

**DOCTORAL (Ph.D.) DISSERTATION**

**KHANDSUREN BADGAR**

**DEBRECEN**

**2022**

**UNIVERSITY OF DEBRECEN**  
**DOCTORAL SCHOOL OF ANIMAL SCIENCE**

*Head of Doctoral School:*

**Prof. Dr. István Komlósi**

professor

*Supervisor:*

**Dr. József Prokisch**

associate professor

**STUDYING THE TOXICITY AND TESTING OF NANOSIZE ELEMENTAL  
SELENIUM**

*Author:*

**Khandsuren Badgar**

Ph.D. candidate

**DEBRECEN**

**2022**

**STUDYING THE TOXICITY AND TESTING OF NANOSIZE ELEMENTAL  
SELENIUM**

Dissertation in order to attain the doctoral degree (Ph.D.)  
in **Animal Science**

Written by: **Khandsuren Badgar** (Ph.D. candidate)

**Name of Ph.D. school:** Doctoral School of Animal Science

**Head of Ph.D. school:** Prof. Dr. István Komlósi

**Supervisor:** Dr. József Prokisch

**Review committee:**

	Name	Sc. Degree	Signature
Chairman:	_____	_____	_____
Member:	_____	_____	_____
Secretary:	_____	_____	_____
Opponents:	_____	_____	_____
	_____	_____	_____

**Date of Ph.D. defence:** 2022.....

## TABLE OF CONTENTS

ABBREVIATIONS AND ACRONYMS .....	6
1. INTRODUCTION .....	9
2. LITERATURE REVIEW.....	12
2.1. The synthesis of selenium nanoparticles.....	12
2.1.1. Biological synthesis .....	12
2.1.2. Chemical synthesis.....	20
2.1.3. Techniques of characterization .....	23
2.1.4. Measurement of selenium concentration .....	26
2.2. The effects of selenium on the health .....	28
2.2.1. Selenium supplementation in animals .....	31
2.2.2. The bioavailability of selenium nanoparticles .....	38
2.3. The application of selenium nanoparticles in nanomaterial.....	43
3. MATERIALS AND METHODS.....	51
3.1. Production of selenium nanoparticles .....	51
3.1.1. Biological method.....	51
3.1.2. Chemical method .....	52
3.1.3. Characterization .....	52
3.2. Determination of antidote effect of selenium nanoparticle.....	54
3.2.1. Determination of the toxic level .....	55
3.2.2. Determination of antidote effect of selenium nanoparticles .....	55
3.3. Production of selenium nanoparticles enriched nanofibers .....	55
3.3.1. Preparation of polymer solution.....	56
3.3.2. Enrichment of polymer solution with selenium nanoparticles .....	56
3.3.3. Electrospinning .....	56

3.3.4. Characterization .....	57
4. RESULTS AND DISCUSSION .....	58
4.1. Production of selenium nanoparticles .....	58
4.2. Coating of selenium nanoparticles .....	65
4.3. Production of selenium nanopowder.....	69
4.4. Determining the protective effect of selenium nanoparticles .....	75
4.4.1. Toxic concentrations of selenium nanoparticles and toxic substances .....	76
4.4.2. The antidote effects of selenium nanoparticles .....	79
4.5. Investigation of selenium nanoparticles in nanofiber production.....	82
4.5.1. Nanofibers enriched with pre-synthesized selenium nanoparticles .....	84
4.5.2. Nanofibers enriched with in-situ synthesized selenium nanoparticles .....	87
5. CONCLUSION .....	91
6. NEW SCIENTIFIC RESULTS.....	93
7. PRACTICAL APPLICABILITY OF RESULTS .....	94
8. SUMMARY .....	95
9. REFERENCES.....	100
10. PUBLICATIONS ON THE TOPIC OF THE DISSERTATION.....	134
11. DECLARATION .....	137
ACKNOWLEDGEMENTS.....	138

## ABBREVIATIONS AND ACRONYMS

AgNPs	Silver nanoparticles
ALT	Alanine Aminotransferase
AST	Aspartate Aminotransferase
ATPase	Adenosine triphosphate
CAT	Catalase
CCD	Charged-coupled device
CRP	C-reactive protein
CVMP	Committee for Medicinal Products for Veterinary Use
DIO	Deiodinases
DLS	Dynamic Light Scattering
DM	Dry Matter
DNA	Deoxyribonucleic acid
EC	European Commission
EDS	Energy Dispersive X-ray Spectroscopy
EMA	European Medicines Agency
EFSA	European Food Safety Authority
EU	European Union
FAO	The Food and Agriculture Organization
FT-IR	Fourier transform resonance spectroscopy
GGT	Gamma-Glutamyl Transferase
GPx	Glutathione Peroxidase
GSH	Glutathione
JCPDS	The Joint Committee on Powder Diffraction Standards
kV	Kilovolts
lg C	Logarithmic Concentration
LC50	Lethal Concentration 50
LC95	Lethal Concentration 95
LD50	Lethal Dose 50
LD95	Lethal Dose 95
MDA	Malondialdehyde
MRL	Maximum Residue Levels

MRS	De Man, Rogosa and Sharpe
MTL	Maximum Tolerable Levels
NDA	Nutrition and Allergies
NRC	The National Research Council
PEEK	Poly(ether ether ketone)
PBS	Phosphate-buffered saline
pH	Potential of Hydrogen
PAN	Polyacrylonitrile
PCL	Poly- $\epsilon$ -caprolactone
PEO	Poly (ethylene oxide)
PVA	Polyvinyl Alcohol
PVB	Polyvinyl Butyral
PVC	Polyvinyl Chloride
PVP	Poly(vinyl pyrrolidone)
PRDX1-6	Peroxiredoxin 1
Rpm	Revolutions Per Minute
RDA	Recommended Dietary Allowance
ROS	Reactive Oxygen Species
SAED	Selected Area Electron Diffraction
SOD	Superoxide Dismutase
Se	Selenium
Se <sup>0</sup>	Elemental selenium
Se <sup>+IV</sup>	Selenite
Se <sup>+VI</sup>	Selenate
SeO <sub>2</sub>	Selenodioxide
SEM	Scanning Electron Microscope
SeNPs	Selenium Nanoparticles
SelCys	Selenocysteine
SeMet	Selenomethionine
Se-MetSeCys	Selenomethylselenocysteine
SEPP1	Selenoprotein P
SEP15	Selenoprotein F
SELENBP1	Selenium-binding protein 1

SOD	Superoxide Dismutase
TAC	Total Antioxidant Capacity
TEM	Transmission Electron Microscopy
TRs	Thioredoxin reductase
TRx	Thioredoxin
TRXNRD1-2	Recombinant Human Thioredoxin Reductase 1
T3	Triiodothyronine
T4	Thyroxine
XRD	X-ray diffraction analysis
$2\theta$	2-Theta
$\text{\AA}$	Angstrom
cm	Centimeter
M	Molar
mL	Milliliter
mg	Milligram
ml/min	Milliliter/minute
$\text{mL h}^{-1}$	Milliliter per hour
mg/L	Milligrams per liter
mg/mL	Milligrams per milliliter
mg/kg	Milligrams per kilogram
mM	Millimeter
m/m	Mass per cent concentration
$\text{mm}^2 \text{s}^{-1}$	Square millimeter per second
nm	Nanometer
$\mu\text{g}$	Microgram
$\mu\text{m}$	Micrometer
$\mu\text{L}$	microliter
g/L	Gram per liter
$\text{g mL}^{-1}$	Grams per square meter
v/v	Volume per volume
w/v	Weight per volume
w/w	Weight per weight

## 1. INTRODUCTION

Selenium (Se) was first discovered as a toxic element in 1817. Then it was identified in 1950 as an essential biological element as a cofactor of selenoproteins including glutathione peroxidase (GPx), thioredoxin reductase (TRs), and deiodinases (DIO). Selenium provides much support for maintaining human and animal health and preventing disease by its functional properties. However, not all organisms can produce it, so it should be taken from food for health reasons. Several types of organic and inorganic selenium are obtained in nature. Worldwide, the total selenium content in soils is around 0.01 mg/kg to 2.0 mg/kg, with an average of 0.4 mg/kg (RAYMAN, 2008; ZHENLI et al., 2010). However, daily selenium intake must be increased depending on the area or illness deficient in selenium. Indeed, soil shortage contributes to the consequent deficiencies of plants, animals, and humans. Several methods have been applied to prevent deficiency symptoms, such as the fortification of selenium mineral salts, feed supplementation, the fortification of selenium in soils, plants, water, and injections and rumen bolus (SUTTLE, 2010; SADEGHIAN et al., 2012; WALLACE et al., 2017; RASHNOO et al., 2020; MILEWSKI et al., 2021).

Selenium intake by animals and humans in various countries, including Europe and Africa, is low, causing selenium deficiency and health problems (ROEKENS et al., 1986; MARTIN et al., 2006; RAYMAN, 2012). Globally, selenium deficiency in animals and humans is commonly observed due to low selenium levels in local soil, water, and food chain and is more prevalent than selenium toxicity (ANNA et al., 2007). In livestock animals, selenium deficiency causes white-muscle disease, heart and skeletal muscle myopathy, ill-thrift, and impaired fertility and immune response, mainly affecting sheep, cattle, poultry, and horses (RAYMAN, 2000). Farm and domestic animals are also affected by selenium deficiency, leading to financial losses (DERMAUW et al., 2013; ZELST et al., 2016). The National Research Council (NRC) has recommended that daily intake of selenium for animals; 0.1 mg/kg dry matter (DM) for beef cattle and calves, 0.3 mg/kg DM for dairy cow (NRC, 2001), 0.1–0.2 mg/kg DM for sheep (NRC, 1985), and 0.1 mg/kg DM of feed for goats (PAPAZAFEIRIOU et al., 2016). In humans, selenium deficiency has been shown to lead to Keshan disease and Kashin-Beck disease (endemic), leading to heart weakness and cartilage tissue atrophy and necrosis. It has been found in the middle of China (STONE, 2009), some countries of Europe, Saudi Arabia, Nepal, and

Egypt (ZHILIN et al., 2015). Selenium deficiency is also correlated with increased cancer occurrence and death, cardiovascular disease, weakened immune system, and male sterility (FORDYCE, 2007; ANNA et al., 2007). Additionally, selenium deficiency is associated with iodine deficiency, observed in Africa (COMBS, 2001). An estimated 500 million to a billion people worldwide are affected by selenium deficiency due to low selenium consumption (PRABHU and LEI, 2016; STONEHOUSE et al., 2020) well documented, especially in Siberia, China, Denmark, Finland, and New Zealand (COMBS, 2001). The Food and Agriculture Organization of the United Nations/World Health Organization has recommended that the daily nutritional requirements of selenium in an adult human diet is 40–400 µg per day (FAO/WHO, 2001). Globally, selenium production is estimated at 2,500 to 2,800 tones annually for various applications, including Japan (551 tones), Canada (384 tones), Belgium (200 tones), and Germany (100 tones). The United Kingdom, Finland, Belgium, and Germany are primary producers and importers of selenium in Europe. The fortification of the soil, water, plants, food, *etc.* with less toxic, more positive effects of selenium, is a new challenge and an essential strategy.

In Europe, selenium content is much lower in most parts than in the United States, especially in the eastern region, where the average selenium intake is lower than in the western region (PRABHU and LEI, 2016). The European Food Safety Authority (REGULATION (EC) № 1924/2006) has admitted the positive effects of selenium on health, including maintaining normal hair, nails, joints, thyroid function, and immune system, and protecting deoxyribonucleic acid (DNA), lipids, and proteins from oxidative damage, and also protecting against heavy metals (EC, 2006a; EFSA PANEL ON DIETETIC PRODUCTS, NUTRITION, and ALLERGIES (NDA), 2010). Dietary selenium like sodium hydrogen selenite and sodium selenate or selenite was included in the list of “vitamins and minerals” that can be added to food (Regulation (EC) № 1925/2006) (EC, 2006b). According to the regulation, the recommended daily allowance (RDA) for adults is 55–70 µg/day (EFSA PANEL ON DIETETIC PRODUCTS, NUTRITION AND ALLERGIES, 2014). The Panel on Additives and Products or Substances used in Animal Feed (FEEDAP) has provided 0.50 mg/kg selenium as selenium-enriched yeast, selenomethionine, and sodium selenite as a feed additive for all animal species (EFSA PANEL ON ADDITIVES AND PRODUCTS OR SUBSTANCES USED IN ANIMAL FEED (FEEDAP), 2012; 2016).

Notably, the nutritional value of selenium depends primarily on the concentration and its chemical forms in the source. Because there is a little space for the beneficial and harmful effects of selenium. Many studies reported that selenium nanoparticles (SeNPs) are more bioavailability (WANG et al., 2007; ZHANG et al., 2008; SHI et al., 2011) and much less toxic (ZHANG et al., 2008; BENKŐ et al., 2012) than other chemical forms. Their applicability is governed by several actual sizes, shapes, structures, atomic arrangements, and surface charges. Therefore, the production of selenium nanoparticles and their applications has recently received increasing attention. Generally, biological and chemical methods are widely used to synthesize nanoparticles that convert metal ions into atoms with the help of reducing agents. The conversion of bulk selenium to nanoform has emerged as a wise approach to obtaining their multifunctional properties. The applications of selenium nanoparticles have been investigated in food supplementation, food packaging systems, nanomedicine, medical devices, and nanomaterials (RAMOS and WEBSTER, 2012; WANG et al., 2015; VERA et al., 2016; CHUNG et al., 2016; SKALICKOVA et al., 2017; DOOSTMOHAMMADI et al., 2021) according to their functional properties including high antioxidant, anticancer, antibacterial, antiviral, antifungal, antidiabetic, immune-stimulatory, and detoxification effects.

Based on the above information, research on the synthesis and application of selenium nanoparticles is progressing in various fields. The present work aims to produce different selenium nanoparticles and seek their applicability in the agricultural sector. Therefore, the following specific objectives have been pursued throughout the research.

- ❖ To synthesize selenium nanoparticles by biological and chemical methods
- ❖ To study the toxic and antidote effect of selenium nanoparticles with an animal model
- ❖ To test selenium nanoparticles in the production of nanofibrous membrane

## 2. LITERATURE REVIEW

### 2.1. The synthesis of selenium nanoparticles

Nanotechnology creates and manipulates materials at the atomic level, and nanosystems are identified by small sizes, complex internal structures, and high surface-to-volume ratios. Three-dimensional, electrostatic, hydrophobic, and hydrogen or coordination bonds are required to stabilize them. The best way to obtain stable nanoparticles is to reduce the number of ions in the polymer solution. To date, reduction methods have been commonly used to prepare selenium nanoparticles, which include  $\gamma$ -radiolytic reduction, chemical reduction, bacterial reduction, *etc.*

#### 2.1.1. Biological synthesis

The biological transformation of nanoparticles is primarily triggered by bacterial and plant metabolites and supports the reduction and stability of nanoparticles. Many studies have been reported the biosynthesized selenium nanoparticles by bacteria, fungi, plant extract, *etc.* Eszenyi and co-workers reported that bacterial synthesis is more effective than other reduction processes with high purity, economical, quicker, and better control parameters (ESZENYI et al., 2011). When cultured in selenium-rich media such as selenium-resistant strains are reached by two different processes such as selenites and selenium salts: reduction process to the elemental selenium, or metabolic conversion to organic forms such as selenomethionine and selenocysteine (ANDREONI et al., 2000; ESZENYI et al., 2011). As is now well established, various positive and negative bacterial species can convert selenium nanoparticles and selenium amino acids with non-toxic from several kinds of inorganic selenium, including selenate ( $\text{Se}^{\text{VI}}\text{O}_4^{2-}$ ) and selenite ( $\text{Se}^{\text{IV}}\text{O}_3^{2-}$ ) oxyanions. As summarized in Table 1., the selenium nanoparticles with various sizes have been synthesized by gram-negative and gram-positive probiotic or pathogenic bacterial strains.

Table 1.

## The synthesis of selenium nanoparticles by bacteria

Bacterial species	Selenium nanoparticle		References
	Size (nm)	Shape	
<b>Gram-positive</b>			
<i>L. acidophilus</i>	100-300	Amorphous	PROKISCH and ZOMMARA, 2011
	15-50	Amorphous	VISHA et al., 2015
	11-23	Amorphous	KAUR et al., 2018
<i>L. helveticus</i>	160 ± 24	Amorphous	MORENO-MARTIN et al., 2017
	10-20	Amorphous	RAJASREE and GAYATHRI, 2015
	100-300	Amorphous	PROKISCH and ZOMMARA, 2011
<i>L. reuteri</i>	130 ± 23	Amorphous	MORENO-MARTIN et al., 2017
<i>L. plantarum</i>	60-80	Amorphous	RAJASREE and GAYATHRI, 2015
<i>L. rhamnosus</i>	60-80	Amorphous	RAJASREE and GAYATHRI, 2015
<i>L. bulgaricus</i>	176 ± 13	Amorphous	MORENO-MARTIN et al., 2017
<i>L. casei</i>	50-80		XU et al., 2018
<i>Bifidobacterium</i>	400-500	Amorphous	ESZENYI et al., 2011; PROKISCH and ZOMMARA, 2011
<i>S. thermophilus</i>	50-100	Amorphous	ESZENYI et al., 2011; PROKISCH and ZOMMARA, 2011
<i>E. faecalis</i>	29-195	Amorphous	SHOEIBI and MASHREGHI, 2017
<i>S. aureus</i>	90-150	Amorphous	MEDINA CRUZ et al., 2018
<i>S. carnosus</i>	439-525	Amorphous	ESTEVAM et al., 2017
<i>S. minutiscleroticus</i>	10-250	Amorphous	RAMYA et al., 2015
<i>B. megaterium</i>	200	Amorphous	MISHRA et al., 2011
<i>B. subtilis</i>	50-400	Monoclinic	WANG et al., 2010
<i>B. cereus</i>	150-200	Amorphous	DHANJAL and CAMEOTRA, 2010
<b>Gram-negative</b>			
<i>E. coli</i>	100-183	Amorphous	KORA and RASTOGI, 2017
	90-150	Amorphous	MEDINA CRUZ et al., 2018
<i>R. eutropha</i>	40-120	Amorphous	SRIVASTAVA and MUKHOPADHYAY, 2015a
<i>P. aeruginosa</i>	47-165	Amorphous	KORA and RASTOGI, 2016
<i>P. alcaliphila</i>	50-500	Trigonal	ZHANG et al., 2011
<i>P. agglomerans</i>	30-300	Amorphous	TORRES et al., 2012
<i>Z. ramigera</i>	30-150	Monoclinic	SRIVASTAVA and MUKHOPADHYAY, 2013
	100-550	Amorphous	FESHARAKI et al., 2010
<i>K. pneumoniae</i>	90-320	Amorphous	KAZEMPOUR et al., 2013

Generally, the mechanism of transformation of selenium nanoparticles by bacterial metabolism is explained in the following phases:

- Transfer of selenium oxoanions into the cell
- Redox reactions of selenium oxoanions in the cell. The conversion process of selenate or selenite to elementary selenium in the cytoplasm or the cytoplasmic membrane is an enzymatic process that includes membrane-bound selenate reductase (RIDLEY et al., 2006), thiol or glutathione reductase called Painter-type reactions (KESSI and HANSELMANN, 2004), nitrite reductase (BASAGLIA et al., 2007), fumarate reductase (SONG et al., 2017), and sulfite reductase (WANG et al., 2018).
- Export of elementary selenium ( $\text{Se}^0$ ) from the cell
- Formation of elemental selenium into nanoscale form in the nuclei (ANNA and ALEXANDER, 2017). The mechanism of this step has been poorly studied and is not completely clear. However, some studies have reported that small particles coalesce into large particles due to the high surface energy (KESSI and HANSELMANN, 2004). Other studies reported that proteins, polysaccharides, and extracellular polymeric substances react in the formation as a cover and capping agents, which is observed on the nanoparticle's surface (JAIN et al., 2015; XU et al., 2019).

Lactic acid bacteria have been commonly used to bioconversion of selenium nanoparticles with amorphous shapes in different sizes due to their non-pathogenic, readily available, and probiotic properties. They can reduce selenium ions to their elemental form intracellularly and extracellularly. However, their ability to resist selenium sources and transport glutathione inside the cell is strain-dependent (POPHALY et al., 2012; PUSZTAHELYI et al., 2015). The production of elemental selenium form by lactic acid bacteria has been explained by alcohol dehydrogenase or glutathione reductase activities, which can reduce selenite by oxidizing glutathione (PUSZTAHELYI et al., 2015; LAMPIS et al., 2017).

Probiotic strains have synthesized selenium nanoparticles with various sizes in diameter (ESZENYI et al., 2011; PROKISCH and ZOMMARA, 2011). In detail, the selenium nanoparticles with 50–100 nm, 100–300 nm, and 400–500 nm were synthesized by bacterial species of *Streptococcus thermophilus* (*S. thermophilus*), *Lactobacillus* sp.,

(*L. casei*, *L. acidophilus*, *L. helveticus*), and *Bifidobacterium*, respectively. In the conversion method, bacterial culture was inoculated in MRS broth enriched with sodium hydrogen selenite at 37 °C for 24–36 hours. The selenium nanoparticles were transformed primarily in bacterial cells. Therefore, at the end of the incubation, the bacteria cell wall was hydrolyzed by HCl at room temperature for 5 days to recover selenium nanoparticles. The nanoparticles were purified by centrifugation at 6000 rpm and rinsed with distilled water. Finally, the suspension has filtered to remove the bacterial biomass. The biosynthesized selenium nanoparticles showed higher antioxidant activity than other selenium sources in animal experiments with sheep, chicken, and fish (BENKŐ et al., 2012; UNGVÁRI et al., 2013; GULYÁS et al., 2016).

RAJASREE and GAYATHRI (2015) reported that selenium nanoparticles synthesized with sizes ranging from 10–20 nm by *L. acidophilus* and from 60–80 nm by *Lactobacillus rhamnosus* (*L. rhamnosus*) and *Lactobacillus plantarum* (*L. plantarum*) in amorphous shape. In the procedure, 1–4 mM of sodium selenite as a selenium source was mixed with 100 mL of bacterial culture medium and incubated at 35 °C for 2 days, shaking at 170 rpm. After the color of the culture, the medium changed from yellow to bright red, and the medium was centrifuged at 10,000 rpm for six minutes, followed by washing with distilled water and ethanol repeatedly. The biosynthesized selenium nanoparticles were shown an inhibitory effect against *Aspergillus niger* (*A. niger*) and *Candida albicans* (*C. albicans*).

*L. acidophilus* and *L. casei* synthesized selenium nanoparticles smaller than 100 nm through a similar conversion method. In brief, a freshly prepared bacterial culture medium with 200 mg/mL selenite was with anaerobe at 37 °C for 24 hours. After the reaction, the selenium nanoforms were released from the bacteria by heating at 121 °C for 20 minutes. Subsequently, the medium was centrifugated at 14,000 rpm for 15 minutes and washed with pure water repeatedly. Finally, the suspension was ultrasonicated for 15 minutes to rupture the cohesive selenium spheres. Due to this method, selenium nanoparticles with a size of 15–50 nm were purified from *L. acidophilus* (VISHA et al., 2015).

*L. casei* converted amorphous selenium nanoparticles accumulated by 50–80 nm in the cell. The fermentation process was conducted using 200 mg/mL sodium hydrogen selenite at an anaerobe condition at 37 °C for 24 hours. After fermentation, the organic ingredients were purified by centrifugation at 12,500 rpm for 10 minutes, followed by

two washes with phosphate buffer. This selenium-enriched *L. casei* showed anticancer activity against the human liver tumor cell line (HepG2). They also stimulated the intestinal porcine epithelial cells, macrophages derived from human acute monocytic leukemia cells, and human colonic epithelial cells (XU et al., 2018).

A recent study reported that *L. casei* transformed amorphous selenium nanoparticles with a mean diameter of 360 nm from hydrogen sodium selenite. In a typical procedure, 20 mg/mL of selenium was mixed with a bacterial culture medium and maintained at 37 °C for 96 hours. After incubation, the culture medium was centrifuged at 7,000 x g for 15 minutes at 4 °C and washed with PBS. The bacterial supernatant was resuspended in 0.1 M NaOH, incubated at 37 °C for 90 minutes, and cleaned with deionized. Eventually, the mixture was sonicated by 20 rounds of five seconds and filtered by a membrane filter with a pore size of 2 to 0.45 µm to purify selenium nanoparticles. The biosynthesized selenium nanoparticles within their converter bacteria showed a high inhibitor effect against the growth of colon carcinoma (SPYRIDOPOULOU et al., 2021).

*Lactobacillus reuteri* (*L. reuteri*), *L. acidophilus*, and *L. delbrueckii subsp. bulgaricus* converted selenite to spherical selenium nanoparticles with 130 nm, 160 nm, and 176 nm, respectively, determined by dispersive light scattering. Shortly, 25 mg/L of sodium selenite as selenium precursor was added into a freshly activated bacterial culture, and the mixture was incubated at 37 °C for 24 hours. After completion of the reaction, the mixture was ultrasonicated for 2 minutes and centrifuged at 9449 rpm for 10 minutes. Subsequently, the pellet was resuspended in 0.1% sodium dodecyl sulfate (w/v), 1M sodium hydroxide by ultrasonication and centrifugation conditions as mentioned above. At last, selenium nanoparticles were purified by resuspension in distilled water and filtering by 0.45 µm and 0.22 µm nylon filters. This study was mentioned that *L. reuteri* accumulates the highest amount of selenium and has the most incredible resistance at high concentrations of selenium (MORENO-MARTIN et al., 2017). The concentration of selenium source in the medium and bacterial strain plays a critical role in bacterial conversion. Some studies reported that the resistant strains, including *L. reuteri* (LAMBERTI et al., 2011; PESCUA et al., 2017), *L. acidophilus* (PESCUA et al., 2017), *L. bulgaricus* (PALOMO-SIGUERO et al., 2016), and *L. plantarum* (CHEN et al., 2019).

According to KAUR et al. (2018), selenium nanoparticles with sizes 11–23 nm were synthesized by a strain of *L. acidophilus* intracellularly. In a typical procedure, MRS broth as a medium was enriched by 30 mg of sodium selenite as a selenium precursor. Then bacteria were inoculated in 100 mL of selenium-enriched medium and incubated at 37 °C for 36–48 hours with a shaker. After incubation, the mixture media was centrifuged at 8,000 rpm for 15 minutes, and the pellets were rinsed with distilled water repeatedly. Then, the bacterial cell wall was ruptured by acidic hydrolysis (37% HCl) for five days at the ambient temperature. Finally, the suspension was centrifuged for 10–15 minutes at 6,000 rpm, rinsed with distilled water, and ultrasonicated for 10–15 minutes to purify selenium nanoparticles. The biotransformed selenium nanoparticles were exhibited a robust antimicrobial effect against the bacterial strains of *Klebsiella*, *Bacillus subtilis*, *Staphylococcus aureus*, *Candida albicans*, *Pseudomonas aeruginosa*, and *Escherichia coli*. However, several studies reported that these bacterial strains could be converted from selenium source to elemental form. For instance, MEDINA CRUZ and co-workers have used these bacterial strains such as *Escherichia coli* (*E. coli*), *Pseudomonas aeruginosa* (*P. aeruginosa*), and *Staphylococcus aureus* (*S. aureus*) as reducing agents for the biosynthesis of selenium nanoparticles with the sizes of 90–150 nm in diameter. In the formation process, two mM sodium selenite as selenium precursor was added to the bacterial culture medium and was incubated at 39 °C with a shaker at 200 rpm for 3 days. After this process, the mixture solution centrifuged at 7500 rpm for 15 minutes, and the particles were washed with PBS and resuspended in Tris/HCl buffer. Finally, selenium nanoparticles were purified by ultrasonication and hyperthermia-based approaches. Interestingly, these synthesized selenium nanoparticles with a 25–250 mg/mL concentration exhibited antibacterial activity against foodborne pathogens and no significant cytotoxic effect on dermal fibroblasts for 24 hours (MEDINA CRUZ et al., 2018). Likewise, *P. aeruginosa* has successfully converted selenium nanoparticles with spherical, polydisperse, ranging from 47 to 165 nm with aerobic conditions. In brief, bacterial culture ( $10^7$  CFU/mL) 100 mL was mixed with the nutrient broth containing 0.25–1.0 mM sodium selenite and incubated for 24–72 hours at 37 °C under aerobic conditions. Finally, the selenium nanoparticles were purified from the bacterial fragments by centrifugation for 10 minutes at 10,000 rpm (KORA and RASTOGI, 2016).

*Bacillus subtilis* (*B. subtilis*) was synthesized monoclinic nanoscale selenium with 50–400 nm size. Briefly, 1 mL fresh bacterial culture and four mM sodium selenite as

selenium source with 100 mL medium were inoculated at 35 °C for 48 hours with shaking incubator at 170 rpm. After incubation, the bacterial fragments were removed from the culture medium by centrifugation for a few minutes at 10,000 rpm and washing twice with redistilled water and alcohol (WANG et al., 2010).

*Klebsiella pneumoniae* (*K. pneumoniae*) was synthesized spherical selenium nanoparticles in diameter size from 100 to 550 nm (FESHARAKI et al., 2010), 90 to 320 nm (KAZEMPOUR et al., 2013) by the same conversion method. In the production, 1% (v/v) of a freshly activated culture of *K. pneumoniae* in tryptic soy broth (TSB) was supplemented with 559.19 mg of selenium chloride (which means 200 mg/L selenium) and were multiplied at 37 °C for 24 hours. At the end of the incubation, the mixture culture was autoclaved at 121 °C, 1.2 kg/cm<sup>2</sup> for 20 minutes to cell lysis, and centrifuged at 25,000 x g for 15 minutes. Following washed three times with distilled water and sonicated for 10 minutes to clean the selenium nanoparticles from the bacterial organelles.

The biotransformation of selenium nanoform has been associated with fungi and some plant extracts. Few studies were reported that fungi could convert inorganic selenium into its elemental form, including such as *Gliocladium roseum* (SRIVASTAVA and MUKHOPADHYAY, 2015b), *Aspergillus terreus* (ZARE et al., 2013), *Alternaria alternata* (SARKAR et al., 2011), *Lentinula edodes* (VETCHINKINA et al., 2013), and *Mariannaea sp. HJ* (ZHANG et al., 2019). However, their mechanism for converting selenium ions into nanoparticles is currently unknown.

ZARE with co-authors (2013) reported that amorphous selenium nanoforms with an average diameter of 47 nm were transformed by *Aspergillus terreus* (*A. terreus*). Shortly, 80 mL of sodium selenite (100 mg/mL selenium) was mixed with 20 mL of *A. terreus* supernatant and incubated for one hour at ambient temperature. Then, the synthesized selenium nanoparticles were separated from fungus through centrifugation at 20,000 ×g for ten minutes and washing several times with distilled water.

The selenium nanoparticles were synthesized in intracellular with average size 45.19 nm and extracellular with 212.65 nm by fungus strain like *Mariannaea sp. HJ*. In the conversion processes, one mM selenium dioxide as selenium source with 1% (v/v) of fungus medium was incubated at 30 °C under aerobic condition until grown. Subsequently, the culture medium was filtered via a filter paper with pore sizes 180 mm and washed with distilled water repeatedly. The authors reported that intracellular and

extracellular synthesized selenium nanoparticles are obtained by ultrasonication at 4 °C for 30 minutes and centrifugation with 12,000 x g for 30 minutes and filtration, respectively (ZHANG et al., 2019).

The plant-based biosynthesis of selenium nanoparticles has received much attention because of its environmentally friendly, inexpensive, non-toxic, and procurable methodology that provides a concerted and one-step technique for the biogenic conversion of selenium nanoparticles (PAGAR et al., 2019). Moreover, the biomolecules contained in the extract are thought to make the nanoparticles more stable and enhance their effectiveness as antibacterial and antioxidant activities. The plant extracts have been prepared from different parts, including leaves, peel, flowers, seeds, fruits, etc.

Fruit extract of *Embllica officinalis* was transformed into selenium nanoparticles of 15–40 nm size. Two mL of fresh extract was mixed dropwise to ten mL of sodium selenite (10 mM) with continuous stirring in the reduction process. After that, the reaction was maintained at 27 °C, on an orbital shaker with 120 rpm for a day in dark conditions. Eventually, the biosynthesized selenium nanoparticles were shown a wide range of antimicrobial activity on pathogenic bacterial strains like *Escherichia coli*, *Listeria monocytogenes*, *Staphylococcus aureus*, *Enterococcus faecalis*, and also antifungal effect (GUNTI et al., 2019).

Leaves extract of *Withania somnifera* was synthesized amorphous selenium nanoparticles in the 45 nm to 90 nm size range. Shortly, 100 mL of leaves extract was supplemented by 50 mM selenious acid under stirring and incubated at ambient temperature. At the end of the reaction, the selenium nanoforms were collected by centrifugation at 1500 rpm, followed by washing with distilled water and acetone and drying. Finally, selenium nanoparticles were resuspended in PBS by ultrasonication and centrifugation (ALAGESAN and VENUGOPAL, 2019).

Flower extract of *Bougainvillea spectabilis* was synthesized hollow and spherical selenium in nanoform with an average size of  $24.24 \pm 2.95$  nm. In the conversion method, 90 mL of 10 mM selenium selenate was mixed with 10 mL of a fresh flower extract and incubated with a shaker at 250 rpm at 36 °C for 5 days (DEEPA and GANESAN, 2015).

The seed extract of *Fenugreek* has been converted to nano selenium in a size range of approximately 50–150 nm. For the synthesis procedure, a mix of 1 mL of seed extract with 10 mL of selenite (30 mM) and 200  $\mu$ L of ascorbic acid (40 mM) was incubated for

24 hours at room temperature. In this case, ascorbic acid was used as the initiator of the reduction reaction. After incubation, the mixture was centrifuged at 10,000 x g for 30 minutes, and the pellet was rinsed with double-distilled water and ethanol repeatedly. Subsequently, ultrasonication and centrifugation were used to resuspend selenium nanoparticles in PBS (RAMAMURTHY et al., 2013).

### **2.1.2. Chemical synthesis**

Reduction and sedimentation methods as chemical synthesis have converted nanoparticles, which means a reaction between selenium source and reducing agents. Also, stabilizing agents need to the stability of nanoparticles by leading to aggregation and controlling to diameters, such as bovine serum albumin (VERMA and MAHESHWARI, 2018; CHUNG et al., 2020), lactoglobulin, or dextrin (MALHOTRA et al., 2014), polysaccharides (ZHANG et al., 2010; LUESAKUL et al. 2016), and some polymers like polyethylene glycol (PEG) (ZHENG et al., 2012), polyvinyl alcohol (PVA) (SHAH et al., 2007), *etc.* Owing to their nontoxicity and ecofriendly, polysaccharides, monosaccharides, amino acids, vitamins, *etc.* are recognized as “green” reducing agents for the reduction of bulk selenium into their nanoform with different structures and sizes, including fructose (VIEIRA et al., 2017), lactose (CAVALU et al., 2018), ascorbic acid (GANGADOO et al., 2017; ANGAMUTHU et al., 2019; VAHDATI and TOHIDI MOGHADAM, 2020; SHAHABADI et al., 2021), glutathione (VERMA and MAHESHWARI, 2018), glucose (CHEN et al., 2011), L-cysteine (PRASANTH and SUDARSANAKUMAR, 2017; LI et al., 2010), *etc.*

Trigonal and amorphous selenium nanoparticles in shapes with an average size at 80 nm were synthesized by D-fructose. In brief, five mL sodium selenite (1.0 mmol/L) as precursor was slowly dropped to 10 mL reductant (1.0 mmol/L fructose), and the mixture was stirred for 15 minutes at 45 °C. The amorphous selenium nanoforms were harvested after 15 minutes, and trigonal selenium nanoforms were collected after 20 minutes. They were purified by centrifugation at 13,000 x g for 10 minutes and washed with deionized water in the next step. Eventually, the synthesized amorphous and trigonal selenium nanoparticles exhibited a potentially toxic effect on the sarcoma cells and a non-toxic effect on human healthy fibroblast cells (VIEIRA et al., 2017).

Moreover, lactose was converted amorphous form of selenium nanoparticles from sodium hydrogen selenite. In a typical method, the same amount of selenium solution (10,000 mg/L selenium) and lactose were mixed in a ratio of 1:8 (w/w) under a magnetic stirrer at 120 °C for three minutes. After heating, the mixture was cooled down, centrifuged at 6000 rpm for ten minutes, and rinsed with pure water. The centrifugation was repeated four times and filtered (CAVALU et al., 2018).

Rod-shaped selenium nanoparticles in the 74.29 nm size were synthesized by glutathione as a reducing agent with bovine serum albumin as a stabilizer. In the procedure, the same amount of sodium selenite (25 mM Se) and glutathione (100 mM), and 0.15 grams of stabilizer were mixed to 9 mL of double-distilled water in a safety cabinet. The pH of the media is set to alkaline with NaOH. In the final step, the media was centrifuged at 13,000 x g at -4 °C to collect the synthesized nanoparticles (VERMA and MAHESHWARI, 2018).

Spherical-shaped selenium nanoparticles with a size of about 20–80 nm have been converted from bulk selenium as a sodium selenosulfate using sulphuric acid with polymer stabilizer PVA. In a particular procedure, pre-prepared 0.25 mol/L sodium selenosulfate with 0.1 % PVA was mixed, then sulfuric acid was added to them and stirred for 1 minute at ambient temperature (SHAH et al., 2007). A similar result reported that spherical selenium nanoparticles with a mean diameter of less than 60 nm were synthesized from L-cysteine and selenous acid reactions. In the typical method, the same amount of 10 mM L-cysteine and 20 mM selenous acid was mixed and heated at 105 °C for an hour. After heating, the selenium nanoparticles were harvested by washing a few times with distilled water and dried at 60 °C for 8 hours in a hot air oven (PRASANTH and SUDARSANAKUMAR, 2017).

One of the most commonly applied reducing agents in forming gold, silver, and selenium nanoparticles is ascorbic acid. A spherical shape of selenium nanoparticles less than 100 nm in size was formed from a reaction of 5 mM selenium tetrachloride, 100 mM ascorbic acid, and 0.1% (v/v) poly (sodium 4-styrenesulfonate) as a protective agent. In the conversion process, 2.5 mL of the protective agent was mixed with 15 mL of selenium source, then 2.5 mL of ascorbic acid from their stock solutions under stirring at 160 °C until the color turned to deep red for 1–2 minutes. After the reaction, 20 mL of the mixture was diluted with 20 mL of Milli-Q water, centrifuged at 1008 x g. The supernatant was

resuspended with 40 mL of Milli-Q water and then centrifuged at 8500 rpm for 25 minutes. The supernatant was resuspended in Milli-Q water, and this wash step was repeated three times. Interestingly, less than 100 nm of selenium nanoparticles were harvested during the first wash, and smaller than 50 nm of particles were obtained from the second wash (GANGADOO et al., 2017).

According to ANGAMUTHU and co-workers (2019), amorphous selenium nanoparticles with a mean size ranging 15–18 nm were also transformed via ascorbic acid. Specifically, 100 mM sodium selenite as selenium precursor was mixed with 50 mM ascorbic acid in a ratio of 1:4 with stirring at room temperature for 30 minutes. After mixing, the reaction was centrifuged at 3000 rpm to separate the supernatant. These ascorbic acid-mediated selenium nanoparticles exhibited a high antibacterial effect against foodborne germs like *Staphylococcus aureus*, *Escherichia coli*, and *Pseudomonas aeruginosa*. A similar study reported a spherical selenium nanoparticle with  $35.6 \pm 7.5$  nm converted from sodium selenite by ascorbic acid with polysorbate as a stabilizer. In this case, ten mL of 56.7 mM ascorbic acid solution was mixed dropwise to selenium precursor solution (30 mg sodium hydrogen selenite dissolved 90 mL of Milli-Q water under stirring). After adding the first 2 mL of ascorbic acid, a 10  $\mu$ L stabilizing solution was added. The reaction was centrifuged at 12,000 rpm, and the pellets were resuspended in sterile double distilled water to purify selenium nanoparticles (VAHDATI and TOHIDI MOGHADAM, 2020). Likewise, spherical shape with a mean diameter at 146 nm selenium nanoform was also converted by 0.1 M ascorbic acid. In this case, 300 mL of ascorbic acid was dropped to 600 mL of sodium hydrogen selenite under mild stirring at room temperature for 24 hours. After the reaction, the synthesized selenium nanoparticles were harvested via centrifugation at 8,000 rpm for several minutes and washed with deionized water (SHAHABADI et al., 2021).

The cubic structure with 300 nm, spherical particles with 200 nm in selenium nanoparticles synthesized ascorbic acid with different stabilizers like folic acid-gallic acid-N, N, N-trimethyl, and chitosan, respectively. In special procedures, five mM sodium selenite, 0.5% (w/v) chitosan in 0.5% acetic acid, 0.5% (w/v) folic acid-gallic acid-N,N,N-trimethylammonium in 0.5% acetic acid (which is modified chitosan), and 20 mM ascorbic acid were previously prepared, then, chitosan or modified chitosan was mixed with 200  $\mu$ L of selenite, following added dropwise 200  $\mu$ L of ascorbic acid, which was reconstituted with distilled water to 1 mL of the final volume. The mixture was

treated by high temperature at 80 °C for 2 hours. The synthesized cubic selenium nanoparticles exhibited a better uptake of breast cancer cells and lesser toxicity towards non-cancer cells (LUESAKUL et al., 2016).

The molar ratio of ascorbic acid to sodium selenite and the stirring speed were studied by Chung and co-workers. In this case, 50 mM ascorbic acid was mixed dropwise to one mL of 100 mM sodium selenite and ten mg/mL bovine serum albumin as a stabilizer. The reaction was continued for 30 minutes. After that, the selenium nanoparticles were separated by centrifugation at 11,000 rpm for 15 minutes and washed at least twice by double-distilled water. The selenium nanoparticles were converted with diameters between 23 nm 47 nm in ratios of 1:5 and 1:6 at 100 and 600 rpm. Finally, the synthesized selenium nanoparticles have supported the growth of fibroblast and inhibited the growth of *Staphylococcus aureus* (CHUNG et al., 2020).

In addition, ascorbic acid with other reducing agents can be converted selenium nanoparticles from bulk selenium. For example, ascorbic acid with polysaccharides of *Undaria pinnatifida* has transformed selenium nanoparticles between 44 nm and 92 nm, with a mean diameter of 59 nm. Eight mL of 60 mM ascorbic acid was mixed with 1 mL of 0.1% polysaccharide under magnetic stirring in a synthesis procedure. Subsequently, 1 mL of sodium selenite (30 mM) was added and sonicated for 5 minutes. Finally, the formed nanoparticles were purified by washing with ultrapure water. The synthesized selenium nanoparticles with an IC<sub>50</sub> value of 3.0–14.1 μm were exhibited an inhibition effect against human cancer cell lines, namely melanoma cells, hepatocellular carcinoma cells, nasopharyngeal carcinoma cells, and breast adenocarcinoma cells (CHEN et al., 2008).

### **2.1.3. Techniques of characterization**

The synthesis processes of selenium nanoparticles and their morphological properties have been characterized by several techniques, including UV-visible spectrophotometry, Dynamic light scattering (DLS), Energy dispersive X-ray (EDS), Scanning electron microscopy (SEM), Fourier transform infrared spectroscopy (FT-IR) analysis, Transmission electron microscopy (TEM), and X-ray diffraction analysis (XRD).

UV/Vis spectrophotometry is the fundamental and essential technique for identifying and characterizing the formation of nanoparticles. It discovers the “absorption maximum” of nanoparticles depending on the concentration of the reagents like precursor sources, reducing agents, or other reaction ingredients. Various absorption peaks were detected during the chemical and biological transformation of selenium nanoparticles caused by reducing agents. For chemical synthesis, L-cysteine and lactose-induced selenium nanoparticles were shown absorption maximum at 580 and 270 nm, respectively (LI et al., 2010; CAVALU et al., 2018). For biological synthesis, *B. megaterium* mediated selenium nanoparticles were shown maximum spectrum at 200–300 nm (MISHRA et al., 2011), and *B. cereus* mediated nanoparticles were presented the absorption maximum at 590 nm (DHANJAL and CAMEOTRA, 2010).

The dynamic light scattering (DLS) analysis has been applied to determine the nanoparticles' surface charge (z-potential). It provides the hydrodynamic diameter of the nanoparticles and a good insight into their stability/aggregation by measuring their Brownian motion (KAPUR et al., 2017).

Electron microscopic techniques such as SEM and TEM with EDS are well-known techniques for characterizing nanoparticles. They can determine nanoparticles' structure, morphology, size distribution, and elemental composition (Figure 1). For instance; these analyses were indicated that the probiotic bacteria mediated amorphous selenium nanoparticles in shape with a size ranging 100-500 nm, which are formed intracellular and extracellular (ESZENYI et al., 2011), and was also shown aggregation of nanoparticles to bacterial cell mass (DHANJAL and CAMEOTRA, 2010).

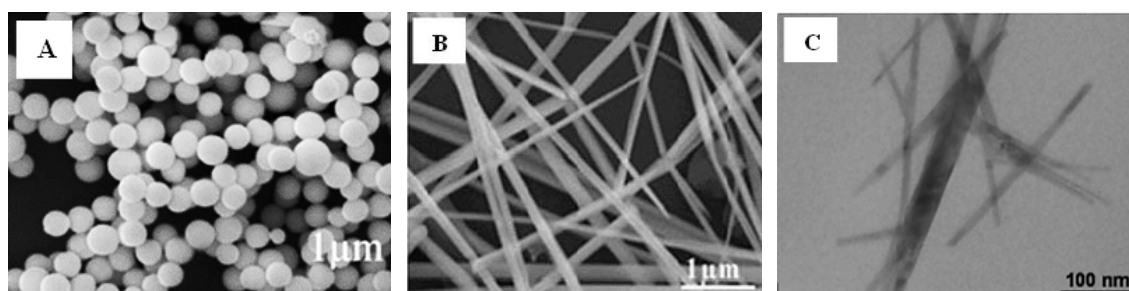


Figure 1: SEM and TEM images for amorphous (A), monoclinic (B), and trigonal (C) selenium nanoparticles synthesized by glucose, *B. subtilis*, and *R. eutropha*, respectively. [Source: CHEN et al., 2011; WANG et., 2011; SRIVASTAVA and MUKHOPADHYAY, 2013]

Fourier transform infrared spectroscopy (FT-IR) is an efficient analysis that enables reproducible analyses to reveal the presence of active groups on the nanoparticle's surface. These groups can reduce metal ions and, or the nanoparticle capping, ensuring colloidal stability (WADHWANI et al., 2017). For instance, ANGAMUTHU et al. (2019) determined active groups of selenium nanoparticles synthesized by ascorbic acid. The spectrum was shown tensile functions at 2919.69, 1630.51, 1380.78, and 1076.09  $\text{cm}^{-1}$  wavelength corresponded to C–H, C=C, O–H, and C–O, respectively. The 2361  $\text{cm}^{-1}$  band is the C–H stretch of acryl acid. The intensive bands were detected at 1654  $\text{cm}^{-1}$  is, indicating C=C elongation of the aromatic ring, N–H bending of amines, and C=O elongation of polyphenols.

X-ray diffraction analysis (XRD) has been applied to study the components and phases of nanoparticles. Several selenium allotropes occur, including black form with an irregular crystal structure, red forms with monoclinic crystalline structure, and grey form with a hexagonal crystalline structure. Red forms of selenium can be found as amorphous and monoclinic crystalline ( $\alpha$ ,  $\beta$ ). Grey hexagonal crystalline form is also known trigonal selenium, and is the most termodinamically stable form. Generally, XRD determines (Figure 2) a lattice structure, crystallinity, and crystallite of nanoparticles size using the Debye–Scherrer equation (GARCÍA et al., 2020). Nanoscale selenium presents a standard XRD pattern (23, 30, 43) that confirms its nanoscale properties and resembles selenium nanoparticles originating from all different sources. In biological synthesis, selenium nanoparticles exhibit a clear pattern during XRD analysis, with no sharp reflections of Bragg, noisy and broad. Consequently, this pattern exhibits the amorphous shape of the selenium nanoform, which is synthesized by *Bacillus cereus*, *Bacillus megaterium*, and *Stenotrophomonas maltophilia* (DHANJAL and CAMEOTRA, 2010; MISHRA et al., 2011; CREMONINI et al., 2016). The XRD pattern of the chemically synthesized selenium nanoparticles sometimes shows broad and strong peaks at around  $2\theta = 23^\circ$ , but it is not crystal form (CAVALU et al., 2018). In addition, reflections (100), (101), (110), (102), (111), (201), (003), (202), (210) and (211) are corresponded to the diffraction peaks of  $2\theta = 23.6^\circ$ ,  $29.9^\circ$ ,  $41.4^\circ$ ,  $43.8^\circ$ ,  $45.4^\circ$ ,  $51.8^\circ$ ,  $55.9^\circ$ ,  $61.8^\circ$ ,  $65.3^\circ$  and  $68.3^\circ$ . They indicate the pure hexagonal crystalline form of selenium nanoparticles converted by the bacterial strain of *Gliocladium roseum*. The lattice constants were  $a = 4.366 \text{ \AA}$  and  $c = 4.9536 \text{ \AA}$  according to the JCPDS №06–0362 (SRIVASTAVA and MUKHOPADHYAY, 2015b). It is also observed that the crystalline phases (100), (101), (110), (102), (111), (201),

(112), and (103) corresponds to diffraction peaks at  $2\theta = 23^\circ, 29^\circ, 41^\circ, 43^\circ, 45^\circ, 51^\circ, 55^\circ, 61^\circ,$  and  $65^\circ$ . These peaks are indicated to the trigonal phases of selenium nanoform converted by fructose as a chemical reducing agent.

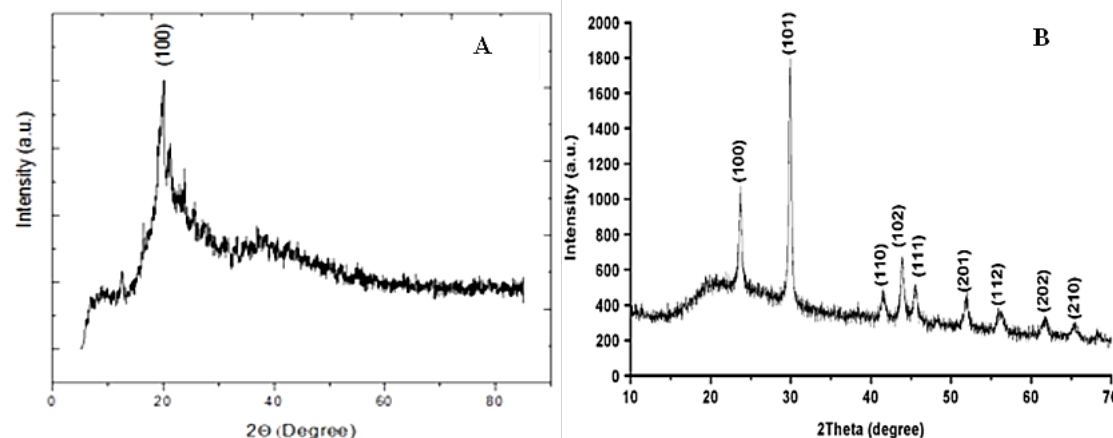


Figure 2: **The XRD patterns of amorphous (A) and crystalline (B) selenium nanoparticles obtained from the biological synthesis.** [Source: CAVALU et al., 2018; SRIVASTAVA and MUKHOPADHYAY, 2015b]

#### 2.1.4. Measurement of selenium concentration

Total selenium concentration can be measured by several basic techniques such as atomic absorption spectrophotometry (AAS), inductively coupled plasma-optical emission spectrometry (ICP-OES), inductively coupled plasma-mass spectrophotometry (ICP-MS), atomic fluorescence spectrophotometry (AFS), *etc.*

Atomic absorption spectrophotometry (AAS) is an analytical technique applied to measure the content of elements in a sample in the ranges from parts per million (ppm) to parts per billion (ppb). The metal ions are sprayed into a high-temperature flame as a fine spray, where they are reduced to atoms and then absorb the light from the element-specific hollow cathode lamp. Generally, this instrument works on the principle that an atom absorbs light of a specific wavelength. When the light of a specific wavelength is given, energy (light) is absorbed by the selenium atom. The electrons of the selenium atom move from the ground state to the excited state. The total selenium concentration in the sample can be calculated after measuring the amount of absorbed light.

Inductively coupled plasma-optical emission spectrometry (ICP-OES) is a routinely applied method for measuring the number of specific elements of different sample types in the ranges of parts per billion (ppb) to parts per trillion (ppt). It works on the principle that an atom absorbs energy, and its energy source is heated from an argon plasma operating at 10,000 Kelvin. This depends on the light emission of a specific wavelength as the excited atom transitions to a lower energy level. The type of atom and the energy level at which the electrons move determine the wavelength of the emitted light. The amount of emitted light at each wavelength is proportional to the number of transitioning atoms. When the excited electrons of the selenium atom return to the ground state, they emit light at a particular wavelength. This instrument measures the amount of emitted light at each wavelength and uses them to calculate the concentration of selenium in the samples. The calibration curve determines the relationship between the intensity of emitted light and the selenium concentration in the sample.

Inductively coupled plasma-mass spectrophotometry (ICP-MS) is one of the best analytical techniques that measure the concentration of elements in the ranges of parts per billion (ppb) to parts per trillion (ppt) of non-interfering low background isotopes. It is superior in speed, accuracy, and sensitivity to atomic absorption spectrometry. Atomic elements are sent through the plasma source from which they are ionized, and then the ions are classified based on their mass. The inductively coupled plasma (ICP) manipulates the argon carrier gas to aerosolize the sample, passing through the chamber and supplying only the smallest droplets to the argon plasma torch. After passing through the ICP, the mass spectrometry (MS) separates the ions by mass-to-charge ratio, and the detector counts the number of selected ions per second. This allows the instrument to measure the concentration of each selected element.

Atomic fluorescence spectrophotometry (AFS) is one of the sensitive techniques for measuring the concentration of a particular element in a sample at parts per trillion (ppt) level. It works by converting the sample into gaseous atoms, where the element of interest is excited by a light source to a higher electron energy level. Solution or solid analysis requires desolvation, vaporization, and spraying of atoms of the object to be analyzed at relatively low temperatures in heat pipes, flames, or graphite furnaces. Hollow cathode lamps or lasers provide resonant excitation to propel atoms to higher energy levels. Atomic fluorescence is scattered and recorded by a monochromator and photomultiplier, similar to an atomic emission spectroscope. The frame atomizer consists of a nebulizer

that turns the sample into an aerosol and is supplied to the burner. The burner system for AFS is a combination of acetylene/nitrous oxide and hydrogen/oxygen/argon by rectangular flame. Monochromators or interference filter systems are used to separate narrow bands of wavelength. Photomultiplier tubes convert radiant energy into electrical signals.

## **2.2. The effects of selenium on the health**

Selenium is a multifunctional element that must be present at certain levels in humans and animals and plays an active role in cell metabolism. The biological activities of selenium are primarily driven by selenoproteins, which are encoded by 25 genes in humans and 24 genes in mice. They are concerned with glutathione-dependent removal of hydroperoxide, reduction of thioredoxins, synthesis of selenophosphate, activation and inactivation of thyroid hormones, thioredoxin-dependent reduction of oxidized methionine residues, protein degradation associated with the endoplasmic reticulum, and other critical biochemical processes. Most of the known selenoproteins are directly or indirectly involved in the antioxidant function and decrease cells and tissues injuries by reducing reactive oxygen species (ROS) and free radicals. Among them, glutathione peroxidase (GPx or GSH-Px) is an essential and most well-known selenoprotein, which creates functional groups to protect cells from oxidation caused by free radicals. Thioredoxin reductase (TRs) is also a selenoprotein regulating intracellular redox processes. The following important selenoprotein is deiodinases, especially iodothyronine deiodinase. They are an essential factor in the metabolism of the thyroid hormone. Selenoprotein P (SEPP) is involved in the transport of selenium and fulfills its antioxidant function, and selenoprotein W is a small protein whose function is unknown, but it is required for muscle metabolism. It is found in the highest concentrations in the muscles, testes, and brain. Many genes, including SEPP1, SEP15, TRXNRD1-2, PRDX1-6, SELENBP1, CAT, GPx1,3,4, and SOD1,2,3, are associated with the antioxidant properties of selenium (CHAN et al., 2016). For example, superoxide dismutase (SOD) helps reduce oxidative stress by effectively suppressing the superoxide radicals and forming them into hydrogen peroxide. Subsequently, the catalase enzyme (CAT) is broken down into water and oxygen to prevent DNA damage. SOD activity is reduced due to low consumption of selenium and other antioxidants, while free radicals cause

carcinogenesis (GALADARI et al., 2017) and other pathological processes. The general metabolism of selenium in the body is imagined in Figure 3, adapted and modified from NICASTRO and DUNN (2013).

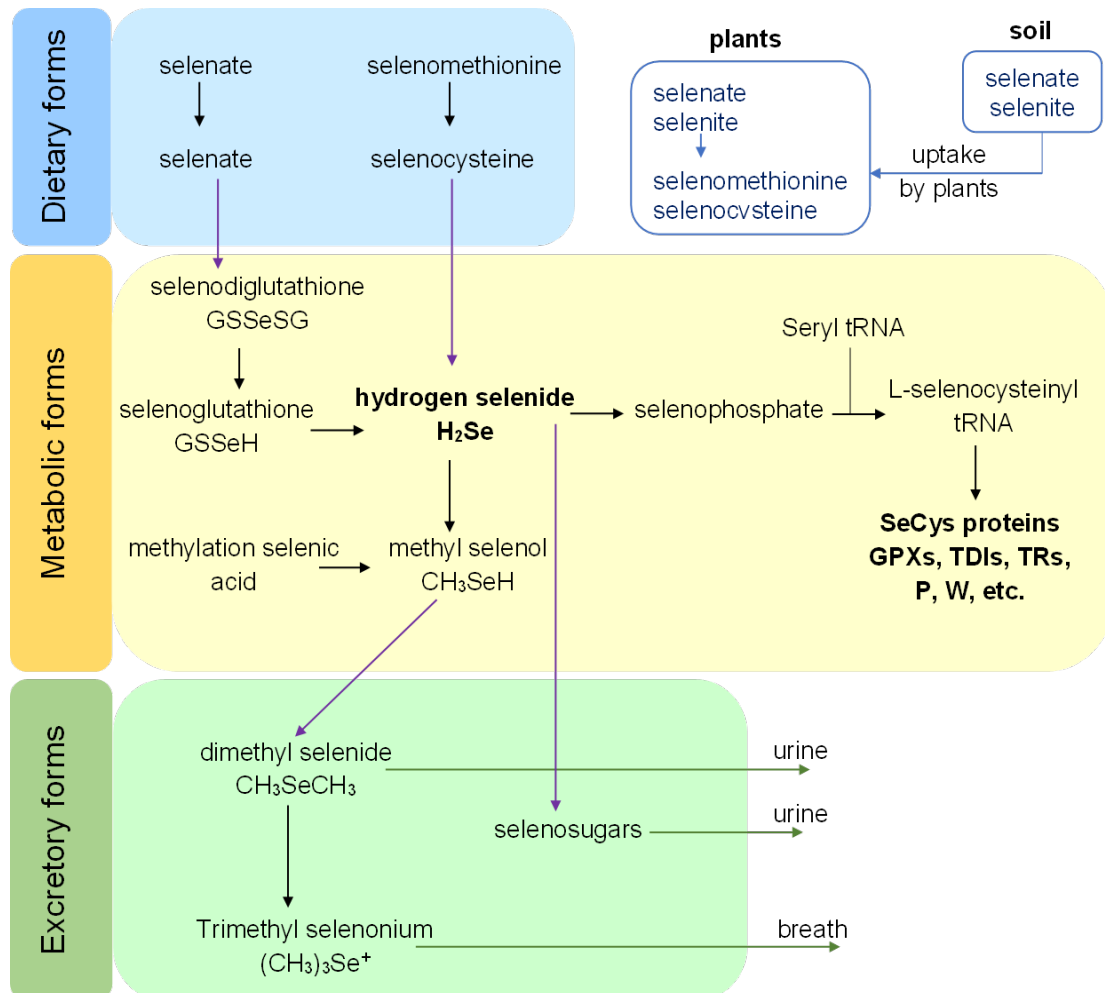


Figure 3: **Intermediary metabolism of selenium in mammals (GPXs: glutathione peroxidases, TDIs: iodothyronine 5'-deiodinases, TRs: thioredoxin reductases, P: selenoprotein P, W: selenoprotein W)**

There is a small space between the essential and toxic concentrations of selenium for animals and humans, reported worldwide (LI et al., 2015). For animals, the toxic concentration of selenium in animal nutrition is around 2–5 mg/kg dry matter (DM), with a lower limit is described as 0.05–0.10 mg/kg DM (GUPTA and SHIKHA GUPTA, 2017). Maximum tolerable levels (MTL) for animal's feed: 5 mg/kg for the horse, cattle, and sheep, 4 mg/kg DM for pigs, 3 mg/kg DM for poultry, and 2 mg/kg DM for fish, have been recommended by The National Research Council (NRC, 2005). In Europe,

dietary selenium of 2–5 mg/kg DM can cause asymptomatic toxicity in all animals, and 25 mg/kg DM can cause acute toxicity in laboratory animals, which is recommended by The European Medicines Agency/Committee for Medicinal Products for Veterinary Use (EMA/CVMP/2015, EUROPEAN PUBLIC MRL ASSESSMENT REPORT). According to the European Food Safety Authority, for humans, the daily maximum selenium level is 300 µg/person (EFSA PANEL ON DIETETIC PRODUCTS, NUTRITION AND ALLERGIES, 2014). However, a dose of selenium greater than 250 mg, or multiple doses of 25–30 mg, such as sodium selenate or selenite, and potassium selenate, can cause acute toxicity (EMA/CVMP/187590/2015). Selenium's chronic toxicity as selenosis is detected at doses above 400 µg/day (FAO/WHO, 2001; KIELISZEK and BŁAŻEJAK, 2016; GUPTA and SHIKHA GUPTA, 2017).

The bioavailability of selenium is caused by some factors, including its form, concentration, solubility, other dietary ingredients, and animal physiology. Nevertheless, its health-promoting and toxic effects depend on its concentration and chemical forms (LIU et al., 2012). Acute exposure to selenium can induce neurotoxicity, and chronic exposure can affect endocrine, primarily thyroid hormone regulation (VINCETI et al., 2001; 2014). Some kinds of selenium, especially selenate and selenite, are toxic to the organism because they are the oxidative form in organisms. Ilona and co-workers reported that the toxic effects of the selenium form could be decreased from selenate to selenite to nano selenium (ILONA et al., 2012). The higher toxicity of selenite, selenocysteine (SeCys<sub>2</sub>), and selenodioxide (SeO<sub>2</sub>) are linked with their potential of proteins to begin oxidation of thiol groups (KIM et al., 2003), which can convert the activity of essential enzymes, including sulfhydryl groups (SPALLHOLZ and HOFFMAN, 2002).

LD50 value for in vivo toxicity of selenium at nano form was approximately 4–6 times lower than selenomethylselenocysteine (Se-MetSeCys) and selenomethionine (SeMet) (ZHANG et al., 2005; WANG et al., 2007; ZHANG et al., 2008). The effect of SeMet compared to the same concentration of selenium nanoparticles was indicated in mice that had significantly increased status of liver enzymes including alanine aminotransferase (ALT), aspartate aminotransferase (AST), and lactate dehydrogenase in the blood, over a long time, which shows acute severe liver damage (WANG et al., 2007). Selenium nanoparticles also had much lower acute toxicity in mice (GAO et al., 2000). The LD50 value was about 18-fold compared to selenite (BAI et al., 2017). A similar result demonstrated that the subchronic toxicity of selenite was compared with selenium

nanoparticles and high-selenium protein for 13 weeks in rats. At the dose of three mg/kg selenium, there was no toxic effect and no change due to the administration of nano selenium. The administration of selenite and high-selenium protein resulted in severe growth inhibition, and hepatocyte degradation was observed (JIA et al., 2005). Therefore, a critical issue is what kind of selenium, how much, and how long to apply as a functional additive in food supplements.

### **2.2.1. Selenium supplementation in animals**

Generally, several kinds of selenium supplementation methods have been used, including injection, rumen boluses, selenium fertilization of forage crops, salt-mineral mixes, and selenium fortified feeds (BRUMMER et al., 2014).

Different concentrations of injections containing inorganic selenium are available for different animals. Selenium injection can increase the blood level of selenium for a short time under veterinarian approval. Therefore, they are often used to prevent and treat white muscle disease (BRUMMER et al., 2014). Recently, El-Deep and his colleagues studied 10, 20, and 30  $\mu\text{g}$  injectable biosynthetic selenium nanoparticles for hatching rates, immune responses, and histopathological changes in hatched chicks. Eggs 18 days old were injected once with 0.5 mL of selenium. The selenium nanoparticles-injected groups showed an increase in the hatchability of the entire hatched egg. The groups injected with 10 and 20  $\mu\text{g}$  per egg had lower total lipid and cholesterol content and increased TAC, CAT, GPx, SOD, and globulin compared to the untreated group. High levels of total blood protein and phagocytosis were significantly detected in the groups injected with 10, 20, and 30  $\mu\text{g}$  selenium nanoparticles/eggs. Maximum final body weight and weight gain were observed with 20  $\mu\text{g}$  selenium nanoparticles/eggs (EL-DEEP et al., 2020). Another study reported that selenium as barium selenate (Ballinskelligs Veterinary Products Ltd., 50 mg/mL) was administrated by injection at 1 mL/50kg (1 mg/kg selenium) to pregnant ewes between 70 and 90 days of pregnancy and young lambs between 4 and 7 days of ages. In the treatment of ewes, selenium content in serum and milk was significantly increased, and high concentrations of fat and DM characterized their milk. Milk production and protein and lactose content in the milk were unaffected by selenium supplementation. The selenium supplementation of lambs has high selenium content in serum and humoral and cellular immunity, including lysozyme activity, gamma globulin

contents, ceruloplasmin activity, phagocytic RBA and PKA, and proliferation of mitogen-stimulated lymphocytes (MILEWSKI et al., 2021). Barium selenate for all food-producing species has been authorized by Regulation (EU) No 2015/446, European Medicines Agency, Committee for Medicinal Products for Veterinary Use (EMA/CVMP, 2015).

Intra-ruminal administration as a bolus can release selenium slowly in the gastrointestinal tract. It has the advantage of giving selenium to ruminants in grazing areas where supplementation is not practicable. RASHNOO et al. (2020) reported that selenium supplementation as an intra-lumen bolus in the late pregnancy improved the milk yield of grazing goats and their kid's performance. The boluses containing the daily amount of 0.25 mg selenium were administered for four weeks before kidding time. After supplementation, milk yield, milk fat ratio, daily production of milk ingredients, and selenium concentration in milk were higher in selenium supplemented goats. Their kid's average daily gain and bodyweight at weaning were more significant than the non-supplemented group. In addition, serum selenium, T3 level, and whole blood GPx activity were dramatically higher in goats, and their kids in the selenium supplemented group.

Biofortification or fertilization is the most promising and widely accepted way to increase dietary selenium by enhancing edible parts of food and forage crops. Different types of fortification methods have been summarized by LI et al. (2021), as presented in Figure 4. Selenium fertilization in pastures can increase the presence of animals and humans in the diet, in addition to the productivity benefits of animals. Fertilizations containing inorganic selenium such as selenite and selenate are mainly used to increase their soil content and then enhance selenium concentration in the crop (MARTIN et al., 2006; HALL et al., 2013; WALLACE et al., 2017).

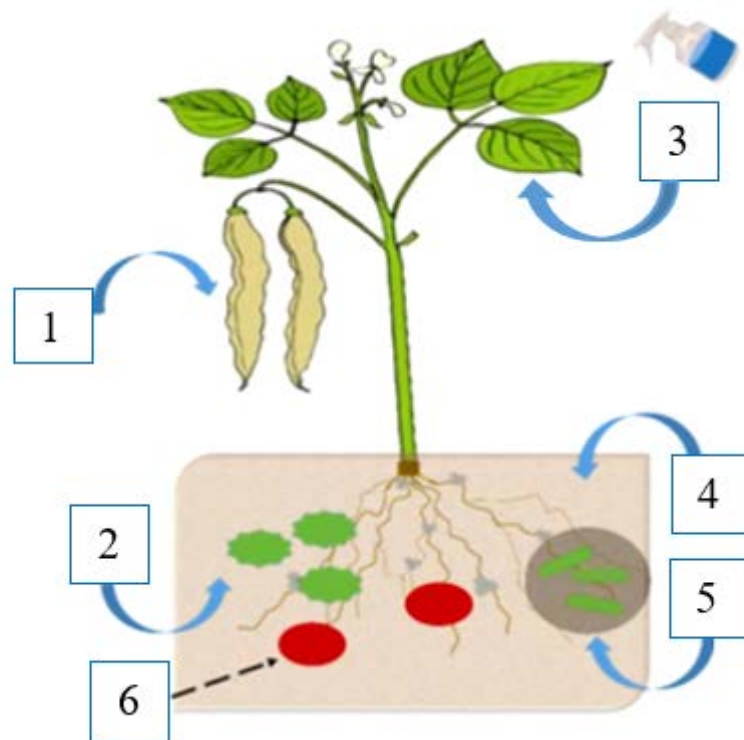


Figure 4: **The fortification methods of selenium in plants (1): conventional plant breeding and genetic engineering, (2): selenium-enriched organic materials as selenium fertilizers, (3): foliar application of selenium fertilizers, (4): soil application of organic selenium fertilizers, (5): microbial assistance, and (6): nano-selenium for biofortification** [Source: (LI et al., 2021)]

For example, the soil or alfalfa field was fortified with selenium as sodium selenate with water and spray, and then the grass was harvested and studied as feed. Feeding with selenium fortified alfalfa hay is increased whole blood selenium levels in weaned beef calves (HALL et al., 2013) and pregnant beef cows and their newborns (WALLACE et al., 2017). Also, colostrum selenium and immunoglobulin G (IgG1) were increased effects of supplementation using selenium fortified alfalfa hay (WALLACE et al., 2017). Recently, the application of selenium nanoparticles has been suggested for selenium fortification, which gradually releases selenium for uptake into plants, resulting in reduced selenium loss compared to rapid leaching of inorganic selenium (EL-RAMADY et al., 2020). Selenium in its nanoform has much less toxic for plants than inorganic forms like selenite and selenate (EL-RAMADY et al., 2020; YUANXIA et al., 2020). They can be rapidly oxidized to selenate and incorporated into plants converted to organic selenium

species such as SeCys, SeMet, MeSeCys in plant roots (WANG et al., 2020). Selenium is not a nutrient mineral for plants and has a chemical resemblance to sulfur. They share the same support membrane and the same biochemical pathway for uptake into plants (LIMA and SCHIAVON, 2021).

Selenium supplementation has been used as a feed or feed additive to provide a more consistent selenium intake for livestock animals. In this case, the most important thing is whether the selenium supplement is organic or inorganic. Organic selenium forms can maintain higher selenium content while minimizing the risk of toxicity to animals. Generally, inorganic and organic forms of selenium, including selenite, selenate, selenomethionine, selenium-enriched algae, selenium-enriched yeast, and selenium nanoparticles can be used as animal supplements. Numerous studies have compared organic and inorganic selenium in feed supplementation. For instance, selenium yeast supplementation was much more effective in increasing selenium content in blood and milk than supplementation with selenate and selenite.

Nevertheless, all selenium supplementation has dramatically increased the activity of glutathione peroxidase (GSH-Px) in the erythrocytes compared to the control group (ORTMAN and PEHRSON, 1999). A similar study reported by Ran and co-workers that both selenium yeast and sodium selenium supplemented group was increased selenium content in blood and milk, the activity of glutathione peroxidase (GPx1) in the erythrocytes and milk percentages of polyunsaturated fatty acids and linoleic acid compared with the group not receiving supplemental selenium. Especially, the selenium yeast supplemented group had significantly higher selenium content in blood and milk than other groups (RAN et al., 2010). Also, selenium supplementation with selenium yeast and selenium nanoparticles on the rumen fermentation and urine purine derivatives in sheep was studied by XUN et al. (2012). In this case, mean pH in the rumen, ammoniacal nitrogen, the molar proportion of propionate, and the ratio of acetate to propionate were significantly lower in sheep who received selenium nanoparticles than the selenium yeast or non-supplemented sheep. The rumen's total volatile fatty acid (VFAs) was higher in the selenium yeast supplemented group. Also, molar proportions of acetate and butyrate were not affected by both selenium supplementation. Another study presented those supplementations with one mg/kg of sodium selenite and one mg/kg of selenium nanoparticles have increased as the indicator of oxidative stress as a thiobarbituric acid reactive substance (TBARS) in blood plasma in sheep. Also, white

blood cells were dramatically increased in the selenium nanoparticles supplemented group, but red blood cells and packed cell volume were not affected by both selenium supplementation (SADEGHIAN et al., 2012). The body weight, selenium content in blood, serum, and tissue, and serum antioxidant parameters are affected by the daily supplementation with 0.3 mg/kg of selenium yeast, sodium selenite, and selenium nanoparticles. Especially, serum GSH-Px, SOD, CAT, and selenium content in blood and serum, and some organs like liver, spleen, and testis were higher in selenium nanoparticle supplemented group than other selenium supplemented groups (SHI et al., 2011). Another study reported that supplemental selenium nanoparticles at 0.3 mg/kg in goats was significantly increased selenium content in testes and activities of GPx and ATPase in the ejaculate (SHI et al., 2010). In addition, selenium supplementation as selenium nanoparticles has improved fetal hair follicles in cashmere goats. 0.5 mg/kg of selenium nanoparticles have dramatically improved the expression of GSH-Px and insulin-like growth factor (IGF-1 and IGF-1R), activities of GSH-Px and SOD, and concentrations of selenium, IGF-1, and total antioxidant capacity in both fetal serum and skin (WU et al., 2011).

As mentioned above, selenium supplementation is used in animal husbandry and veterinary practice based on its therapeutic and prophylactic properties. However, it also aims to increase the selenium content, other functional ingredients, and product quality in animal-derived foods such as meat, eggs, and dairy products. Such foods are potentially a unique source of supplement for human dietary selenium. It is a chain of animal health, animal-derived products, and human health. For example, LING et al. (2017) produced selenium-enriched cheese from selenium supplemented milk of Estonian Red dairy cows. In that case, the selenium supplementation was carried out by adding organic and inorganic selenium to the dairy cows. The feeding process consisted of 2 steps. First, inorganic selenium as sodium selenite (20 mg/kg) feed for 64 days. After that, a complex of organic and inorganic selenium (20 mg/kg Se yeast; 20 mg/kg sodium selenite) with fed for 57 days. After supplementation, in blood and milk, selenium concentrations increased from 186.5 to 287.9  $\mu\text{g}/\text{kg}$  and 17.1 to 51.8  $\mu\text{g}/\text{kg}$ , respectively. The selenium content also increased from 146 to 361  $\mu\text{g}/\text{kg}$  in the final product like cheese. The produced cheese showed high oxidative stability and low linoleic acid (oxylipins).

Milk rich in selenium was made by feeding 1–6 mg selenium-enriched yeast containing SeMet, SeCys (Sel-Plex2300) for eight weeks. After supply, selenium

concentration in cow milk was significantly increased from 18  $\mu\text{g}/\text{kg}$  to 94  $\mu\text{g}/\text{kg}$ . Finally, the authors produced selenium-enriched dairy products such as yogurt (58.5  $\mu\text{g}/\text{kg}$  Se), telemea cheese (138.1  $\mu\text{g}/\text{kg}$  Se), curd cheese (156.5  $\mu\text{g}/\text{kg}$  Se), orda cheese (163.7  $\mu\text{g}/\text{kg}$  Se), and mixed curdling cheese (200  $\mu\text{g}/\text{kg}$  Se). Also, the selenium concentration in whey dramatically enriched from 8.8–9.7  $\mu\text{g}/\text{kg}$  to 20.1–25.8  $\mu\text{g}/\text{kg}$ . The study also reported that selenium levels in milk decreased to baseline levels six weeks after discontinuation of the supplement (CSAPÓ et al., 2015).

Selenium levels in eggs can increase with increasing selenium content in the broiler breeder diet (PAPPAS et al., 2005; SCHEIDELER et al., 2010). Aseel chicken was supplemented by organic selenium as a selenium-enriched yeast and inorganic from a sodium selenite at 0.3 mg/kg for 22–42 days. Selenium-enriched Yeast has shown more effective than sodium selenite on eggs' selenium content and performance. Precisely, the selenium content in whole eggs was measured to be 11.70  $\mu\text{g}$  for organic selenium, 9.13  $\mu\text{g}$  for inorganic selenium, and 7.77  $\mu\text{g}$  for the control group. These differences of selenium content in the yolk and white were the same. Also, the group supplemented with organic selenium has shown early sexual maturity, high body weight, and high egg production and egg mass compared to the inorganic selenium supplemented group or unsupplemented group (ZIA et al., 2016). Similarly, the egg production and mass, vitelline membrane strength of stored egg were improved by selenium supplementation containing sodium selenite and Sel-Plex (selenized yeast containing 63% SeMet, Alltech, Nicholasville, KY, USA) at 0.55 or 0.75 mg/kg for 12 weeks. Also, selenium levels in egg yolk increased with selenium supplementation and were more efficiently deposited when fed with Sel-Plex than sodium selenite (SCHEIDELER et al., 2010). However, another study reported that these types of selenium supplementation (up to 0.8 mg/kg) did not significantly affect the quality of eggshells, such as shell deformation, destructive shell power, shell index, and shell thickness (PAVLOVIĆ et al., 2010).

Selenium levels in serum or blood are among the most critical indicators of the animal's body, and selenium levels in muscle are an essential component of selenium-rich meat. Meat fortification with selenium is also treated with selenium-rich feeds. Increasing dietary selenium intake to livestock is a common strategy for producing selenium-rich meat, as selenium status and selenium deposition are susceptible to dietary selenium levels. For example, selenium content in beef was measured after 105 days of feeding selenium-rich alfalfa, wheat, and corn with 11.9 or 0.62 mg/kg selenium. Steers were

collected from low and high selenium areas of geography (at toxicity levels). The selenium content of the meat was increased by the high selenium area and high selenium supplementation, which was the same in different cuts of meat. These groups also increased liver and kidney selenium levels. Based on these results, the authors suggested that cattle fed a selenium-rich diet accumulated significant amounts of selenium in their meat without showing symptoms of selenium toxicity. They can regulate selenium levels by accumulating in several organs (HINTZE et al., 2002). ŠEVČÍKOVÁ et al. (2016) fortified broiler chicken by ingesting organic selenium such as selenium-enriched yeast and selenium-enriched alga *Chlorella* at 0.3 mg/kg selenium for 42 days. Selenium levels in the parts of chest and thigh muscles, feathers, excrement, and liver were improved in both organic selenium-supplemented groups compared non supplemented groups. At the same time, the selenium-enriched yeast-supplied group showed exceptionally high levels. These selenium supplementations also enhanced the concentration of microelements in muscles and feathers. In addition, organic selenium as Sel-Plex at 0.3 mg/kg is supplied to pigs for 80 to 100 days to produce selenium-rich pork. Finally, the selenium content of pork (*musculus semimembranosus*) was  $1.045 \pm 0.10$  mg/kg for selenium-supplemented pigs and  $0.701 \pm 0.05$  mg/kg for unsupplied pigs (MRÁZOVÁ et al., 2020).

In Europe, EFSA has approved that selenium-enriched yeast (Selemax) is a safe and efficient source of selenium as a feed additive for all animal species (EFSA PANEL ON ADDITIVES AND PRODUCTS OR SUBSTANCES USED IN ANIMAL FEED (FEEDAP), 2012). Selemax1000/2000 containing 1000 or 2000 mg/kg selenium as selenomethionine shall be incorporated into the feed in the form of a premixture with a maximum level of 0.50 mg/kg selenium for all animal species. In addition, sodium selenite is approved as a safe source of selenium for all animal species/categories (EFSA PANEL ON ADDITIVES AND PRODUCTS OR SUBSTANCES USED IN ANIMAL FEED (FEEDAP), 2016). Likewise, selenium sources, including sodium selenite, coated granulated sodium selenite, and zinc-L-selenomethionine for all animal species, have been authorized by Commission Implementing Regulation (EU) 2019/49 until 2029 (EUROPEAN COMMISSION, DIRECTORATE-GENERAL FER HEALTH AND FOOD SAFETY, 2019).

- Sodium selenite (ID:3b801), as a powder with a minimum content of 45% selenium, shall be incorporated into the feed in the form of a premixture with a maximum level of 0.50 mg/kg selenium for all animal species.

- Coated granulated sodium selenite (ID: 3b802), as a granulated film with a content of 1.0%–4,5% selenium, coating, and granulating agents, shall be incorporated into the feed in the form of a premixture with a maximum level of 0.50 mg/kg selenium for all animal species.
- Zinc-L-selenomethionine (ID: 3b818), a solid containing zinc-L-selenomethionine with a selenium content of 1–2 g/kg, shall be incorporated into the feed in the form of a premixture with a maximum level of 0.50 mg/kg selenium for all animal species.

They belong to the additive category "Nutrition Additives," and the functional group, "Compounds of Trace Elements," are approved as feed additives for animal nutrition (REGULATION, №1831/2003) (EC, 2003).

### **2.2.2. The bioavailability of selenium nanoparticles**

Selenium nanoparticles have excellent bioavailability, which is indicated by the improvement in the antioxidant serum status and the selenium concentration in blood and tissue (SHI et al., 2011), improved chemotaxis and respiratory burst activities (KOJOURI et al., 2012), and much lower toxicity compared to other chemical types as indicated by median lethal concentration, acute liver damage, survival time, and short-term toxicity (ZHANG et al., 2008; JIA et al., 2005). Selenium nanoparticles seem to be more effective in inducing selenoproteins such as GPx and TRx than other selenium sources such as selenate, selenite, SeMet, and Se-Met SeCys. Therefore, its potent antioxidant activity appears to effectively prevent oxidative DNA damage (PENG et al., 2007). The primary biological function of selenium nanoparticles has summarized by LIN et al. (2021), which was included chemotherapeutic and protective effects in cell apoptosis and autophagy induction, drug delivery, and chemotherapy (Figure 5).

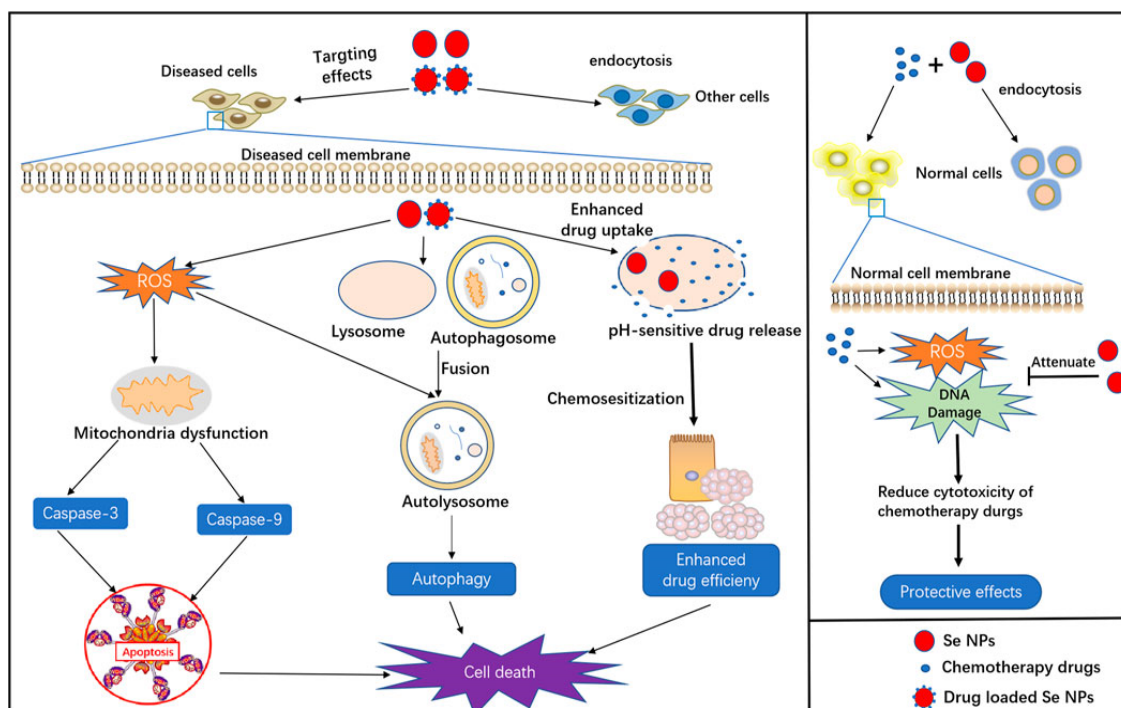


Figure 5: **The biological functions of selenium nanoparticles** [Source: LIN et al., (2021)]

Theoretically, anticancer effect of selenium nanoparticles explains by inducing ROS-mediated cell death when they accumulate in cancer cells, while at low doses, they cause antioxidation and cancer prevention in healthy tissues (ZHUANG et al., 2020). Selenium nanoparticles have also received considerable attention in treating infectious diseases, using the advantages of small dimensions and high surface area to simplify the reaction of biological molecules. The general mechanism of biofilm destruction helps suppress pathogens' growth (VALLET-REGI et al., 2019), and microbial resistance primarily corresponds to the cell wall and membrane. High selenium ion content destroys cell membrane integrity, impairs intracellular homeostasis and microbial dysfunction, and causes microbial cell death (BAPTISTA et al., 2018). As summarized in Table 2, selenium nanoparticles have been shown to have high antioxidant, anticancer, antimicrobial, and immune-stimulatory properties. They also play in the feed digestibility (WENJUAN et al., 2010, 2012; GALBRAITH et al., 2016) and reproductive system (WILDE, 2006; SPEARS and WEISS, 2008; SHI et al., 2010; BADADE and NARSHETTY, 2011; FERNANDES et al., 2012).

Table 2.

**The biological properties of selenium nanoparticles**

<b>Properties</b>	<b>Special action</b>	<b>References</b>
<b>Antioxidant</b>	GPx activity in plasma, liver, and kidney in mice	WANG et al., 2007
	High level of GSH-Px, SOD, and CAT in serum and blood in goat	SHI et al., 2011
	EC50 (effective concentration required to inhibit 50% of free radicals)	GUNTI et al., 2019
<b>Anticancer</b>	Human melanoma cells A375	CHEN et al., 2008
	Human cervical carcinoma cells HeLa	LUO et al., 2012
	Human breast carcinoma cells MDA-MB-231	LUO et al., 2012
	Human breast-cancer cells MCF-7	RAMAMURTHY et al., 2013
	Human liver tumor cell line (HepG2)	XU et al., 2018
<b>Immune-stimulatory</b>	Neutrophil activation	KOJOURI et al., 2012
	T-cell activation	REN et al., 2012
<b>Antibacterial</b>	<i>Escherichia coli</i>	ESTEVAM et al., 2017; SRIVASTAVA and MUKHOPADHYAY, 2015a; GUNTI et al., 2019
	<i>Staphylococcus aureus</i>	SRIVASTAVA and MUKHOPADHYAY, 2015a; MEDINA CRUZ et al., 2018; VYAS and RANA, 2018; GUNTI et al., 2019; ALAM et al., 2019
	<i>Bacillus subtilis</i>	VYAS and RANA, 2018
	<i>Enterococcus faecalis</i>	GUNTI et al., 2019
	<i>Pseudomonas aeruginosa</i>	SRIVASTAVA and MUKHOPADHYAY, 2015a
	<i>Streptococcus pyogenes</i>	SRIVASTAVA and MUKHOPADHYAY, 2015a
	<i>Listeria monocytogenes</i>	GUNTI et al., 2019
	<i>Proteus sp.</i> ,	MENON et al., 2019
	<i>Proteus Vulgaris</i>	MULLA et al., 2020

<b>Antifungal</b>	<i>Aspergillus brasiliensis</i>	KAZEMPOUR et al., 2013; GUNTI et al., 2019
	<i>Aspergillus flavus</i>	GUNTI et al., 2019
	<i>Aspergillus oryzae</i>	GUNTI et al., 2019
	<i>Aspergillus ochraceus</i>	GUNTI et al., 2019
	<i>Aspergillus niger</i>	RAJASREE and GAYATHRI (2015)
	<i>Candida albicans</i>	KAZEMPOUR et al., 2013; RAJASREE and GAYATHRI (2015)
	<i>Fusarium anthophilum</i>	GUNTI et al., 2019
	<i>Saccharomyces cerevisiae</i>	ESTEVAM et al., 2017
	<i>Colletotrichum coccodes</i>	FARDESADEGH et al., 2019
	<i>Rhizopus stolonifer</i>	GUNTI et al., 2019
	<i>Penicillium digitatum</i>	FARDESADEGH et al., 2019
<b>Antiparasitic</b>	<i>Steinernema feltiae</i>	ESTEVAM et al., 2017
	<i>Schistosoma mansoni</i>	DKHIL et al., 2019
<b>Antiviral</b>	Dengue virus	RAMYA et al., 2015
	H1N1 influenza virus	CHANGBING et al., 2020

In addition, it has long been known and one of the confirmed properties that selenium has a protective activity against heavy metal-mediated toxicity and reduces the adverse effects of metals (IKEMOTO et al., 2004; ZWOLAK and ZAPOROWSKA, 2012). Metal-induced toxicity has been linked with oxidative damage in living organisms (COLLÉN et al., 2003). Several studies have reported that the effect of selenium against toxicity induced by chromium, mercury, arsenic, and cadmium (FREITAS et al., 2009; COGUN et al., 2012; TRABELSI et al., 2013; PRASAD and SELVARAJ, 2014; HAO et al., 2017; WANG et al., 2017; ANSAR et al., 2017; VICAS et al., 2021a; 2021b).

The selenium supplementation with a concentration of 0.63 mg/kg was protected unusual alterations in the amount of decreased GSH, mitochondrial membrane potential, and  $\text{Ca}^{2+}$ -ATPase activity of chromium ( $\text{Cr}^{\text{VI}}$ )-mediated injury in the chicken brain (HAO et al., 2017). A similar study also reported that selenium nanoparticles have a protective effect on chromium (VI)-induced thyroid damage in the rats due to correcting the free T3 and T4 levels and GSH, CAT, SOD, and MDA (HASSANIN et al., 2013).

Moreover, selenium can reduce the symptoms of mercury-induced toxicity in cell culture (WANG et al., 2017), fish (COGUN et al., 2012), and adult mice (FREITAS et al., 2009). The antagonistic effect of selenium on mercury-induced toxicity is explained

by the formation of a selenium-mercury complex or antioxidant ability of selenium to prevent oxidative stress or reduce mercury body burden.

The biosynthetic selenium nanoparticles obtained from *Terminalia arjuna* leaves have shown an antigenotoxic effect on arsenic-induced toxicity. They had prevented DNA damage and death of lymphocytes by decreasing As(III)-mediated ROS production (PRASAD and SELVARAJ, 2014).

Recent studies have demonstrated that nano selenium-enriched probiotics (0.4 mg/kg for a month) as functional food can eliminate the toxic effect of cadmium on the liver and kidney. The protective effects of selenium nanoparticles were indicated by the recovery of liver markers (AST, ALT, GGT, total bilirubin), antioxidant enzymes (CAT, GPx) in blood, and morphological changes (VICAS et al., 2021a). For kidney toxicity, selenium nanoparticles supplementation was dramatically decreased the blood marker (creatinine), gene expression of kidneys inflammatory markers such as (TNF- $\alpha$ , IL-6, NF-kB), and morphological changes in a dose-dependent manner (VICAS et al., 2021b).

Another study reported that silver nanoparticles-mediated oxidative stress in the liver is also attenuated by selenium. Selenium supplementation (0.2 mg/kg) was significantly reduced AgNP-induced biochemical alterations, including levels of total antioxidant capacity (TAC), C-reactive protein (CRP), and serum transaminases (AST, ALT) (ANSAR et al., 2017).

Based on these properties, nano selenium consumption is increasing day by day. Due to chemical pollution, there are growing environmental, public health, and food safety concerns. Selenium in its nanoform can be an ideal additive to address these problems jointly. For instance, the selenium nanoparticles-based food package showed higher antioxidant activity than the non-selenium nanoparticle package. This is because it extends the shelf life and reduces food oxidation (VERA et al., 2018). Therefore, studies on antidote substances in the scientific study are increasing. Based on the above information, one of our objectives is to focus on a quick and easy way to determine the detoxification effect of biosynthetic selenium nanoparticles using animal models.

Protozoan cells have been widely used as biological indicators of chemical contamination and toxicity in aquatic environments (MORTUZA et al., 2005), and one of them is *Paramecium caudatum* (*P. caudatum*). Acute toxicity test of *P. caudatum* is susceptible to studying the direct toxicity of chemical compounds (KOMALA, 1995).

They simplify the examination of physiological alterations and effects of water pollutants, including pesticides, metals, mineral oils, and others through controlling their morphology, locomotion, and mortality (VENKATESWARA et al., 2006; HUSSAIN et al., 2008; RAO et al., 2008; AMANCHI and HUSSAIN, 2010; BENBOUZID et al., 2015). The sensitive response of stress due to water pollution (LITTLE and FINGER, 1990) is the movement of the ciliary body, which is mainly controlled by the action potential of the cell membrane (ECKERT and NAITOH, 1972; VAN HOUTEN, 1978). Their backward swimming correlates with membrane depolarization (NAITOH, 1966, BREHM and ECKERT, 1978), and forward swimming correlates with hyperpolarization (ECKERT and NAITOH, 1972). Their behavior is considered the preferred device in ecotoxicology, and these studies are becoming important in evaluating the toxicity in unicellular organisms. On the other hand, their sensory apparatus enables the control of different concentrations of chemical substances and the detection of temperature, light, etc. For instance, *P. caudatum* exposed to more than 100 mg/L of monocrotophos as organophosphate insecticide for 10 minutes was dramatically affected. They showed schematic changes in their shape by forming from irregular blebbing (single and multiple) of the cell membrane to cell death/lysis (VENKATESWARA et al., 2007). In addition, their locomotor behaviors such as backward swimming, forward swimming, and swimming speed are indicators of stress caused by toxicants or poisons. These changes can be easily detected with a microscope.

### **2.3. The application of selenium nanoparticles in nanomaterial**

Several kinds of nanomaterials have been developed with unique properties by developing nanotechnology. The properties of nanomaterials, especially their dimensions, offer a variety of different advantages over the original form of the material, and the versatility that may adjust them to extraordinary claims value them. Their high porosity also increases their use in many industries again. Nanomaterials' vast surface area to volume ratio is advantageous in the biomedical field, allowing cells to bind to the active ingredient. Hence there is the apparent benefit of improving the possibility of successfully fighting various diseases.

Nanofibers are getting a lot of attention due to their unique characteristics including high porosity, large specific surface area, and interconnected pore structures, which have

been successfully manufactured from more than 50 different synthetic and natural polymers using the electrospinning technique (HUANG et al., 2003); Natural polymers including cellulose (KIM et al., 2005), silk fibroin (JEONG et al., 2007; CHUNG et al., 2016), chitosan (OHKAWA et al., 2004; BHATTARAI et al., 2005), gelatin (HUANG et al., 2004), collagen (RHO et al., 2006; TONG et al., 2015) and alginate (BHATTARAI and ZHANG, 2007; SURYADININGRAT et al., 2021), and synthetic polymers, such as poly (L-lactic acid) (PLA) (XINHUA et al., 2002) and poly( $\epsilon$ -caprolactone) (PCL) (KAMARUZAMAN et al., 2017; 2021; DOOSTMOHAMMADI et al., 2021), polyvinyl alcohol (PVA) (AADIL et al., 2018; SADAT-HOSSEINI et al., 2021), poly(vinyl pyrrolidone) (PVP) (IGNATOVA et al., 2007), polyurethane (JOO KIM et al., 2014; KHIL et al., 2003), polyamide (SUPAPHOL et al., 2005), polyvinyl butyral (PVB) (YALCINKAYA et al., 2016; JALIL and ISMAIL, 2019; YALCINKAYA and KOMAREK, 2019; LU et al., 2021), *etc.* Natural polymers are generally biocompatible and elicit an immune response in the body, but most of these require mixing with synthetic polymers or strong and dangerous solvents. Synthetic polymers greatly simplify electrospinning over natural polymers based on a well-defined molecular structure and well-controlled molecular weight.

Electrospinning techniques have been identified and recognized since the 1930s, and this process has received much attention as it has excellent potential to produce nanofibers with exceptional and specific properties, such as higher permeability and surface area with a volume ratio of a smaller diameter. This is a simple process and consists of a positive or negative high voltage power supply, a syringe pump with a capillary or tube to transfer the polymers from the syringe to the needle, and a conductive collector such as aluminum foil or metal screen with any shapes such as flat plate, rotating drum, *etc.* (Figure 6). A high-voltage electric field produces a charged jet from a polymer solution. This jet evaporates during drying to form nanofibers. Simply put, the polymer solution is retained by the surface tension of the needle-tip exposed to the significant difference between the spinneret and the anode surface (collector). The electric area creates an electric charge on the polymer surface, transforming a hanging droplet into a falling jet while it reaches a critical value. The electrical repulsive force overcomes the surface tension. Eventually, an unstable charged jet of polymer solution is pushed out of the tip of the Taylor cone. As a result, an unstable and rapid impact jet is created between the

needle or capillary tip and the collector. The resulting evaporation of the solvent creates the polymer nanofibers on the surface of the collector (DALTON et al., 2007).

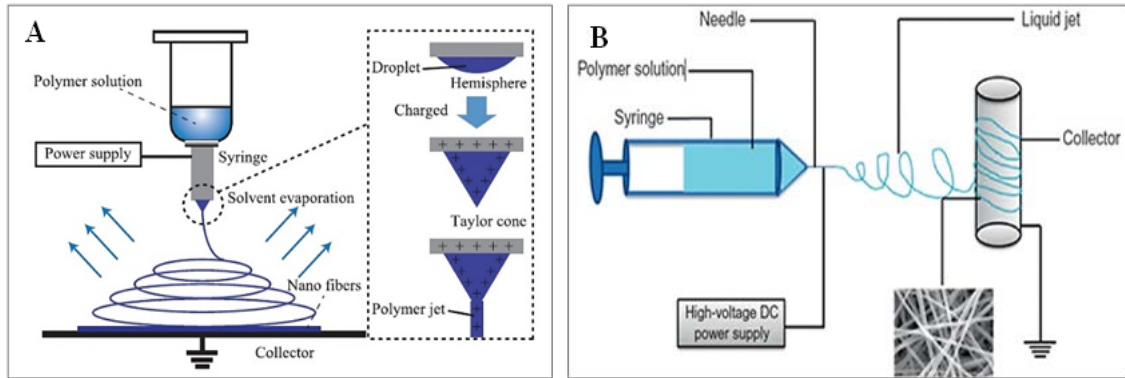


Figure 6: **Working principle of electrospinning setup technique (A) vertical and (B) horizontal setup** [Source: MAEDA et al., 2015; UNNITHAN et al., 2015]

The structural and morphological properties of electrospun nanofibers influence both by process parameters such as voltage, a flow rate, a distance from needle tip to collector, spinning environment, and collector type or movement, and material parameters like polymer and solvent types, viscosities, concentrations, net charge densities, and surface tensions of polymer fluids. For instance, increasing the used voltage increases the polymer flow rate from the needle, resulting in a faster deposition rate. The distance from needle-tip to collector surface affects the deposition time, evaporation speed, and whipping or instability interval. Moreover, flow rate affects jet speed and material transfer speed. The solvent type and vapor pressure determine the evaporation speed and the drying time, and solvent volatility affects the phase separation process. The concentration of the polymer establishes the limits of fiber formation due to fluctuations in viscosity and surface tension.

Generally, electrospinning with beneficial parameters produces fibers with a diameter size of ten nm to several hundred nanometers. It enables the production of ultra-thin fiber mats with exceptional control over their structures and features, creating them an ideal alternative for applications. For instance, there are various applications of nanofibers from medical to consumer products such as drug delivery systems (MATTHEWS et al., 2002; KIM and YOO, 2010; COOPER et al., 2013), wound healing (LEU et al., 2012; RAMYA et al., 2015; KWAN et al., 2016; DOOSTMOHAMMADI et al., 2021), filtration (SUNDARRAJAN et al., 2014; SOLOMIN et al., 2017), nano

composites (KANG et al., 2007; CHUNG et al., 2016), biological functional tissue scaffolds (HUANG et al., 2001; MATTHEWS et al., 2002), protective textiles (MONTAZER et al., 2014; YUAN GAO and CRANSTON, 2008; CHUNG et al., 2016), catalysis (JIA et al., 2002), enzyme immobilization (MENG et al., 2010; DONG et al., 2015; BOAKYE et al., 2015), and sensor (AHMED et al., 2019). Electrospun nanofibers also have been used in agricultural sectors such as veterinary medicine (TONG et al., 2015; KARUPPANNAN et al., 2017; SCHNEIDER et al., 2011; SADAT-HOSSEINI et al., 2021), food industry (PRAKAASH et al., 2021; DUAN et al., 2021; FORGHANI et al., 2021), plant protection (FARIAS et al., 2019; OSANLOO et al., 2020), and water treatment or filtration (JOO KIM et al., 2014; MOHAMMAD et al., 2015; SUNDARAN et al., 2019; LI et al., 2020). For example, nanofibers derived from pullulan/chitin containing curcumin and anthocyanins have shown antioxidant and antibacterial properties in food packaging (DUAN et al., 2021), and cellulose nanofibers were also exhibited antioxidant and antimicrobial activities in food applications (PRAKAASH et al., 2021). In addition, electrospun cellulose diacetate nanofibers with fluopyram as seed coating were shown to have an antifungal effect against the plant pathogen *Alternaria lineariae* (FARIAS et al., 2019).

In livestock, nanofibers containing several bioactive ingredients are used in experimental treatments and organ modeling, including treatment of tendon and bone, activation of progesterone, artificial skin, cartilage, *etc.* However, the application of functional nanofibrous membranes in veterinary medicine and animal husbandry is still inadequate. For example, nanofibrous scaffolds obtained from calcium phosphate nanoparticles and silver-rich poly(lactide-co-glycolide) polymers have shown new bone formation due to the excellent biocompatibility and bone healing of sheep (SCHNEIDER et al., 2011). Electrospun PVA nanofibers contained *Eucalyptus globules* extract also were shown a decreased new angiogenesis, an increased ratio of fibroblasts to fibroblasts, reduced edema, and the low placement of fine collagen fibers during treatment of Achilles tendon injuries compared to the untreated group (SADAT-HOSSEINI et al., 2021). Bovine estrus synchronization was increased by progesterone loaded into electrospun nanofibers. In that case, nanofibers containing 1.2 grams of progesterone released 87.28% progesterone by day 7. This showed a much more robust control of progesterone delivery than high concentrations of progesterone (KARUPPANNAN et al., 2017). Functional 3D models of stromal and epithelial cells for bovine endometrium restoration were obtained

from PGA (polyglycolic acid) nanofiber scaffolds. They showed correct expression of the natural endometrium and cytokeratin and vimentin by the epithelial cells (MACKINTOSH et al., 2015).

Moreover, collagen/chitosan-rich nanofiber scaffolds as a femoral artery model showed increased smooth muscle cells and improved dogs' vascular genes and proteins expression (TONG et al., 2015). Recently, nanofibers for animal nutrition have begun to attract attention. DE OLIVEIRA et al. (2021) suggested that supplying nanofiber in feed can be improved animal performance and productivity. SURYADININGRAT et al. (2021) reported that alginate loaded with PVA nanofibers enhanced hyperglycemia by lowering insulin and glucose-metabolizing enzyme levels in streptozotocin-induced diabetic rats. They have significantly decreased ALT, AST, GGT, TNF- $\alpha$ , and interleukin-1 $\beta$  compared to groups not supplying nutritional nanofibers.

In water treatment, nanofibrous membranes or nanofibers with some bioactive compounds are the essential materials in water treatment or filtration. Nanofibrous membranes can be removed minerals, salts, oils, pathogens (bacteria, viruses, fungus, protozoa, and helminths), and some metals (cadmium, lead, copper, mercury, chromium, arsenic, nickel) from water (HUANG et al., 2014; MOHAMMAD et al., 2015). Their unique properties, such as small pore size with narrow distribution, high porosity, and high specific surface, contribute to the functional activities for water filtration and desalination. For example, Li and co-workers reported that nanofibers with graphene oxide were significantly removed from salt as a membrane distillation (LI et al., 2020). JOO KIM et al. (2014) reported that polyurethane nanofibers with titanium dioxide and fly ash (PU/TiO<sub>2</sub>/FA) show antibacterial effects and adsorption of mercury and lead ions.

Recently, a new challenge is the functionalization of electrospun nanofibers with bio-active ingredients, especially nanoparticles with therapeutic and prophylactic activities. There are generally three methods for producing nanoparticles-loaded nanofiber using electrospinning, and all have their advantages.

- Pre-synthesis method: This involves mixing nanoparticles that have already been synthesized into a polymer solution and using them in an electrospinning process. It has multi-step and time-consuming to prepare a homogeneous polymer. However, it is the most basic and the most common.

- Post-synthesis method: This means including the precursor source in the electrospun nanofibers that form nanoparticles within the nanofibers through a post-electrospinning process.
- In-situ synthesis method. This means that nanoparticles are often converted in a polymer solution prior to electrospinning, or precursors are contained in the polymer, and nanoparticles are synthesized within the nanofibers through an electrospinning process. It is the latest method and has advantages such as simple methodology and scalability.

There are several studies reported on the nanofibers containing silver nanoparticles (JIN et al., 2005; RUJITANAROJ et al., 2008; SAQUING et al., 2009; THOMAS et al., 2015; AADIL et al., 2018; PAN et al., 2019), copper nanoparticles (HASHMI et al., 2019; YALCINKAYA and KOMAREK, 2019), magnetic iron-oxide nanoparticle (BURKE et al., 2017), cerium oxide nanoparticles (RATHER et al., 2018), and selenium nanoparticles (KAMARUZAMAN et al., 2017; 2021; DOOSTMOHAMMADI et al., 2021).

AADIL and co-workers have produced electrospun PVA nanofibers (100–300 nm) enriched with silver nanoparticles (10–50 nm) pre-synthesized by alkali lignin extract. To prepare the mixture polymer solution, the silver nanoparticles were mixed to 10% of PVA with 1% of lignin as a stabilizer under stirring for one hour to give a homogenous solution. After that, the mixture was sonicated for 10 minutes to clean air bubbles. Finally, nanofibers were produced by electrospinning with suitable conditions such as 12 cm of distance from the needle tip to the collector surface, 15 kV of voltage, and 10  $\mu\text{L}/\text{min}$  of flow rate. The produced silver nanoparticles enriched nanofibers were shown antibacterial activity against *B. circulans* and *E. coli* by the diffusion method (AADIL et al., 2018). Another study produced electrospun PVB (polyvinyl butyral) nanofibers that contained silver nanoparticles by the post-synthesis method. PVB polymer solution prepared with silver nitrite as a silver precursor. After forming nanofibers, they were immersed in an ascorbic acid solution to obtain silver nanoparticles. The produced silver nanoparticles rich nanofibers have inhibited the growth of *E. coli* after 4 hours of contact (YALCINKAYA et al., 2016). The mechanism can explain that after silver ions are released from the membrane, they are adsorbed on the cell wall, killing bacteria and reducing the biofouling of attached microorganisms (PAN et al., 2019).

Polyacrylonitrile (PAN) nanofibers with copper nanoparticles (less than 50 nm) were obtained from Sigma-Aldrich, which was produced by HASHMI et al. (2019). In a typical procedure, 8% of PAN dissolved in N,N-Dimethylformamide with stirring for 12 hours at room temperature. Subsequently, copper nanoparticles were added and stirred for 4 hours to make a homogenous solution. Eventually, they formed PAN/CuO nanofibers in the diameter ranges from 161 to 197 nm via the electrospinning process under the conditions of a needle-to-collector distance of 14 cm, a voltage of 13 kV, and a flow rate of 0.5 mL/h. PAN/CuO nanofibers have suppressed the growth of *B. subtilis* and *E. coli*. They also showed suitable properties for use with masks.

Poly (ethylene oxide) (PEO) nanofibers containing in-situ synthesized magnetic iron-oxide nanoparticles are produced by BURKE et al. (2017). Briefly, a polymer solution was mixed with sodium borohydride solution for 5 minutes. Then, ferric/ferrous chloride solution ( $\text{FeCl}_3/\text{FeCl}_2$ ) was added to them, and the mixture was ensured to proceed at ambient temperature for 20 minutes with continuous stirring. After the reaction time, a color change is observed, indicating nanoparticles' formation in a polymer solution. Subsequently, they loaded in the electrospinning process with 17 cm for the distance from the needle to the collector surface, 15 kV for power supply, and 0.5 mL/h for flow rate. Also, PCL-gelatin nanofibers loaded with cerium oxide nanoparticles have shown a SOD mimetic activity, cleaned ROS, and subsequently improved the vitality and proliferation of cells by 3-folds as it reduced the oxidation in the application of wound healing (RATHER et al., 2018).

Selenium nanoparticles are a good candidate for developing functional properties of nanomaterials based on previously mentioned activities such as detoxifying ROS, maintaining redox homeostasis, etc. It is reported that silk scaffolds enriched with selenium nanoparticles drastically inhibit bacterial growth. Otherwise, it significantly improved the metabolic activity of human skin fibroblasts for a short time while lowering the ATP content of *S. aureus* (CHUNG et al., 2016). Kamaruzaman and colleagues reported that nanofibers with a uniform diameter were fabricated from PCL polymer infused with selenium nanoparticles (KAMARUZAMAN et al., 2017; 2021). The 4% PCL polymer was dissolved in a mixture of dimethylformamide and tetrahydrofuran and stirred at 100 rpm overnight during the manufacturing process. Then, the pre-synthesized selenium nanoparticles at 0.2–1.0% (w/v) were added to the polymer and were treated by ultrasonication for one hour. The electrospinning process at 15 cm of distance from needle

and collector, 20 kV of voltage, 3.0 mL/h of flow rate, and at room temperature was performed to form nanofibers. These authors mentioned that the bead formation increases with the increase of selenium nanoparticle's concentration from 0.2% to 1.0% (w/v) (KAMARUZAMAN et al., 2017). They were also reported that the presence of selenium nanoparticles improved the degradation behavior and shortened the degradation time to break, starting after six months of degradation (KAMARUZAMAN et al., 2021). The latest study presented the healing effect of PCL/gelatin nanofibers containing pre-synthesized selenium nanoparticles with vitamin E. This nanofibrous membrane has assisted the proliferation and attachment of dermal fibroblast cells by decreasing edema, inflammation, and oxidation at the injury site. During the treatment, both selenium nanoparticles and vitamin E were released for more than four days (DOOSTMOHAMMADI et al., 2021).

### 3. MATERIALS AND METHODS

#### 3.1. Production of selenium nanoparticles

Chemical reagents like sodium selenite ( $\text{Na}_2\text{SeO}_3$ ), sodium hydrogen selenite ( $\text{NaHSeO}_3$ ), ascorbic acid ( $\text{C}_6\text{H}_8\text{O}_6$ ), and hydrochloric acid (HCl) were obtained from VWR International Ltd. (Lutterworth, Leics, United Kingdom). MRS broth was purchased from VWR International Ltd. (Lutterworth, Leics, United Kingdom).

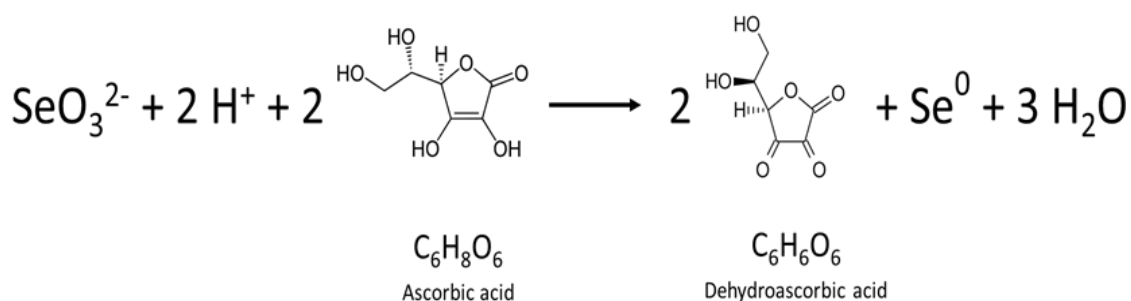
##### 3.1.1. Biological method

Selenium nanoparticles were synthesized by *Lactobacillus acidophilus* (LA-5) according to Prokisch and Zommara (2011). In the procedure, 10000 mg/L of sodium selenite ( $\text{NaHSeO}_3$ ) as an initial solution and 1000 mL of sterilized MRS broth as a culture medium (DE MAN, ROGOSA, SHAPE, 1960) were prepared at the same time by the method. After cooling the medium to 25 °C, 20 mL of selenium solution was mixed with 980 mL of MRS broth, which means around 200 mg/L selenium. Subsequently, ten mL of activated bacterial culture was mixed with them, and the mix solution was placed into the incubator with a shaker at 37 °C for 36–48 hours in aerobic condition. The color of the medium turns red at the end of time due to the synthesized element selenium.

In the purification of the synthesized selenium nanoparticles, the supernatants were separated by centrifugation at 6,000 rpm for 10–15 minutes, and the pellets were rinsed with distilled water repeatedly. The selenium nanoparticles were synthesized mainly intracellular in lactic acid bacteria. Thus, 100 mL of purified selenium nanoparticles were mixed with 150 mL of 37% hydrochloric acid to lysis bacterial cell wall (PROKISCH and ZOMMARA 2011; ESZENYI et al., 2011). After hydrolysis, the mixture was centrifugated at 6,000 rpm for 10–15 minutes and rinsed with pure water until pH returned to neutral. Finally, the solution was ultrasonicated for 10–15 minutes to rupture the cohesive selenium spheres and filtered through a vacuum filter with one plastic filter layer and two paper layers to remove the remaining bacterial cell wall.

### 3.1.2. Chemical method

Selenium nanoparticles are synthesized by a modified chemical method using a reductant agent. In a typical procedure, sodium selenite as selenium precursor was dissolved in distilled water by various concentrations like 25 mg/L, 50 mg/L, 100 mg/L, 150 mg/L, 200 mg/L, 250 mg/L, and 500 mg/L. Ascorbic acid as a reductant agent was dissolved in the same solvent by 1 g/L, 5 g/L, and 10 g/L concentrations before two hours of the experiment. Each concentration of stock solutions is mixed in equal proportions at ambient temperature for one hour. The process of reducing selenite to elemental form ( $\text{Se}^0$ ) follows the following formula:



### 3.1.3. Characterization

#### 3.1.3.1. UV/Vis spectrophotometry

The absorbance of the sample is determined by UV/Vis spectrophotometry (PerkinElmer Lambda2S) using a quartz cuvette (1 cm) at the ambient temperature. Pure water was applied as a control. In this method, the turbidimetry signal was measured because the signal is derived from the light scattering of solid particles rather than light absorption. Early solutions (sodium selenite and ascorbic acid) are not absorbed in 400 nm, but the nanoparticles formed can scatter light and reduce intensity.

#### 3.1.3.2. Dynamic light scattering analysis

The particle size distribution of the generated selenium nanoform was measured by dynamic light scattering techniques (Malvern Mastersizer 2000 particle size analyzer). This analyzer operates in conjunction with an optical bench to detect the actual scattering

pattern from the particle field. The selenium nanoparticle's samples prepared at the varying rotation speeds were reported in the ranges from 0.01  $\mu\text{m}$  to 1000  $\mu\text{m}$ , under the following conditions: 1.33 for water refractive index, 1.590 for particle refractive index 0.01 for particle absorption coefficient, and room temperature. Furthermore, it calculates the particle size distribution from the light scattering data.

#### 3.1.3.3. X-ray diffraction analysis

The examination of phase composition and structure of selenium samples were performed by X-ray powder diffractometer (XRD), operating on a SuperNova X-ray diffractometer (Rigaku Corporation, Tokyo, Japan) with Cu K $\alpha$  source ( $\lambda = 0.15406$  nm). Crystallographic identification was achieved by comparing the experimental patterns (XRD) with the patterns in the Joint Committee on Powder Diffraction Standards (JCPDS) database.

#### 3.1.3.4. Scanning electron microscopy and energy-dispersive X-ray spectroscopy

The morphology, distribution of selenium nanoparticles, and thickness and surface of coated PVC and silicone tubes were analysed by scanning electron microscopy (SEM) using the Hitachi S-4300 model (Hitachi High Technologies, Schaumburg, IL, USA). Before inspecting the sample by SEM, they were coated with a gold layer. Examination of elemental components of the samples was performed by Energy-dispersive X-ray spectroscopy (EDS). This instrument was managed based on the SEM technique, and an acceleration voltage of 20 kV was used to determine. For sample preparation, small pieces of tubes coated with selenium nanoparticles were washed with absolute ethanol and distilled water repeatedly to remove uncoated particles and other contamination. Finally, samples were dried at room temperature.

#### 3.1.3.5. Atomic fluorescence spectrometry

Selenium concentration was measured using Millennium Excalibur (PSA, England) atomic fluorescence spectrometry (AFS) according to methods published and validated

by instrument manufacturers (PS ANALYTICAL, 1999). For the hydride formation reaction, two solutions were used at a flow rate of 1.5 mL/min to generate the selenium hydride. The first is 3M hydrochloric acid (HCL), and the second is 1.4% (w/v) sodium borohydride (NaBH<sub>4</sub>) dissolved in 0.1M sodium hydroxide (NaOH). The formed hydrogen selenide (H<sub>2</sub>Se) gas was purged with 15 liters/min of argon in a double-membrane separator unit called PermaPure. By burning the diffused gas and illuminating it with monochromatic light from a hollow cathode lamp, the selenium in the flame is excited and emits fluorescent light perpendicularly to the plane of the incident light. During the measurement, a 30-second sample aspiration was followed by a 30-second background wash. Each measurement was repeated three times, using the Charlau selenite standard for calibration. For sample preparation, 1 mL of selenium sample was mixed with 5 mL of nitric acid (HNO<sub>3</sub> 65% w/w) at 60 °C for 60 minutes. After that, 3 mL of hydrogen peroxide (H<sub>2</sub>O<sub>2</sub> 30% w/w) was added for further destruction for 4 hours at 120 °C. The samples were then diluted to 15 mL with 3M hydrochloric acid and filtered through filter paper.

### **3.2. Determination of antidote effect of selenium nanoparticle**

The starter culture of *P. caudatum* was obtained from a fish laboratory (Faculty of Agricultural and Food Sciences and Environmental Management, University of Debrecen). Paramecia were multiplied in tap water added with probiotic yogurt powder (1 g/L) at room temperature for two weeks. Yogurt powder was produced by a starter culture (Lyofast Y 250), including *Streptococcus thermophilus* and *Lactobacillus delbrueckii ssp. bulgaricus* was obtained from SACCO Srl (Italy).

The biological synthesized red nano selenium, which contained 800 mg/L selenium in the 250 nm size, was used in this experiment. The production processes of selenium nanoparticles are presented in 3.1.1.

Silver nanoparticles (AgNPs) with a size of 10–20 nm and 20 mg/L of silver were obtained from Dr. Juice Pharma Kft. (Miskolc, Hungary). Silver nitrate (AgNO<sub>3</sub>) was purchased from Reanal Laborvegyszer Kft. (Budapest, Hungary). Sodium hydrogen selenite (NaHSeO<sub>3</sub>) was purchased from VWR International Ltd. (Lutterworth, Leics, United Kingdom), and sodium selenate decahydrate (Na<sub>2</sub>SeO<sub>4</sub> x 10H<sub>2</sub>O) were purchased from Scharlau Chemie S.A. (Barcelona, Spain).

### **3.2.1. Determination of the toxic level**

Initial solutions of 20 mg/L of silver compounds and 80.0 mg/L of bulk selenium compounds were made and then diluted in serial dilutions (up to  $10^{-10}$ ). The exact amount of *Paramecia*'s culture (20  $\mu$ L) with toxic solutions (20  $\mu$ L) was mixed on the microscope slides while monitoring by microscope in control groups. An optical microscope attached to a CCD camera monitors their locomotion, morphology, and mortality. LC95 values for all toxicants were determined, considering the lethal concentration. For liquids, LC50 or LC95 is used instead of LD50 or LD95. Calculate the LC50 concentration value by applying the effects of survival time and concentration. The LC50 value is the concentration when the survival time is 12.5 minutes. The NOEL (No Observed Aid) concentration was defined as when survival was greater than 20 minutes.

### **3.2.2. Determination of antidote effect of selenium nanoparticles**

*P. caudatum* has been supplemented with selenium nanoparticles. In a typical process, 500  $\mu$ L of culture was mixed with the same amount of selenium nanoparticles and kept at room temperature for around 2 hours in experimental groups. After supplementation, 20  $\mu$ L of the supplemented culture was dropped in the center of a glass slide, and 20  $\mu$ L of toxicants was added to them while monitoring under a microscope. At the same time, the survival time, locomotor behavior, and morphological changes of *P. caudatum* are continuously monitored by the camera. Survival vs. concentration has a unique shape that resembles a pH titration curve. The turning point gives the LC50 value. An optical microscope attached to a CCD camera and an SEM with X-ray diffraction analysis indicated the accumulation of the selenium nanoparticles in the cell.

### **3.3. Production of selenium nanoparticles enriched nanofibers**

Polyvinyl butyral (PVB, Mowital LPB 16H, molar mass 16 kDa) in powder was obtained from KURARAY EUROPE GmbH D-65926 (Frankfurt am Main, Germany). Pure ethanol (ethyl alcohol) was obtained from Nógrádi Vegyipari Zrt (Tolmács, Hungary).

### 3.3.1. Preparation of polymer solution

Various concentrations (from 6% to 15%) of polyvinyl butyral (PVB) polymer was dissolved in 96% of ethanol with constant stirring (Heidolph RZR 252) at room temperature until the solution became clear. Then, the solution was kept unstirred for one day.

### 3.3.2. Enrichment of polymer solution with selenium nanoparticles

PVB polymer solution was enriched with red and grey nanopowder and in-situ synthesized selenium nanoparticles. 1%, 3%, 5%, and 10% (w/v) red and grey selenium nanopowder were suspended in PVB polymer and sonicated for 30 minutes to obtain a homogeneous solution (Figure 7A, B). The third polymer solution was prepared by the in-situ synthesis method. In the conversion procedure, sodium selenite as a precursor and the ascorbic acid as a reducing agent were separately dissolved in 80% ethanol with 20% water, followed by a 10% PVB polymer. After dissolving, these solutions were mixed at room temperature in equal proportions, and the mixture was retained for about one hour until red (Figure 7C).

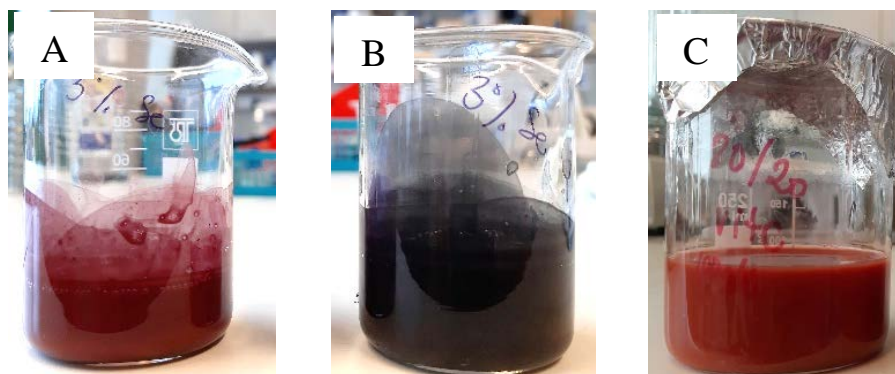


Figure 7: PVB polymer solution suspended with red-SeNPs (A), grey-SeNPs (B), and in-situ synthesized SeNPs (C)

### 3.3.3. Electrospinning

Selenium nanoparticles enriched nanofibers at various concentrations were produced by horizontal electrospinning setup with the following conditions, as presented in Figure

8. The polymer solution was placed in the syringe of 50 mL and injected at a flow rate of 10 mL h<sup>-1</sup> through a stainless-steel blunt needle. The nanofibers were collected in a stainless-steel, flat plate collector located 25 cm from the needle-tip under a voltage of 40 kV (NT-45/P, RWT Vasúttechnikai Kft) at the humidity (RH) 34% and temperature at 24 °C.

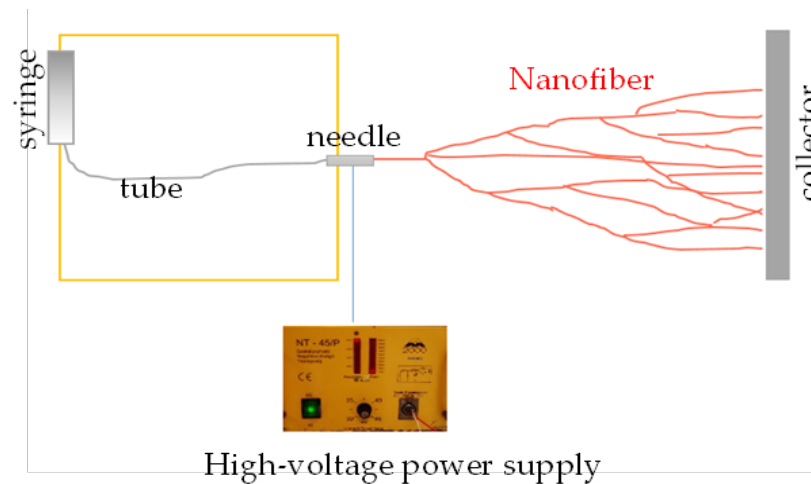


Figure 8: A schematic process of electrospinning

### 3.3.4. Characterization

The morphology, microstructure, surface, and chemical composition of nanofibers were analyzed by scanning electron microscopy (SEM) using a Hitachi S-4300 within Energy-dispersive X-ray spectroscopy (EDS) and simple light microscope (Visiscope® 260, VWR). The nanofibrous sheet was coated with a gold layer for viewing electron microscope. The samples were harvested on a stainless-steel collector covered with textiles and glass slides for characterization.

The fiber lengths are calculated according to the following equation:

$$l = \frac{4V}{d^2\pi}$$

Where “l” is the fiber length in meters, “V” is the volume in m<sup>3</sup>, “d” is the diameter in meters.

## 4. RESULTS AND DISCUSSION

### 4.1. Production of selenium nanoparticles

The reaction of selenium ions with ascorbic acid occurred, and the mixture solution was showed a time- and concentration-dependent color change, which was evident to the eye. The color changes from white to orange to red indicated the reduction reaction to nano form of selenium.

In our results, there was no reaction between 1 g/L of ascorbic acids and all concentrations of sodium selenite, and no color change was observed for more than 1 hour. In 5 g/L of ascorbic acid, moderate selenite reduction was observed but insufficient. The reaction between 10 g/L of ascorbic acids and 500 mg/L of selenite was significantly better than other concentrations, indicating color changes from clear white to deep red. The red color was obtained from 6 minutes of the reaction time. The color changes of the reaction between the concentrations of selenium and ascorbic acid are shown in Figure 9. The color changes of the reaction from yellow to deep red are associated with the increase in particle size (LIN and CHRIS WANG, 2005), and red color indicates amorphous selenium nanoparticles in shape (HAGEMAN et al., 2017).

The color changes demonstrate the reaction rate correlated with hydrogen ion concentration (pH). Figure 10 shows that the pH of the reaction is represented by the relationship between the concentrations of ascorbic acid and sodium selenite. The reduction process is faster in acidic environments with high ascorbic acids concentrations (pH <7.0). Similar to our finding, GANGADOO et al. (2017) reported that a high concentration of ascorbic acids in 100 mM with selenous acid produced selenium nanoparticles smaller than 70 nm and red color. ANGAMUTHU et al. (2019) synthesized amorphous selenium nanoparticles in shape from the reaction of selenium source as sodium selenite (100 mM) and reducing agent as ascorbic acid (50 mM) in various ratios while magnetically stirring at room temperature for 30 minutes. Similarly, MALHOTRA et al. (2014) also produced selenium nanoparticles of about 20–30 nm by mixing sodium selenite and ascorbic acid in 1:3 and 1:4 under stirring at 1000 rpm for 30 minutes.

The concentration of precursors and reducing agents and their ratio, environmental conditions, and the biocompatibility of reducing agents play a principal role in the chemical synthesis/reduction of nanoparticles.

500 mg/L selenite with 1 g/L ascorbic acids



500 mg/L selenite with 5 g/L ascorbic acids



500 mg/L selenite with 10 g/L ascorbic acids



250 mg/L selenite with 10 g/L ascorbic acid



Figure 9: **Color changes of reaction between sodium selenite and ascorbic acid by reaction time**

Ascorbic acid (vitamin C) is a natural antioxidant involved in biochemical processes. It is a commonly proposed reducing agent because of its bioavailability. It is less toxic in animals and humans than other reducing agents (SUN et al., 2009). According to these properties, ascorbic acid has been used to synthesize gold nanoparticles, silver nanoparticles, and selenium nanoparticles (SUN et al., 2009; QIN et al., 2010; VAHDATI

and TOHIDI MOGHADAM, 2020; SHAHABADI et al., 2021). Ascorbic acid contains several hydroxyl groups that are highly reducible and can reduce the tetravalent selenium ions to elemental form. In addition, ascorbic acid, together with other reducing agents, has successfully synthesized selenium nanoparticles. For instance, the mixed reaction of 1 mL plant polysaccharide (Wakame), 8 mL of ascorbic acids, and 1 mL of sodium selenite, and the mix reaction of 0.1% polyvinyl alcohol or 1% chitosan solutions, 50 mM ascorbic acid with 50 mM sodium selenite were used for the production of selenium nanoparticles (CHEN et al., 2008; BOROUMAND et al., 2019). Notably, the selenium nanoparticles converted by ascorbic acid were showed dose-dependent antibacterial and anticancer activities against some pathogenic bacteria such as *Staphylococcus aureus*, *Escherichia coli*, *Pseudomonas aeruginosa*, *Staphylococcus epidermidis*, and human cancer cell lines such as nasopharyngeal carcinoma-CNE2, breast cancer-MCF-7, melanoma-A375, and liver cancer-HepG2 (ANGAMUTHU et al., 2019; BOROUMAND et al., 2019; CHEN et al., 2008).

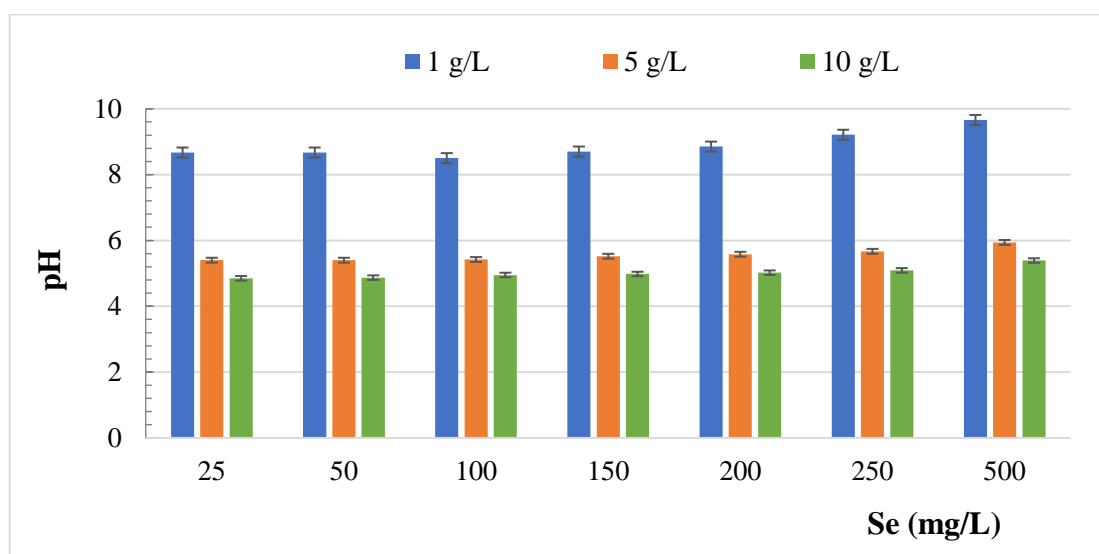


Figure 10: The reaction pH by different concentrations of selenite and ascorbic acid

Light scattering techniques can observe the formation of nanoparticles of various sizes in a liquid. As shown in Figure 11, the most specific experimental feature of nanoparticles is the change in color at various sizes. This is because this color is often different for transparent and reflected light. Thus, the color of the particles that form changes with the size, which are scattered and absorbed in the visible range of the

spectrum. Therefore, light scattering is the most fundamental method for identifying and characterizing nanoparticles.



Figure 11: **The light reflection of selenium nanoparticles in transparent and reflected light**

The reduction process was measured by UV-visible spectrophotometry, one of the widely used methods for the structural determination of nanoparticles. UV/Vis spectrum discovers the “absorption maximum” of nanoparticles depending on the concentration of the reagents like precursor sources, reducing agents, or other reaction ingredients—the absorption changes over time, showing the reaction rate and particles' formation.

Figure 12 illustrates the UV-vis absorption spectra at 400 nm, originating from the reaction between selenium precursor and reducing agent with various concentrations. The concentrations of ascorbic acid in 1 g/L and 5 g/L were not suitable for the reduction reaction with concentrations of selenite from 25 mg/L to 500 mg/L (Figure 12A, B). These results confirm the color changes of the reaction. Incredibly, there was no reaction between 1 g/L of ascorbic acids with all concentrations of sodium selenite. The reaction rate between 10 g/L of ascorbic acids with concentrations of sodium selenite in 25 mg/L to 500 mg/L was significantly greater than 1 g/L and 5 g/L of ascorbic acids. For concentrations of selenium precursor, the reaction rate of 500 mg/L of sodium selenite was dramatically increased until 30 minutes of the reaction time, as exhibited in Figure 12C. These data indicated that the reaction of 500 mg/L of sodium selenite and 10 g/L of ascorbic acids are suitable for forming nano selenium. This ratio may be the least

appropriate option for synthesizing selenium nanoparticles in an aqueous form without any stabilizer. Other studies reported that various concentrations of selenium source as selenite with lactose (CAVALU et al., 2018), cysteine (LI et al., 2010), and ascorbic acid (MALHOTRA et al., 2014; ANGAMUTHU et al., 2019) as reducing agents in various ratios had been used in the formation of selenium nanoparticles.

The absorbance at 400 nm was an excellent point for measuring the selenium nanoparticles. In similar studies, the absorption spectrum of the chemical reduction method synthesized selenium nanoparticles was detected between 265 nm and 580 nm. For example, ascorbic acid-induced nanoparticles were showed firm absorption peaks at 265 nm (VAHDATI and TOHIDI MOGHADAM, 2020), 310 nm (BOROUMAND et al., 2019), 370 nm (ANGAMUTHU et al., 2019), and 390 nm (MALHOTRA et al., 2014). In addition, closely absorption peaks are detected at 400 nm, 410 nm, and 420 nm in the biological synthesis using garlic extract (VYAS and RANA, 2018), *Pseudomonas aeruginosa* (KORA and RASTOGI, 2016), and plant leaf extract (SOWNDARYA et al., 2017), respectively. Several studies have confirmed that resonance peaks in nanoparticles become visible around this area. However, the exact point depends on various factors, like morphology, particle size, material ingredients, and local environmental conditions (JOSHI et al., 2008).

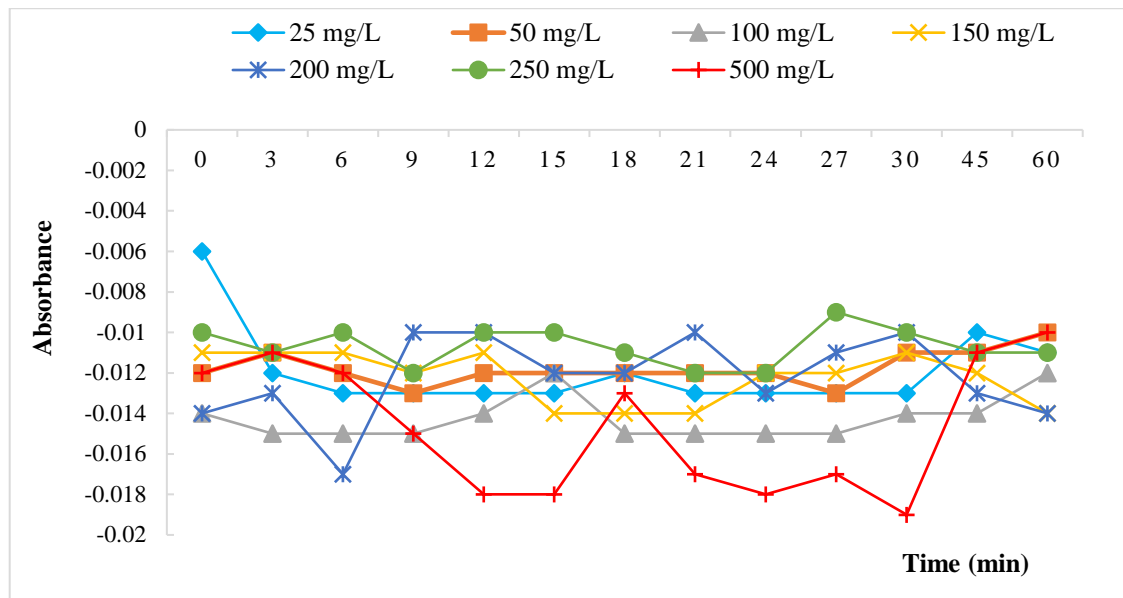


Figure 12A: Reaction rate of selenite with ascorbic acid (1 g/L) for the formation of SeNPs

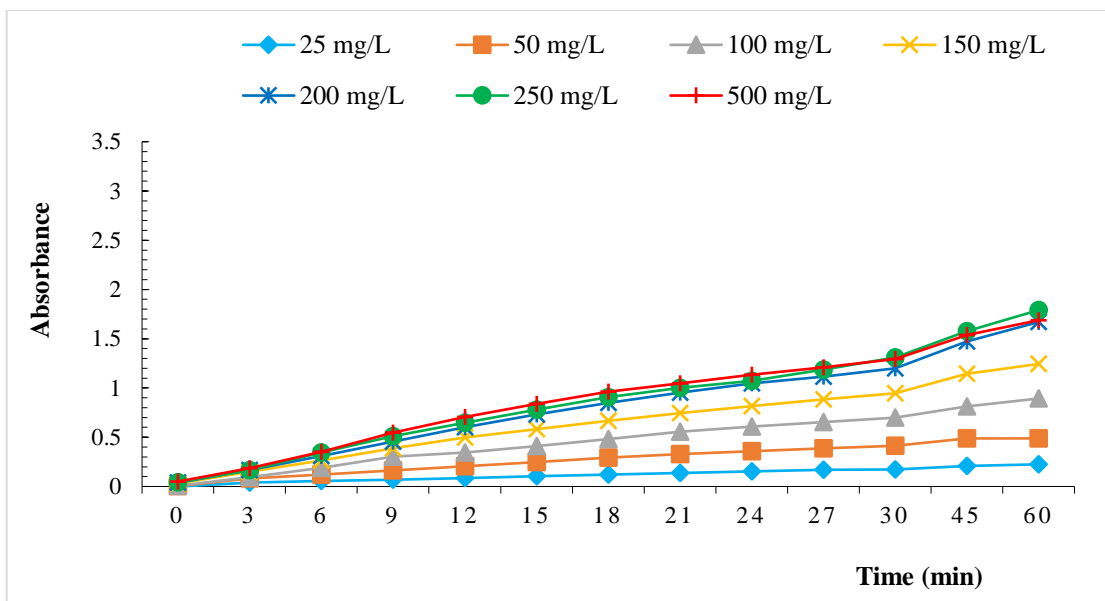


Figure 12B: **Reaction rate of selenite with ascorbic acid (5 g/L) for the formation of SeNPs**

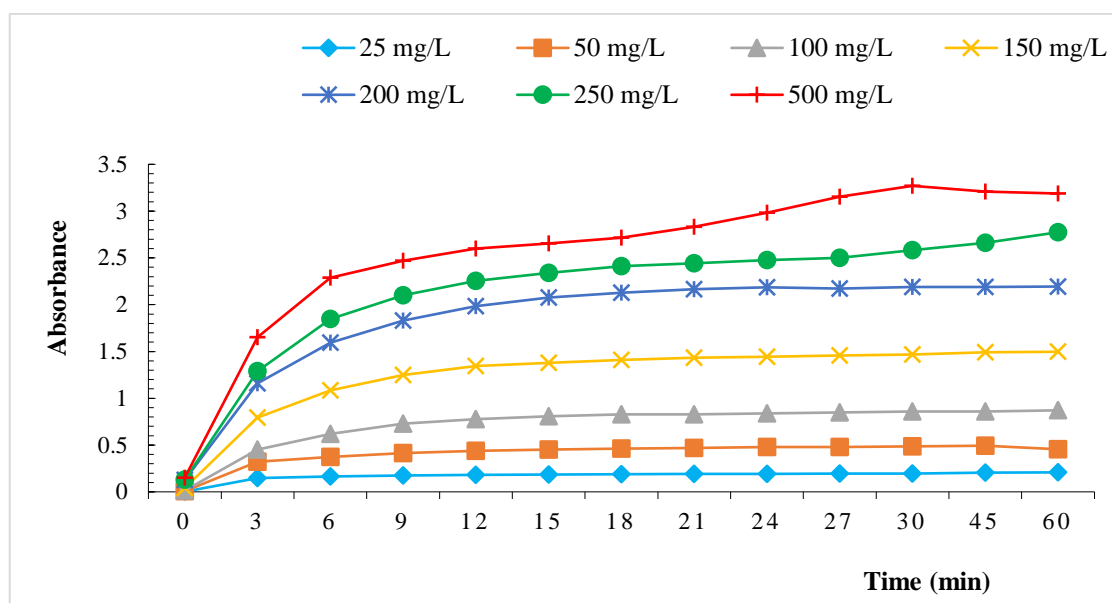


Figure 12C: **Reaction rate of selenite with ascorbic acid (10 g/L) for the formation of SeNPs**

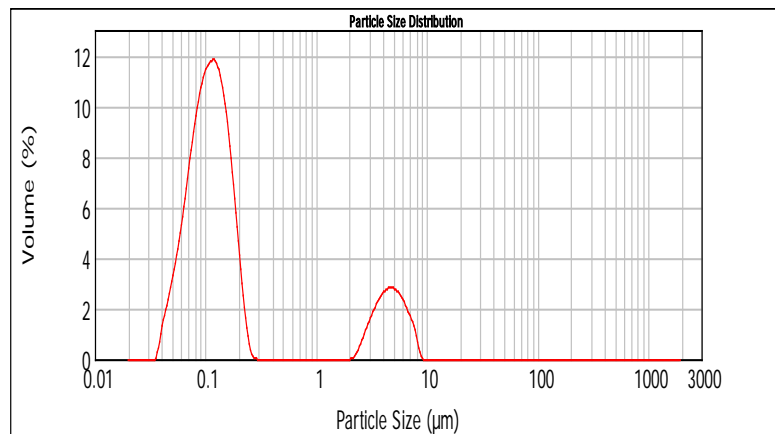
The dynamic light scattering (DLS) technique confirmed the formation of selenium nanoparticles. DLS is most commonly used in the analysis of nanoparticles, and particle size is measured by determining random changes in the intensity of light scattered from the solution. The size distribution curve of selenium nanoparticles obtained from the reaction of 500 mg/L selenite and 10 g/L of ascorbic acids is measured. The synthesized

nanoparticles with a size range from 100 nm to 100  $\mu\text{m}$  are detected. These results are consistent with other studies in the literature showing that ascorbic acid as a reducing agent is a powerful auxiliary tool for the complete conversion of selenium precursor molecules to their nanoscales. As determined by particle size analysis, nanoparticles can aggregate in higher concentrations in liquid form. Over time, the aggregate size increased and finally reached a size of 100  $\mu\text{m}$ . The different measurements for the aggregation were carried out by 10, 20, and 30 minutes of reaction time, as displayed in Figure 13.

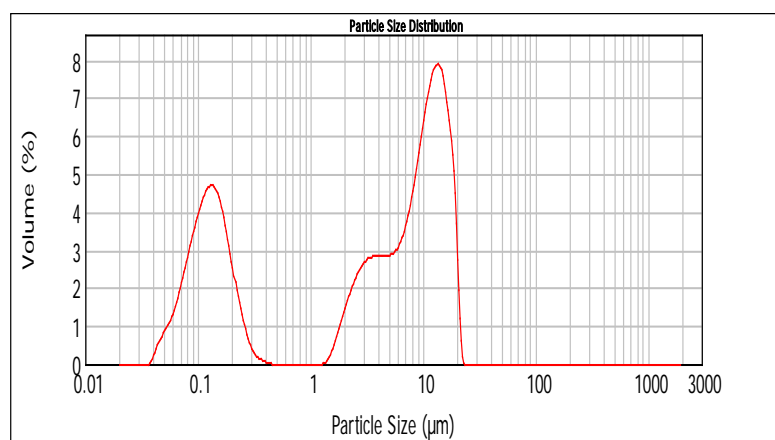
Theoretically, the conversion of metal nanoparticles with different morphology and dimensions occurs by reducing metal ions to neutral atoms by adding reductants. The nucleation atoms can form small clusters, so-called “seeds,” with a stable structure and defined crystallinity (REGAN et al., 2012; XIONG and XIA, 2007). Subsequently, the “seeds” to create nanoparticles of different morphology and structures (XIONG and XIA, 2007). When agglomeration occurs, the surface energy of the metal also increases, and the tiny particles easily interact with each other to create a bigger particle size. This finding was observed in the biological synthesis of nano selenium. For instance, in the transformation of selenium nanoparticles by the bacterial strain of *B. mycoides*, the particle size in the range of 5–100 nm to 50–400 nm increased after 6 hours and 48 hours of fermentation time (LAMPIS et al., 2014). Similarly, the size of the nanoparticles mediated by plant extract (*Azadirachta indica*) is grown from 153 nm to 287 nm after a reaction time of 5 and 10 minutes (MULLA et al., 2020).

The size of one atom of selenium is tiny, but the surface-free energy is tremendous. The agglomeration of selenium atoms reduces the surface-free energy and forms more stable particles, and stabilizer agents can be used. The capping agent or stabilizer protects other agglomeration by forming an electric double layer around the nanoparticles resulting from the adsorption of ions to the surface of the nanoparticles.

10 minutes



20 minutes



30 minutes

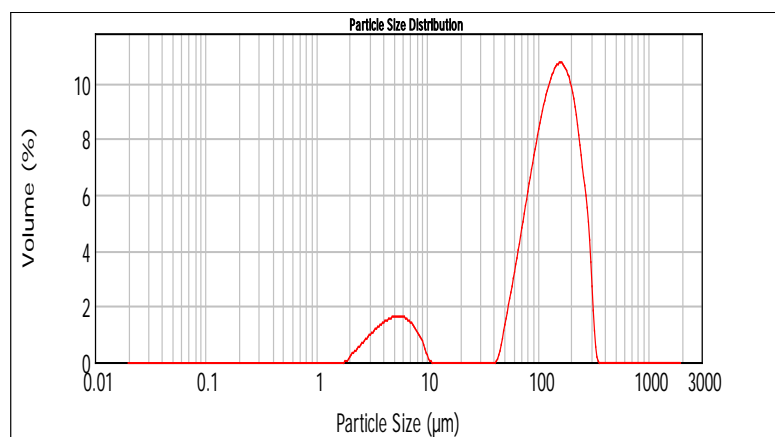


Figure 13: The particle size distribution of SeNPs by reaction time

#### 4.2. Coating of selenium nanoparticles

We observed that selenium nanoparticles adhere to the surface of plastic, iron, and polymer during our experiments. After a while, the polypropylene tube and the

transparent polymer tube (the tube that connects the sample container and the device) turned red. Therefore, we decided to create a nano selenium layer on silicone and polyvinyl chloride tubes. These are the most widely used materials in various fields, especially in the medical field. In that case, the selenium layer in the inner surface tube was created by a circulating flow of selenium nanoparticle's solution using a peristaltic pump with a flow rate of 95 rpm at room temperature for 30 minutes (Figure 14A, B). After stabilizing the red color, it was washed with distilled water several times. Also, the selenium nanolayer with crystal structure was converted at a higher temperature of 85 °C from the red selenium-coated tubes. The red selenium-coated tube (Figure 14B) turned into the grey tube during the heat treatment, as presented in Figure 14C. In this process, the color change is visible, and it indicates the formation of grey hexagonal selenium on the inner surface of the tube.

Our advanced method is a simple, rapid, and low-cost version. These tubes are coated with red and grey selenium nanoparticles, and their applications could be exciting in many fields. This method allows the formation of selenium nanolayers of different thicknesses in tubes of different lengths and diameters, depending on the capacity of the peristaltic pump. Few studies have been conducted on the coating of nano selenium on medical devices. Chiera and co-workers reported that elemental selenium coated in the inner surface of fused silica tubes by a vapor transport system (CHIERA et al., 2015). Wang and co-workers reported that selenium nanoparticles coated on poly(ether ether ketone) (PEEK) medical devices by precipitation. Grey selenium-coated PEEK medical devices were converted at 100 °C for 6 days from red selenium-coated PEEK, and they dramatically suppressed the growth of *Pseudomonas aeruginosa*. The authors also reported no change in selenium concentration and elemental composition before and after heating (WANG et al., 2015).

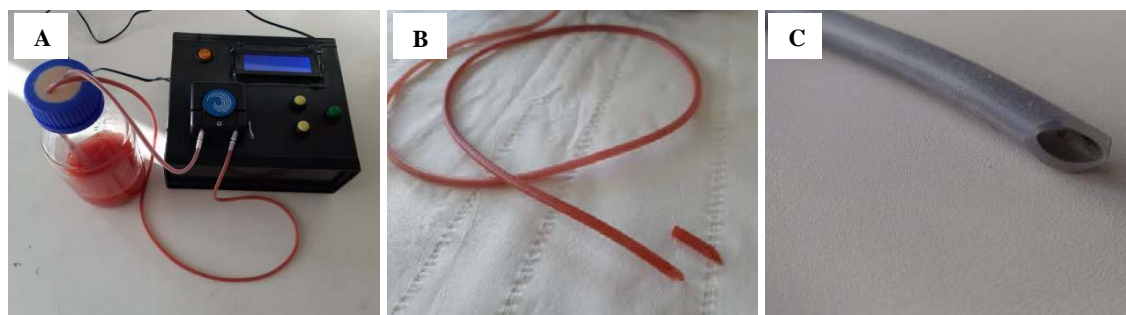
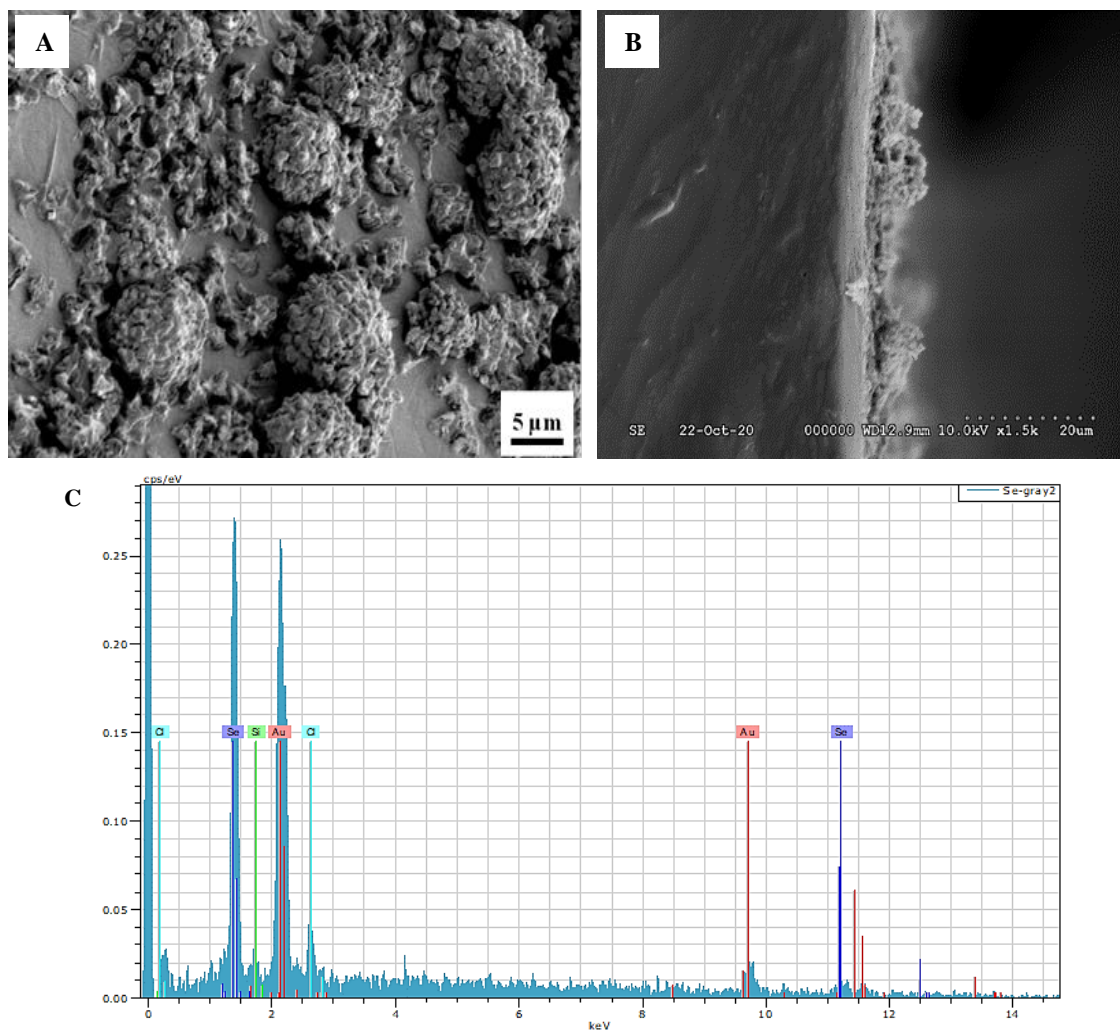


Figure 14: **Preparation of silicone and PVC tubes coated with SeNPs**

The size, morphology, chemical composition of selenium nanoparticles and the thickness of the deposited nanolayer by top-down and cross-sectional area were characterized by scanning electron microscopy (SEM) within Energy Dispersive X-ray spectroscopy (EDS) analysis.

PVC tubes are coated with selenium nanoparticles with a size of 100–200 nm, and these single and small particles attach to form more significant clusters with a size of 2  $\mu\text{m}$  (Figure 15). These structures are detected in the top-down and cross-sectional areas and are unevenly and sparsely distributed within the tube. SEM images with EDS have also exhibited the coating density of PVC and silicone surfaces covered with selenium nanoparticles. The scanning electron microscopic analysis is the most crucial technique for the characterization of nanomaterials. In results, the EDS spectrum was showed that selenium (Se) peaks were detected in silicone and PVC tubes coated with selenium nanoform, which confirmed that the nanoparticles were, in fact, elemental selenium. Also, peaks of chlorine (Cl) and silica (Si) present are from the PVC and silicone substrate; peaks of gold (Au) present are from the sputter-coating process.



**Figure 15: SEM images and X-ray spectra for top-down (A), and cross-sectional areas (B) of PVC surface coated with SeNPs**

The silicone surfaces were also covered with a considerable amount of selenium nanoparticles and are evenly distributed over all surfaces (Figure 16A). The thickness of the nanolayer is approximately 16 μm (Figure 16B). Some studies reported that medical devices coated with selenium nanoparticles such as PVC tubes and PEEK are more effective in suppressing bacterial growth. Coated PVC protects mammalian cells (RAMOS and WEBSTER, 2012; WANG et al., 2015). Therefore, the authors have suggested that selenium nanoparticles have remarkable selectivity for discerning between pathogens and normal cells. It is an excellent option for coating medical devices made of PVC, such as endotracheal tubes. Whether the selenium nanoparticle coating releases selenium, and if so, other issues such as the rate and volume of release in vitro and in vivo need to be addressed in future research.

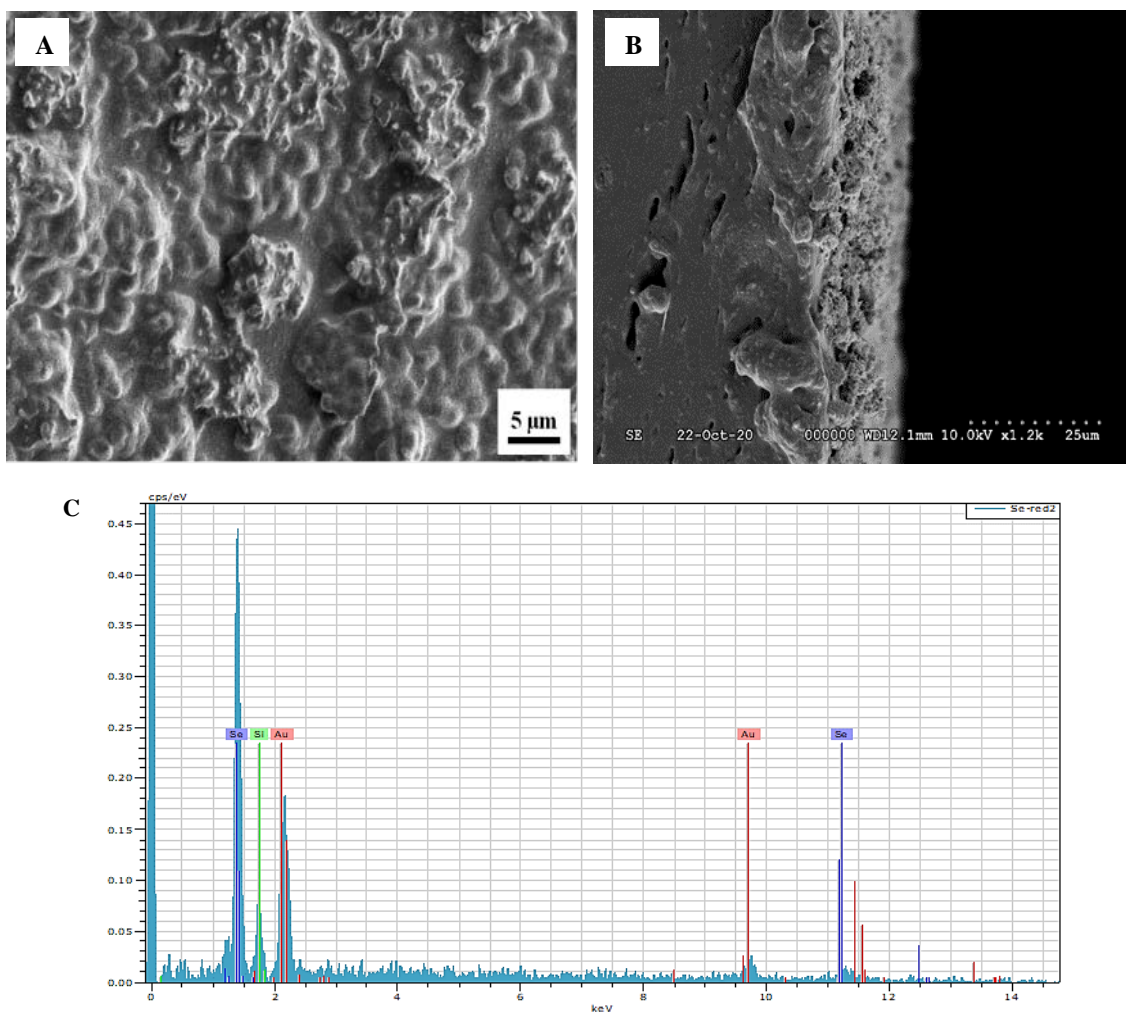


Figure 16: SEM images and X-ray spectra for top-down (A), and cross-sectional areas (B) of silicone surface coated with SeNPs

### 4.3. Production of selenium nanopowder

#### Red and grey selenium nanopowder

Red selenium nanoparticles in an aqueous form were produced by reacting 500 mg/L of sodium selenite and 10 g/L of ascorbic acids, detailed in section 4.1. Grey crystalline selenium in aqueous form was converted by heat treatment at 85 °C for 10 minutes from red selenium solution (Figure 17). The grey hexagonal form is the most thermodynamically stable form of selenium in the temperature range. The red form will gradually become grey after months or years, even at room temperature. The color changes from red to grey correlate with a blueshift when the selenium nanospheres turn into irregular particles (GATES et al., 2002). Transformation of the hexagonal crystalline

structures of selenium nanoparticles from the red amorphous form can be made by high temperature (LENZ et al., 2009) or replacing the aqueous phase with alcohol (LI and YAM, 2006), or chloroform with methanol (TEJO PRAKASH et al., 2009).

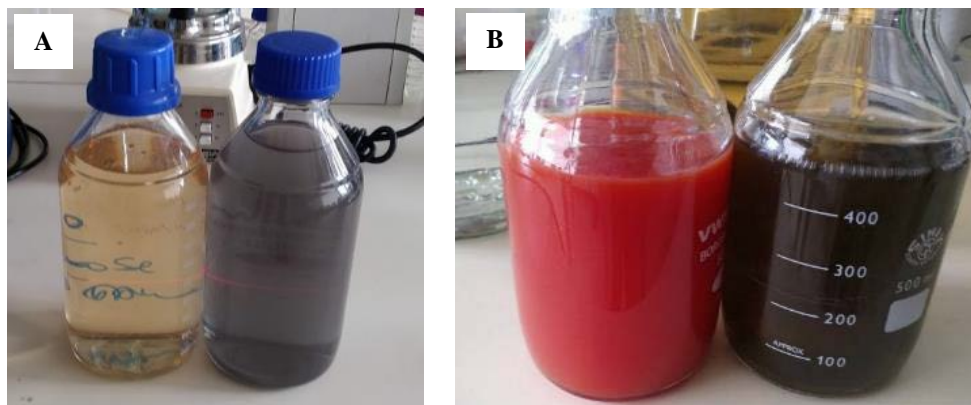


Figure 17: **Red and grey selenium nanoparticles 20 (A) and 200 mg/L of Se (B)**

Selenium nanoparticles in powder form were produced by precipitation, which is the chemical modified method. In a particular procedure, an equal amount of 10,000 mg/L sodium selenite and 100 g/L ascorbic acids were mixed and maintained at ambient temperature for 2 hours. Selenium nanoparticles were converted by the aforementioned general mechanism for 30 minutes. After 30 minutes of the reaction time, the precipitation of the nanogranules began (Figure 18B), and after two hours, they were utterly precipitated, as presented in Figure 18C. Then, the nanogranules were removed by filtration and purified by washing with ethanol and distilled water three times (Figure 18D, E). The purified nanogranules were split to make red selenium nanopowder (red-SeNPs) and grey selenium nanopowder (grey-SeNPs). Red selenium nanogranules were placed at 4 °C until dry (Figure 18F). Grey selenium nanogranules were transformed from red by heating at 85 °C for 10 minutes and dried at room temperature (Figure 18G). Finally, selenium nanogranules were ground using a nano grinder. It is possible to obtain approximately 5 grams of red or grey pure selenium nanopowder from 1000 ml of the aqueous form containing nano selenium nanoparticles from 100 nm to 100  $\mu$ m, as shown in Figure 13 above.

The grey color of selenium has corresponded with particle dimension and morphology as crystalline hexagonal form. The temperature and pH can control the structure, shape, and color of the selenium nanoparticles. These methods illustrate the

phenomenon that red amorphous selenium nanoparticles are first produced. These spheres are transformed into acicular hexagonal crystalline structures in aqueous, nanolayer, and powder form.

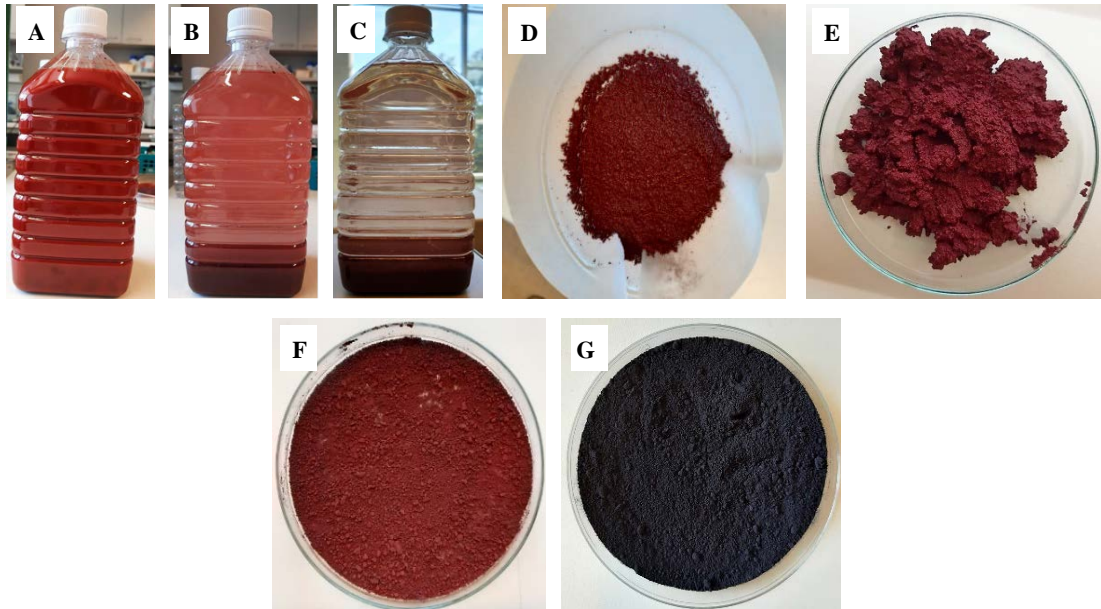


Figure 18: **Schematic illustration (A-G) of the preparation process for red-SeNPs and grey-SeNPs in powder form**

### **Selenium-enriched yogurt powder**

Probiotic yogurt was prepared by bacterial fermentation at incubation at 37 °C for 24-36 hours with 1000 mL of skim milk, 200 mg/L of sodium selenite, and starter culture (Lyofast Y 250: *S. thermophilus* and *L. delbrueckii sp. Bulgaricus*). After incubation, the yogurt turned red, and ascorbic acids (10 mg/L) in powder was added to them. If there is precursor selenium in yogurt, it will be converted into them, also supported extracellular synthesis. Subsequently, the yogurt was maintained at room temperature for 30 minutes and placed in a lyophilizer to obtain a powder (Figure 19).

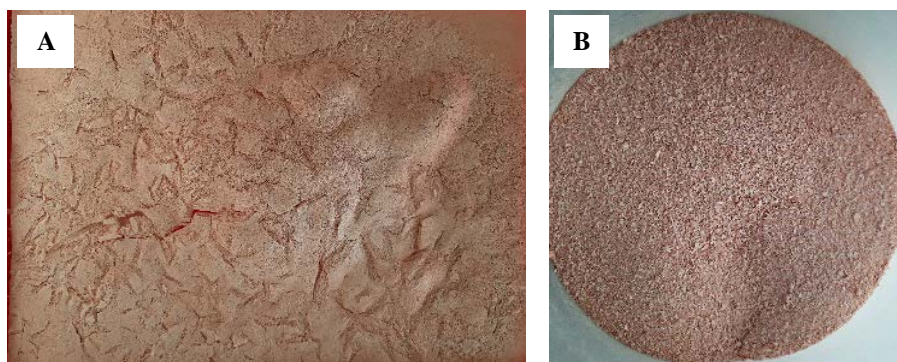


Figure 19: **Selenium-enriched yogurt powder after lyophilization (A) and grinding (B)**

In this case, we can obtain around 120 grams of yogurt powder rich in selenium from 1000 mL of skim milk. This yogurt powder contains about 2000 mg/kg of selenium within 93.8% nano form. During the incubation time, the transformation of selenium nanoparticles with a size ranging 50–500 nm occurred mainly intracellularly in bacteria, confirmed by transmission electron microscopic (TEM) and DLS techniques (Figure 20).

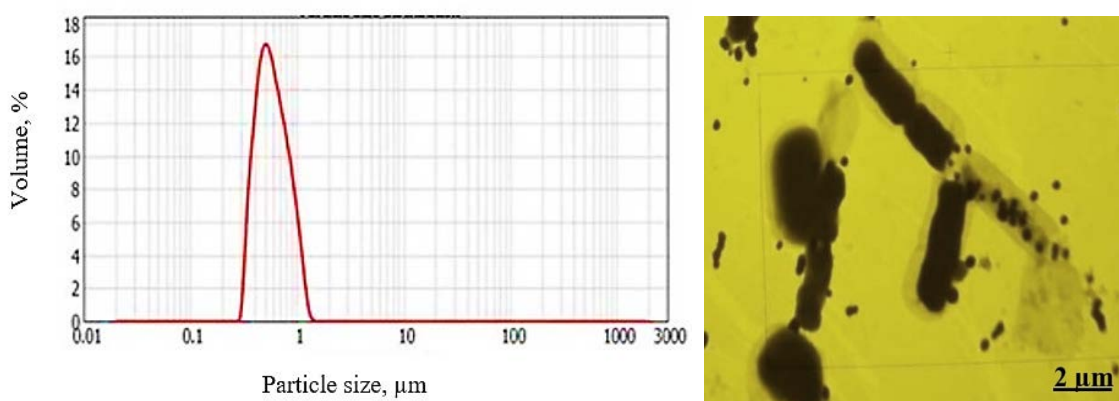


Figure 20: **The particle size distribution of the biosynthesized SeNPs and TEM image of bacteria with SeNPs**

The color of the selenium nanoparticles can be applied as an indicator, but their structure and morphology must also be characterized. Hence, X-ray diffraction analysis with selected area electron diffraction (SAED) and SEM analysis has been used to analyze the composition and phase of the resulting samples of selenium nanoparticles.

As a result, the biogenic red-SeNPs and chemically synthesized red-SeNPs are amorphous in shape, as demonstrated by these characterization techniques. The typical

XRD pattern of the red-SeNPs synthesized by the chemical method was no sharp reflections of Bragg, noisy and broad indicating the amorphous shape of the particles, as presented in Figure 21A. These data are consistent with other studies performed in the chemical conversion of selenium nanoparticles by several types of reducing agents (LI et al., 2010; CHEN et al., 2011; VIEIRA et al., 2017; ANGAMUTHU et al., 2019). Similar results were detected with biologically transformed selenium nanoforms using some bacteria and plants such as *P. aeruginosa* (KORA and RASTOGI, 2016) and extraction of red pepper (LI et al., 2007). However, nanoscale selenium indicates a typical XRD pattern (23, 30, and 43), confirms its nanoscale properties and resembles selenium nanoparticles originating from all different sources. CAVALU and co-workers (2018) reported that the XRD patterns for the nanoscale selenium show broad and robust peaks at around  $2\theta = 23^\circ$ , suggesting that nanoparticles are not crystal-shaped. In the biological synthesis of selenium nanoparticles, the amorphous shape of single and clustered selenium nanoparticles was indicated by SEM analysis after purification from the organic compounds (Figure 21B).

Scanning electron microscopic analysis is one of the basic techniques for morphological characterization. For instance, it was confirmed a spherical shape of selenium nanoparticles synthesized by bacterial species such as *Lactobacillus* (ESZENYI et al., 2011; RAJASREE and GAYATHRI, 2015; MORENO-MARTIN et al., 2017; SPYRIDOPOULOU et al., 2021), *Enterococcus* (SHOEIBI and MASHREGHI, 2017), *Staphylococcus* (MEDINA CRUZ et al., 2018; ESTEVAM et al., 2017) *Actinobacteria* (RAMYA et al., 2015), *Bacillus* (MISHRA et al., 2011; DHANJAL and CAMEOTRA, 2010), and Gram-negative bacterial species (FESHARAKI et al., 2010; KAZEMPOUR et al., 2013; SRIVASTAVA and MUKHOPADHYAY, 2015a; KORA and RASTOGI, 2017; MEDINA CRUZ et al., 2018).

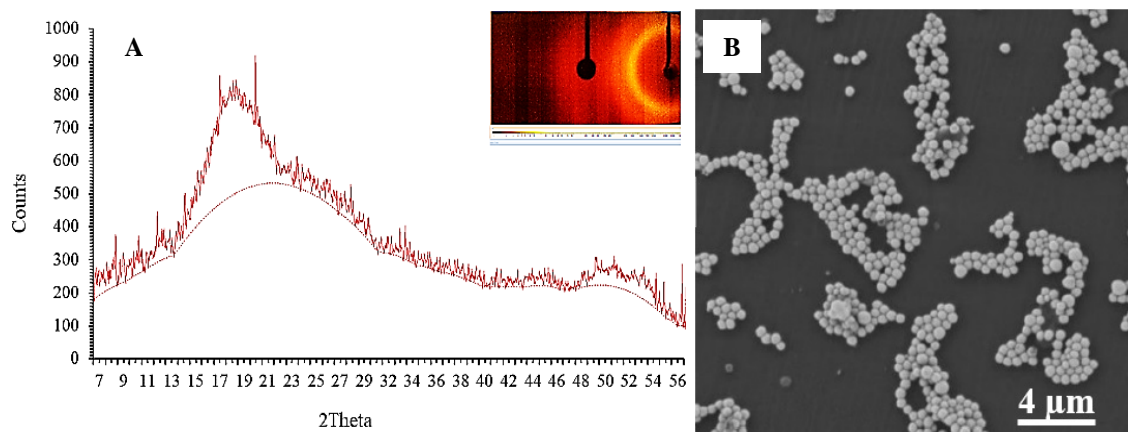


**Figure 21: XRD pattern with the corresponding SAED, and SEM image of red-SeNPs synthesized by chemical (A), biological (B) method**

The grey hexagonal structure of the synthesized selenium nanoparticles (grey-SeNPs) was also confirmed by XRD technique and SEM analysis. Selenium nanoparticles could come in different allotropic forms: amorphous, monoclinic, and trigonal phases. Grey (trigonal) selenium is the densest and thermodynamically stable form, consisting of absolute spiral chains of selenium atoms. This phase features an anisotropic crystal structure in which selenium atoms coordinate with each other via covalent bonds to form an infinite chain (CHEN et al., 2010). Likewise, some studies reported that particles could become highly crystalline at 50 °C for 21 days or longer (HAGEMAN et al., 2017), at 130 °C for six hours (DWIVEDI et al., 2011), and 180 °C within 12 hours (AN and WANG, 2007). The hexagonal selenium particles can raise along the ends of the needle-shaped particles (MONDAL et al., 2008). There is much competition for growth between the tips and sides of the selenium particles, resulting in thicker particles with a better crystallization speed. At higher temperatures, molecules can better disperse through the aqueous phase so that they can grow together with the tips of the needle-shaped particles (MONDAL et al., 2008).

In our study, figure 22 illustrates the XRD typical pattern and SEM image of the hexagonal crystalline structure of the chemically and biologically synthesized selenium nanoparticles, respectively. The sharps and narrow peaks were detected, and impurities peaks were not detected, which indicates the formation of high purity and well-crystallized selenium nanoparticles after heating at 85 °C for 10 minutes. Figure 23A shows the diffraction peaks of selenium are 23.5°, 29.7°, 41.4°, 43.6°, 45.4°, 51.8°, 55.9°,

61.5°, 65.3°, and 71.5° centered at  $2\theta$ , that has corresponded to the reflections (100), (101), (110), (102), (111), (201), (112), (202), (210) and (113), which is indication pure hexagonal phase of selenium crystalline form. Similar results as the lattice parameters confirmed our data were  $a = 4.366 \text{ \AA}$  and  $c = 4.9536 \text{ \AA}$ , these data confirmed by according to the JCPDS №06-0362 (DWIVEDI et al., 2011; CHEN et al., 2011; SRIVASTAVA and MUKHOPADHYAY, 2015b). In addition, the crystalline phases such as (100), (101), (110), (102), (111), (201), (112), and (103) are observed at  $2\theta = 23^\circ$ ,  $29^\circ$ ,  $41^\circ$ ,  $43^\circ$ ,  $45^\circ$ ,  $51^\circ$ ,  $55^\circ$ ,  $61^\circ$  and  $65^\circ$ . The lattice parameters of  $a = 4.3662 \text{ \AA}$  and  $c = 4.9521 \text{ \AA}$  agree with the normal point for selenium with  $a = 4.3662 \text{ \AA}$  and  $c = 4.69536 \text{ \AA}$  according to JCPDS №73-0465 (VIEIRA et al., 2017). However, all the diffraction peaks are indicated to the crystalline phase of nanoscale selenium.

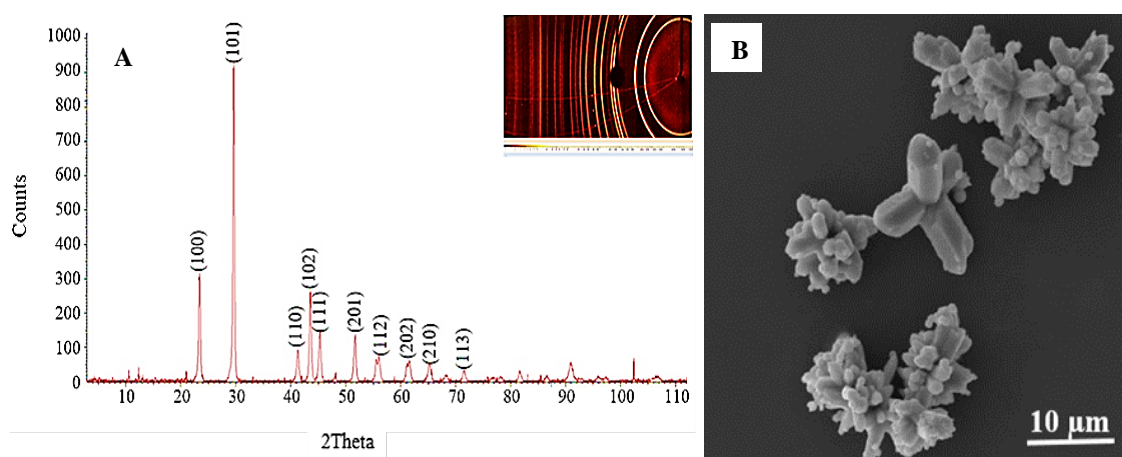


Figure 22: XRD pattern with the corresponding SAED, and SEM image of grey-SeNPs synthesized by chemical (A), biological (B) method

#### 4.4. Determining the protective effect of selenium nanoparticles

The homogenous solution of red amorphous selenium nanoparticles with a size 250 nm size (Figure 23) was produced by the method patented by Prokisch and Zommara (US8003071B2). The characterization of selenium nanoparticles was already published by ESZENYI et al. (2011) and PROKISCH and ZOMMARA (2011). They have already shown higher antioxidant activity than other selenium compounds in animal experiments with sheep, chicken, and fish (BENKŐ et al., 2012; UNGVÁRI et al., 2013; GULYÁS et al., 2016). In this experiment, the animal model organism determined the toxic and

antidote effects of such biosynthesized selenium nanoparticles. *Paramecium caudatum* was fed by adding the same amount of nano-selenium solution to the culture before 2 hours of the experiment.

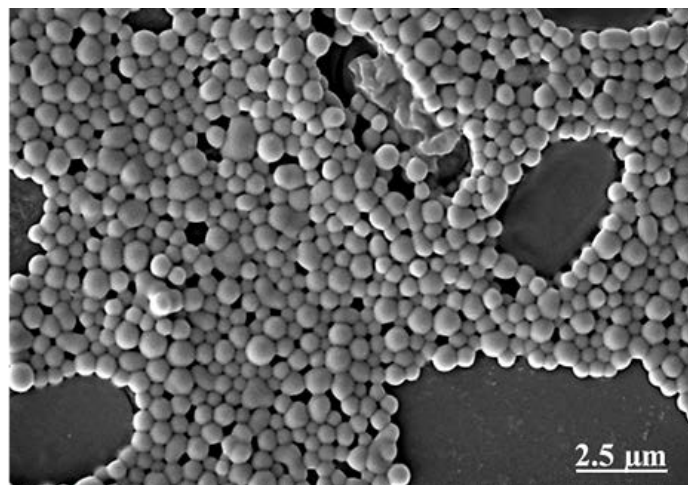


Figure 23: SEM image of biosynthesized selenium nanoparticles

#### 4.4.1. Toxic concentrations of selenium nanoparticles and toxic substances

It was found that selenium nanoparticles above 800 mg/L had no toxic effects on the locomotion and morphology of *P. caudatum*. They like to eat selenium nanoparticles, and after 5 minutes, the selenium particles accumulate inside the cells. Due to its general structure and sensitive features, a combination of a simple light microscope and a computerized video tracking system was used in the study, which was a fully observed diet, locomotion/movement, and morphological change in *Paramecium*. After supplementation, dark spots inside *P. caudatum* are visible under a microscope, resulting from red particles. Moreover, this accumulation of selenium nanoparticles inside the cell was confirmed by scanning electron microscopy (SEM) with X-ray analysis.

X-ray fluorescence mapping indicates the location of selenium on the image and shows ciliates, selenium spheres, and lactobacillus cells. In other words, the selenium nanoparticles inside *Paramecium* are shown as dark and yellow spots by the processed light microscope and SEM microscope, as displayed in Figure 24 and Figure 25. These images show no morphological changes in the *P. caudatum* after supplementation with selenium nanoparticles. Therefore, this result indicates that biosynthesized selenium nanoparticles have no toxic effects on unicellular organisms.

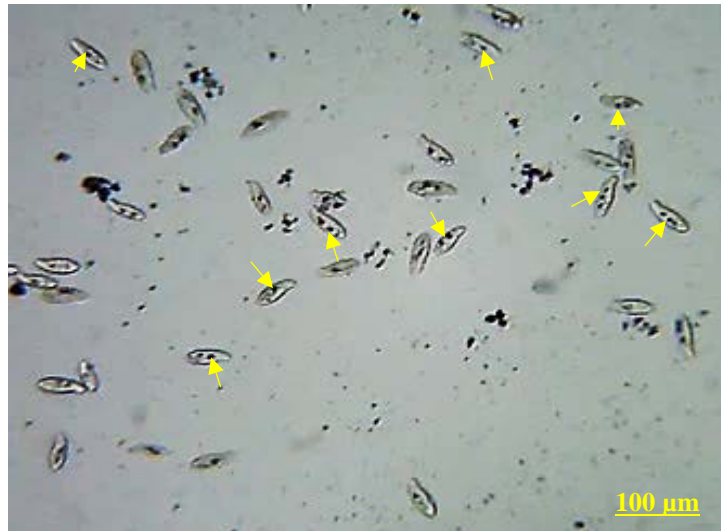


Figure 24. **Optical image (400x) of *P. caudatum* after 5 minutes of supplementation with SeNPs**



Figure 25: **SEM images with X-ray (B) of *P. caudatum* treated with SeNPs**

In results, the lethal concentration of toxic substances on Paramecium was determined, as presented in Figure 27: for bulk selenium;  $\geq 10.0$  mg/L as sodium selenite,  $\geq 20.0$  mg/L as sodium selenate, and for silver;  $\geq 1.25$  mg/L of silver nanoparticles, and  $\geq 2.50$  mg/L as silver nitrate. All cells have died caused by lysis under 18 minutes. The concentration vs. survival time has a unique shape that resembles a pH titration curve, and its turning point offers the LC50 value. Exposure to silver compound and bulk-selenium during the experiment resulted in various alterations in locomotion behavior and morphology of Paramecium.

Due to the high selenium concentration, Paramecium's swimming stopped completely, but his ciliates continued to move until the cells were lysed. As the concentration decreased, continuous changes in swimming speed, changes (circular motion), immobility, and cytolysis were observed. Swimming speed gradually decreases with increasing exposure time, probably caused by toxic substances on cell metabolism and morphological alterations. Similar changes in swimming speed, morphological changes, generation time, *etc.*, were observed when Paramecium is exposed to high concentrations of insecticide as acephate (VENKATESWARA et al., 2006; 2007).

Silver-affected Paramecium showed systematic alterations in its shape, primarily by causing irregular bleb formation of the cell membrane before cytolysis, the same as in Figure 26. Single or multiple blebs (vesicles) have developed on the cell membranes, which is a common occurrence during cell apoptosis. Macronucleus fragmentation and decay were also observed with increasing exposure time. Similar changes in the cell membrane of *P. caudatum* were detected with xenobiotics or insecticides, and they died entirely in 17 minutes (LEON and BERGMANN 1968; VENKATESWARA et al., 2007; RAO et al., 2008).

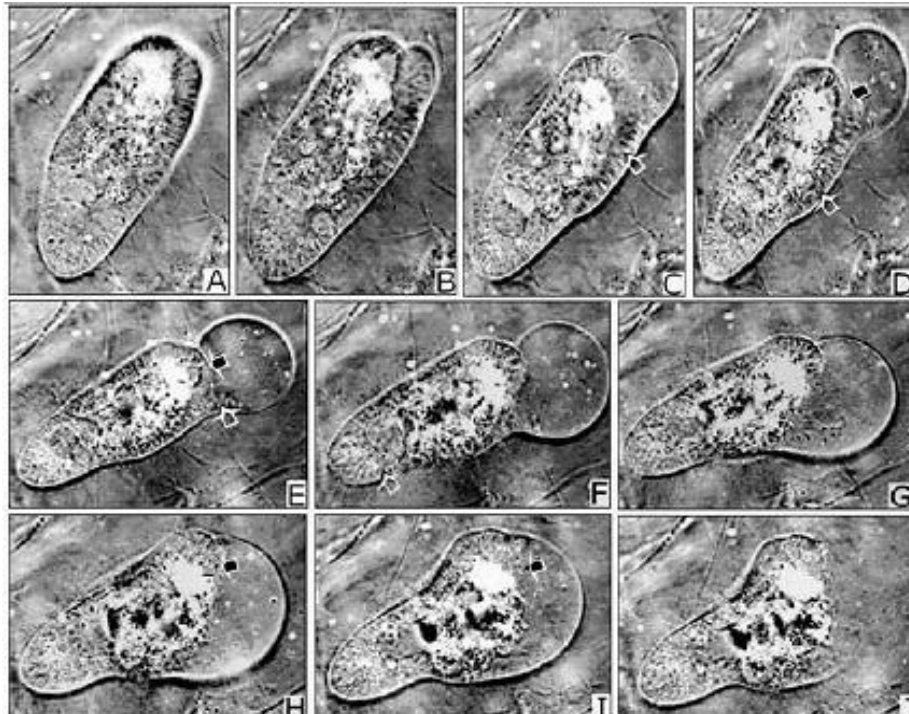


Figure 26: **Scheme of morphological changes from blebbing to cell lysis in *P. caudatum* (1400x).** [Source: VENKATESWARA et al., 2007]

Selenium and silver have been used for the food industry and medicine due to their antibacterial, antioxidant, and other biocompatibility. In the case of selenium, its bioavailability depends on its chemical form and concentration. There is a small space between their essential and toxic concentration for bulk selenium forms compared with nanoform. For instance, sodium selenite and sodium selenate are classified as highly toxic and adequately toxic to tilapia larvae, respectively (RANZANI-PAIVA et al., 2011). Selenium can lead to acute and chronic health problems in all living organisms (VINCETI et al., 2001; 2014). The method and results we used were similar to those of other researchers (KIM et al., 2003; ZHANG et al., 2005; WANG et al., 2007; ZHANG et al., 2008; ILONA et al., 2012). The toxic effects of selenium have been reported by ILONA et al. (2012) to decrease from selenate to selenite and its nanoforms. Several studies have reported that selenium in its nanoform has shown higher bioavailability and is much less toxic than bulk selenium forms (JIA et al., 2005; ZHANG et al., 2008; SHI et al., 2011; KOJOURI et al., 2012).

In the case of silver, there is growing attention to the biological consequences of the extensive use of silver nanoparticles and their potential toxicity to organisms (ANSAR et al., 2017). Silver, and even its nanoparticles, are known to destroy different levels of complex cells in both prokaryotes and eukaryotes. The effective concentration of silver is around 0.1 mg/L (VAZQUEZ-MUÑOZ et al., 2017; TAYLOR et al., 2016). The toxic effect of silver nanoparticles was found with *Paramecium* at around 30–50 µg/L for 15 minutes. In our study, silver nitrate and silver nanoform have a dose-dependent toxic effect on *Paramecia*, similar to other studies. Several studies have reported that silver nanoparticles have shown a toxic effect at the cellular level in all living organisms, including viruses (MEHRBOD et al., 2015), bacteria (YOON et al., 2007), protozoa (KVITEK LIBOR et al., 2009), algae (TAYLOR et al., 2016), fungi (VAZQUEZ-MUÑOZ et al., 2017), *etc.*

#### **4.4.2. The antidote effects of selenium nanoparticles**

In the experimental group supplemented with the biogenic selenium nanoparticles, the lethal dose of toxic substances was significantly reduced 2-fold. In detail, the lethal concentrations of toxic substances after supplementation found silver nanoparticles at  $\geq 2.5$  mg/L, silver nitrate at  $\geq 5.0$  mg/L, sodium selenite at  $\geq 20.0$  mg/L, and sodium

selenate at  $\geq 40.0$  mg/L. All cells have survived for an experimental time under the influence of pre-determined lethal concentrations of toxicants. They also did not show any alterations in locomotion and morphology, including shape, blebbing, lysis, and swimming. In addition, the aforementioned morphological changes lasted longer in the experimental group under the influence of higher than lethal concentrations compared to the control group. Surprisingly, the survival time of *Paramecium* was extended by the supplementation of nano selenium when exposed to all concentrations of toxicants. Figure 27 shows the experimental and control groups' concentration and survival time changes. Theoretically, these results agree with the other studies associated with the protective effect and low toxicity of selenium nanoparticles.

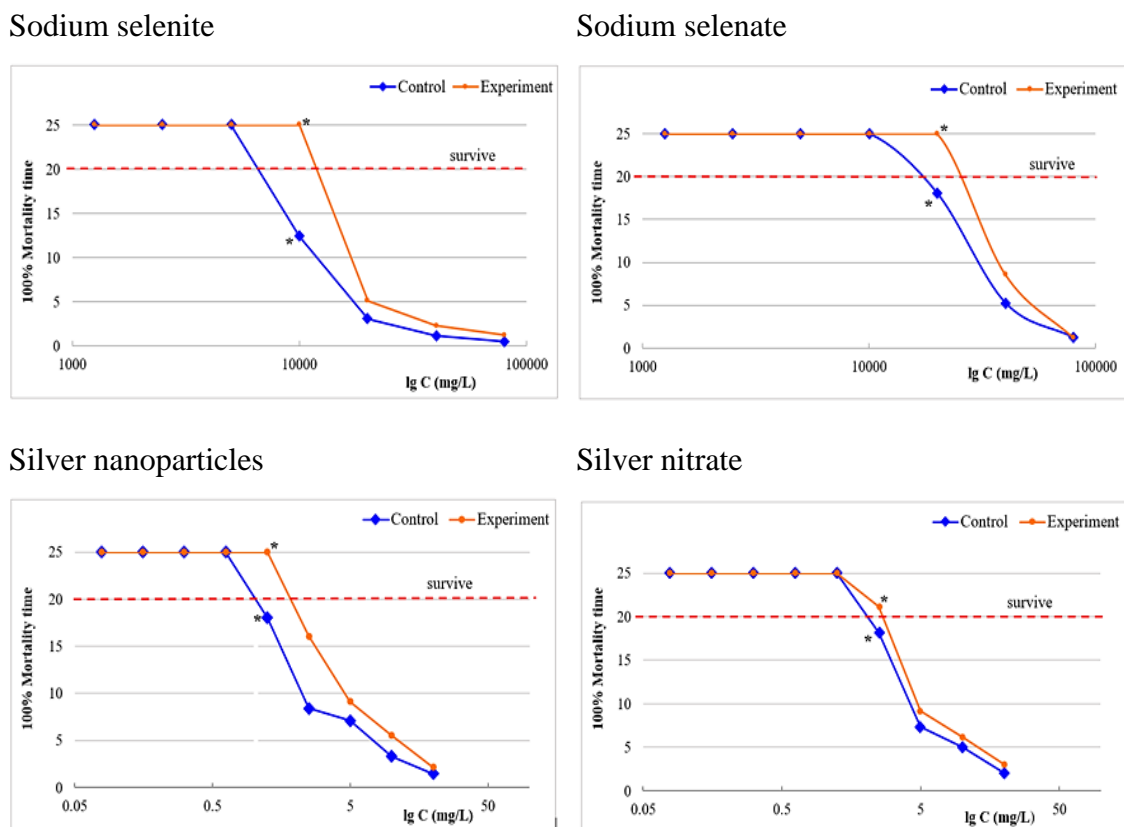


**Figure 27: The correlation between concentration and survival time on a logarithmic scale. *P. caudatum* was supplemented with SeNPs in experimental groups, and control groups not receiving SeNPs**

To date, numerous studies have reported that selenium supplementation consisting of its nanoparticles can cause high efficiency and low toxicity, as mentioned in the literature. For instance, selenium nanoparticles dramatically reduced bulk selenium-

induced acute toxicity by up to 4-fold in rodent models (ZHANG et al., 2001). Also, bulk selenium as a selenite has a higher toxic effect than nano selenium in the order that it adversely affects mouse growth, lipid peroxidation, and liver function (ZHANG et al., 2005). In addition, selenium nanoparticles can protect against some heavy metal or other toxic substances-induced toxicity. The detoxification of selenium nanoforms may be explained by restoring the target selenoproteins activity and intracellular redox state. Degradation of the thioredoxin (Trx) and glutaredoxin (Grx) systems allow intracellular ROS and RNS (reactive nitrogen species) proliferation, leading to mitochondrial damage, lipid peroxidation, calcium homeostasis disorders, protein repair disorders, and cell apoptosis (LU and HOLMGREN 2014). Dietary selenium nanoparticles can be increased antioxidant enzymes, including GSH-Px, SOD, and CAT in blood, liver, and kidney (WANG et al., 2007; SHI et al., 2011). The activity of these enzymes plays a critical role in the poisoning. For instance, several studies reported that selenium reduces the toxic symptoms of mercury in model organisms (FREITAS et al., 2009; COGUN et al., 2012; WANG et al., 2017).

The antagonism of selenium against mercury-induced toxicity is explained by the antioxidant capacity of selenium to prevent the formation of selenium-mercury complexes or oxidative stress or its capacity to reduce the body load of mercury. Mercury binds to the active sites (selenocysteine binding sites) of cytosolic thioredoxin reductase (TXNRD1) and mitochondrial thioredoxin reductase (TXNRD2) and significantly inhibits their function (BRANCO et al., 2014). It is a fundamental problem that metals have a lower affinity for thiol groups and a higher affinity for selenium-containing groups. Therefore, selenium supplementation can play a critical role in balancing proper selenium conditions and reducing mercury toxicity (SPILLER, 2018).

The protective effect of selenium nanoparticles on arsenic-mediated cell destroys and DNA injuries were explained by lowering ROS production (PRASAD and SELVARAJ, 2014). A high concentration of ROS can be damaged normal cells. Besides, the selenium supplementation was prevented chromium-induced symptoms such as the reduction of GSH, membrane potential, and  $\text{Ca}^{2+}$ -ATPase activity (HAO et al., 2017), and reduced oxidative stress in the liver induced by silver nanoparticles (ANSAR et al., 2017).

The toxicity of silver nanoparticles is explained by the release of silver ions in the system or large-scale systemic distribution of silver in tissue, which causes oxidation,

protein or DNA injury, and cell destroys (MACKEVICA et al., 2015; ARORA et al., 2008; GOPINATH et al., 2010). Recently, VICAS et al., (2021a; b) reported the antidote effect of selenium nanoparticles against cadmium-mediated toxicity. The supplementation of selenium nanoparticles with probiotics showed the restoration of blood-liver markers, antioxidant enzymes, and morphological changes in the liver (VICAS et al., 2021a) and reduced creatine, inflammation markers, and morphological changes in kidney toxicity (VICAS et al., 2021b).

#### **4.5. Investigation of selenium nanoparticles in nanofiber production**

In the electrospinning process, *processing* parameters such as polymer types and solvent types, viscosity, concentration, density, surface tension, and *system* parameters such as voltage, flow rate, needle or capillary to collector distance, ambient conditions, and collector types play an essential role in fiber sizes, morphologies and their structures (TEO and RAMAKRISHNA, 2006). The concentration of polymer is a significant parameter that can limit fiber formation. A polymer solution with low concentration makes droplets due to the effects of surface tension, and high-concentration has a high viscosity that prevents fiber formation. For voltage, it has been reported that the applied voltage increases as the fiber size decreases (MEGELSKI et al., 2002). Due to the increased flow rate, the fibers showed significant bead morphology and increased pore size (MEGELSKI et al., 2002). The distance from the needle tip to the collector surface and solvent type also plays an essential role in the evaporation speed, deposition rate, and drying time. However, there are no formal conditions. The conditions differ depending on polymer solution, solvent, and additive used.

Our study measured the density and viscosity of PVB polymer dissolved in pure ethanol at concentrations of 6% to 15%, as displayed in Figure 28 and Figure 29. They are directly linked to concentrations. Excessive or low density and viscosity are not suitable for the electrospinning process. As a result, 10% of PVB polymer with a density of  $0.81 \text{ g mL}^{-1}$  and a viscosity of  $474 \text{ mm}^2 \text{ s}^{-1}$  was compatible with a flow rate of  $10 \text{ mL h}^{-1}$ , a distance of 25 cm between stainless-steel collector and needle tip, and 40 kV of voltage for electrospinning. In addition, the environmental parameters were a humidity of 34% and a temperature of  $24 \text{ }^\circ\text{C}$ . For solvent PVB polymer, they are suitable for dissolving them for electrospinning, including ethanol, methanol, isopropanol, acetic

acid, n-butanol, and dimethylformamide (YALCINKAYA et al., 2016; JALIL and ISMAIL, 2019; YALCINKAYA and KOMAREK, 2019; LU et al., 2021).

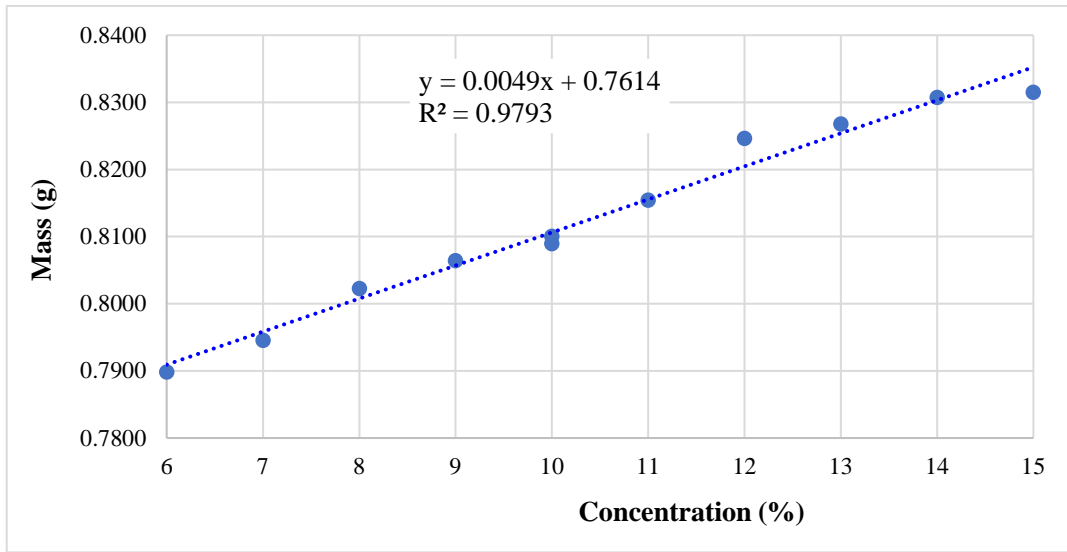


Figure 28: The density of PVB polymer solutions of different concentrations

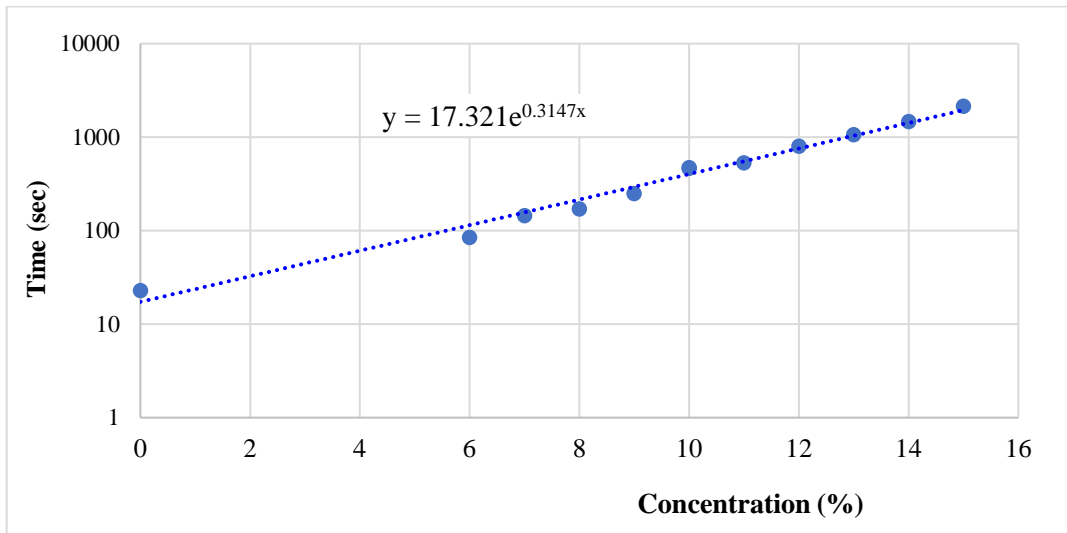


Figure 29: The viscosity of PVB polymer solutions of different concentrations

PVB polymer solution in 10% was proper for resuspension of selenium nanopowder from 1% to 10% by ultrasonication for 30 minutes, as exhibited in Figure 8. The morphology of the electrospun nanofibers was monitored by a conventional light microscope (400×). In this case, some nanofiber layers were applied to the coverslip for viewing through the microscope. The optical images were taken with regular and laser lighting. Figure 30 shows the various multiple structures of nanofibers with cylindrical

shapes, including linear, spiral, zigzag lines, *etc.* These fiber structures are visible under a light microscope, which is a simple method used to characterize the morphology and structures of electrospun nanofibers.

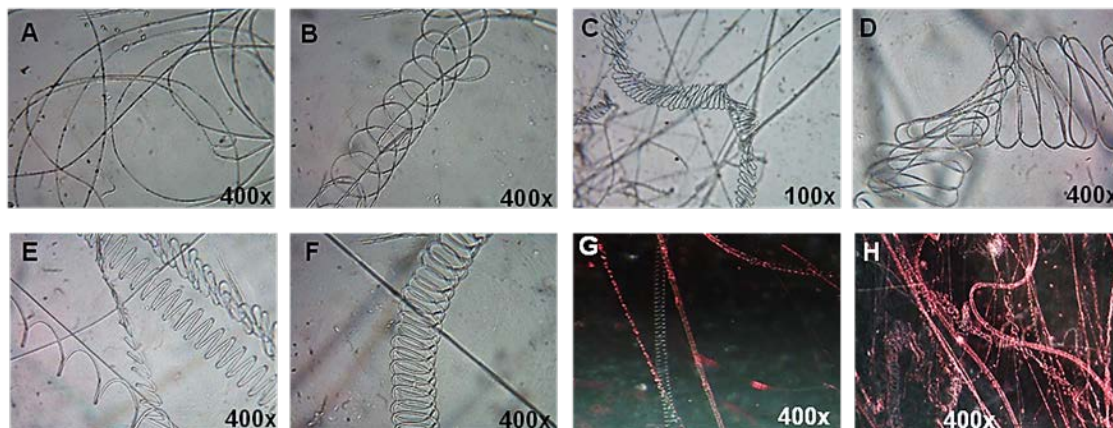


Figure 30: **Optical images of nanofiber's structures enriched with selenium nanoparticles; red-SeNPs (A; B), grey- SeNPs (C; D), aqueous-ethanolic SeNPs (E–H)**

#### 4.5.1. Nanofibers enriched with pre-synthesized selenium nanoparticles

The pre-synthesis method is commonly used for enriching electrospun nanofibers with nanoparticles. In this case, nanoparticles in liquids and powders can be synthesized on a laboratory scale or purchased from producers and mixed with polymer solutions. Electrospun nanofibers enriched with several types of nanoparticles in this way: PVA nanofibers with silver nanoparticles (AADIL et al., 2018), PAN nanofibers with copper nanoparticles (HASHMI et al., 2019), PCL-gelatin nanofibers with cerium oxide nanoparticles (RATHER et al., 2018), PCL nanofibers with selenium nanoparticles (KAMARUZAMAN et al., 2017; 2021).

Our study tested pre-synthesized selenium nanoparticles in powder form with PVB polymer solution to form selenium-enriched nanofiber production. PVB polymer solutions containing 1% to 10% of red-SeNPs and grey-SeNPs were suitable for the formation of nanofibers. Concentrations above 5% of the nanopowder were affected by the viscosity, density, and conductivity of the PVB polymer solution, slowing productivity. As the concentration of selenium nanopowder increases, deeper colored nanofibrous sheets are formed. From light to brighter pink (Figure 31A; B) and black

(Figure 32A; B) nanofibrous sheets with smooth and flexible surfaces originated from 1% and 10% of red-SeNPs and grey-SeNPs.

Interestingly, there was no significant difference in the dimension, structure, or morphology of the nanofibers produced from the amorphous and crystalline forms of selenium, as well as in the electrospinning process, which was identified by scanning electron microscopic technique within X-ray and EDS analysis (Figure 31C; D and Figure 32C; D). They are effective techniques for characterizing the size and morphology of nanofibers. The resulting nanofibers are typically amorphous with a diameter range of 100 nm to 100  $\mu\text{m}$  and a specific surface area of around 4 to 40  $\text{m}^2 \text{g}^{-1}$ . Significantly, the mean diameter was approximately 500 nm with a specific surface area of 8  $\text{m}^2 \text{g}^{-1}$  at all concentrations of selenium nanopowder. In addition, the length of the nanofibers is calculated by the equation for the cylinder's volume and surface, based on their diameter size. As a calculation, the length of the nanofibers is 5093  $\text{km cm}^{-3}$  with a diameter of 500 nm, which is derived from one mL of 10% polymer solution.

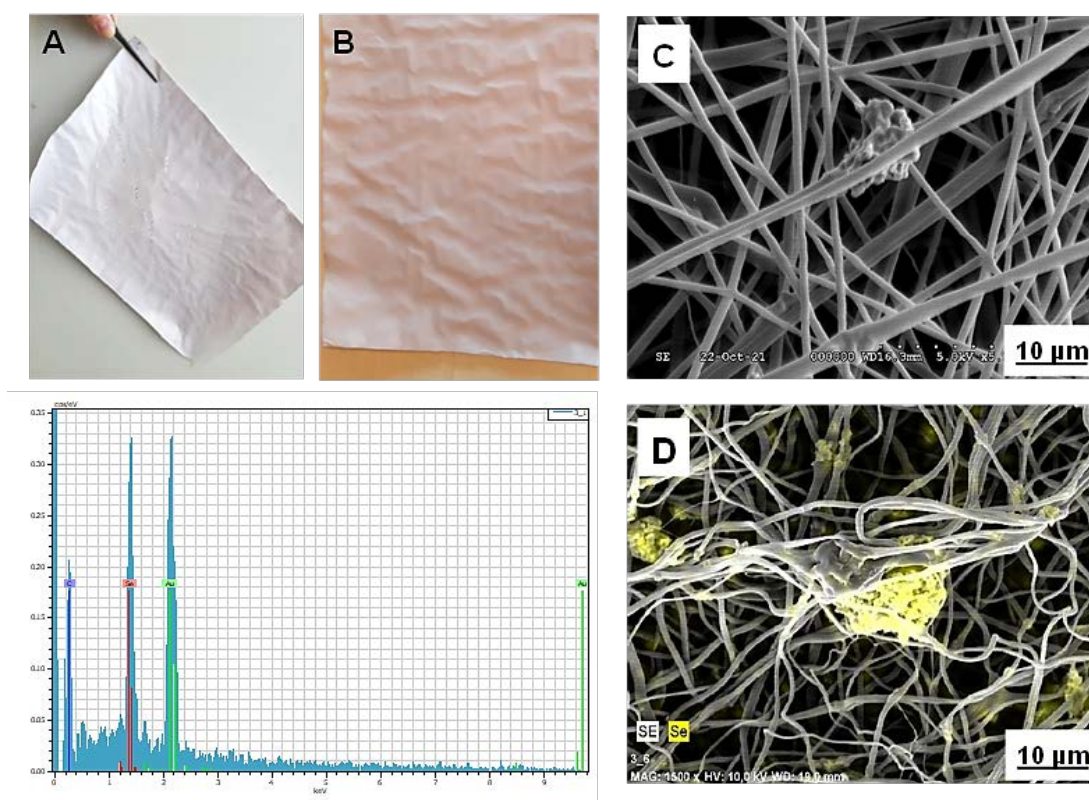


Figure 31: Nanofibrous sheets enriched with red selenium nanopowder and their SEM images with EDS; (A, C): 1% red-SeNPs, (B, D): 10% red-SeNPs

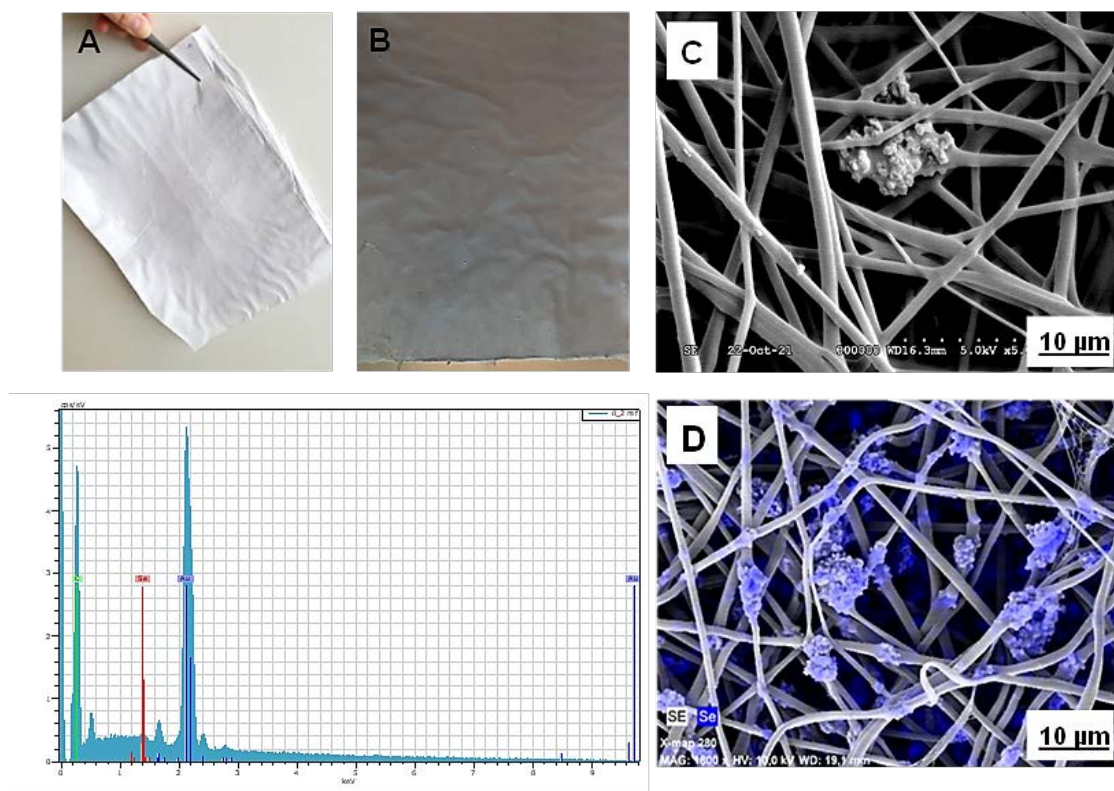


Figure 32: **Nanofibrous sheets enriched with grey selenium nanopowder and their SEM images with EDS; (A, C): 1% grey-SeNPs, (B, D): 10% grey-SeNPs**

The highest concentration of red-SeNPs and grey-SeNPs produced more beads formation than the lowest concentration, which X-Ray and EDS analysis also confirmed. The same phenomenon was reported that bead formation increases due to the high concentration of selenium nanoparticles in PCL polymer (KAMARUZAMAN et al., 2017). The aggregation of nanoparticles forms the beads during electrospinning, and the aggregation occurs because of their higher relative surface area and a higher relative number of surface atoms. Due to solid-state interactions, particles are structured in different orders of magnitude, leading to nanofibers' chain-like structures.

A nanofibrous sheet that contains beads of selenium nanopowder can have both disadvantages and advantages. For disadvantage, the chain-like structure of the beads may influence the mechanical properties like tensile strength of the fibers. For advantage, they contain a large amount of selenium and can be functionalized on the surface due to the basic bioactive properties of selenium. The nanofibrous sheet with more beads can probably release more selenium ions from the sheet. If these nanofibrous sheets are used for the wound healing process in animals, selenium nanoparticles can be controlled the

oxidation process in the injury sites. Because numerous studies reported about preventive and therapeutic properties of selenium nanoparticles, as mentioned in the literature. However, only one study reported that the nanofiber membrane loaded with selenium nanoparticles and vitamin E completed the re-epithelialization of skin injuries through the wound healing process (DOOSTMOHAMMADI et al., 2021).

The control of ROS can explain the therapeutic mechanism of selenium nanoparticle-enriched nanofibrous membranes at the site of injury, which plays an essential role in the wound dressing process. Wound dressings consisted of multiple processes, including hemostasis, inflammation, proliferation, and maturation stages (RIEGER et al., 2013; SELVARAJ and FATHIMA, 2017). Suppose enzymatic and nonenzymatic antioxidation cannot control ROS. In that case, its high levels can damage normal cells such as fibroblasts throughout the inflammatory stage, which are released from neutrophil cells to fight microorganisms (MITTAL et al., 2014; GALLEGO-VILLAR et al., 2014). In this case, the presence of antioxidant additives may improve the wound healing process by reducing the site effect of ROS (GOMATHI et al., 2003).

Nevertheless, there are limited studies on selenium-containing nanomaterials and their treatment effects. CHUNG and colleagues presented the antibacterial effect of scaffold enriched with selenium nanoparticles against the growth of *Staphylococcus* (CHUNG et al., 2016). In addition, due to the antibacterial, antifungal, antiviral activities of selenium nanoparticles, these nanofibrous sheets could be efficient for water treatment, irrigation systems, air filtration, *etc.* For example, studies have shown that bead-containing nanofibrous membranes are more hydrophobic activity than nanofibrous membranes with smooth permeation flux (TIJING et al., 2014; HUIZHEN et al., 2016).

#### **4.5.2. Nanofibers enriched with in-situ synthesized selenium nanoparticles**

Recently, it has focused on developing the in-situ synthesis of nanoparticles in combination with an electrospinning process with fewer steps, simpler and lower production costs, which enables the synthesis of nanoparticles during the electrospinning process, or electrospinning in solution without pre-synthesizing the nanoparticles. Several studies have reported a simple one-step technique for synthesizing nanoparticles and incorporating them into electrospun nanofibers (JIN et al., 2005; RUJITANAROJ et al.,

2008; SAQUING et al., 2009; BURKE et al., 2017). For example, BURKE et al. (2017) produced electrospun PEO nanofiber with in-situ synthesized magnetic iron-oxide nanoparticles. They mixed precursor sources and reducing agents in the polymer solution to obtain nanoparticles.

Our study synthesized selenium nanoparticles in PVB polymer from a reduction of 500 mg/L of sodium selenite by 10 g/L of ascorbic acids. A selenium precursor and a reducing agent were dissolved in 80% ethanol at ultrasonic for 30 minutes in a typical procedure. After dissolving, 10% (w/v) of PVB polymer was mixed and treated with ultrasound for 30 minutes. The sodium selenite and the ascorbic acid-loaded PVB polymer solution were stored separately for one day at room temperature. The next day, these solutions were mixed with ultrasound in equal proportions for 30 minutes to synthesize selenium nanoparticles (SeNPs-PVB). After ultrasonication, the mixture turned red, indicating the formation of selenium nanoparticles, as discussed above. Before electrospinning, this solution was diluted in equal proportions with pure PVB polymer solution to reduce the water phase. Eventually, the solution was used in the electrospinning process, resulting in PVB nanofibers containing selenium nanoparticles.

As a result, a pink nanofibrous sheet with a smooth and soft surface containing 1250 mg/L of selenium was produced by electrospinning under the same conditions, as exhibited in Figure 33A. The SEM technique analyzed the morphology and diameter, size of fiber. The electrospun nanofibers are also amorphous with 500 nm of average diameter size. Their length and specific surface area are similar to nanofibers enriched with selenium nanopowder. Interestingly, nanofibers have contained 50 nm or more small sizes of selenium nanoparticles only inside. The SEM images with low and high magnification showed no particles outside the fiber, as presented in Figure 33B-D.

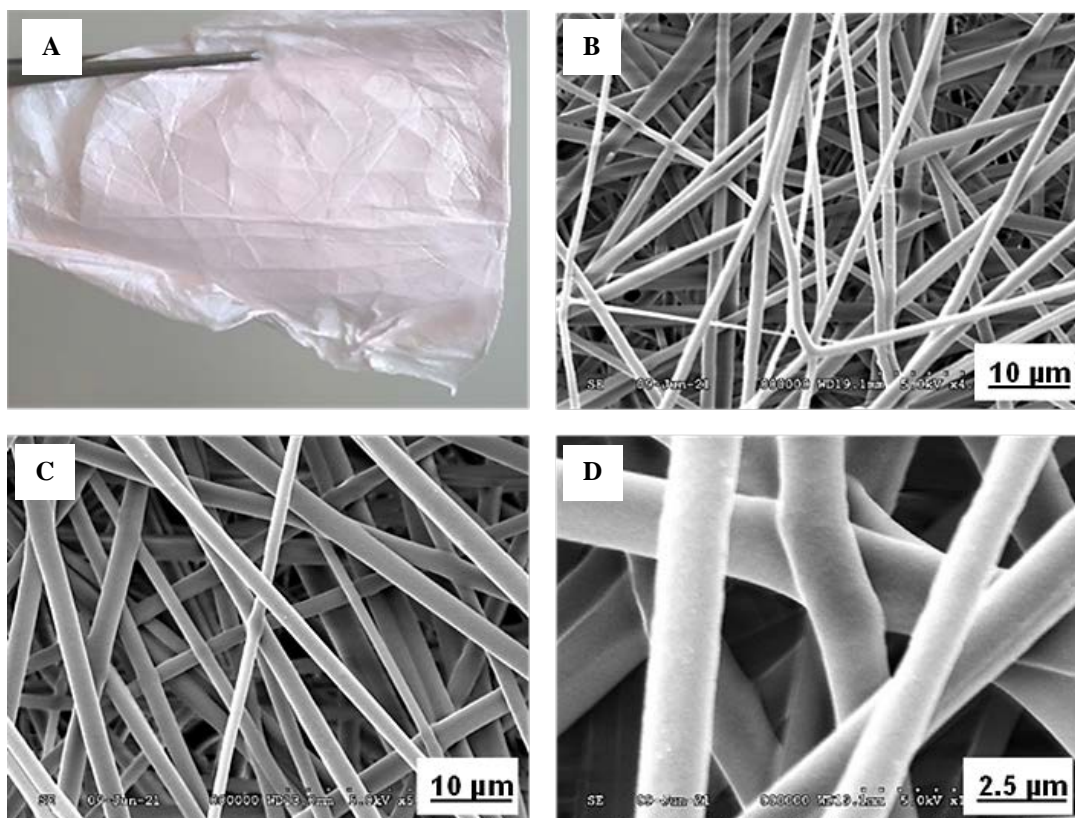


Figure 33: **Nanofibrous sheet enriched by in-situ synthesized SeNPs and its SEM images**

These data demonstrated that the in-situ synthesized selenium nanoparticles are well dispersed in a PVB polymer solution and suitable for forming electrospun nanofibers, a new material. In addition, The PVB polymer solution was an excellent stabilizer in the formation of selenium nanoparticles, so there was no significant agglomeration. Because of its basic properties, including non-toxicity and hydrophobicity (water-insoluble), an economical version, showing elasticity, optical transparency, and excellent adhesion to many surfaces, it has been extensively used in many applications such as nanofibers, drug delivery, medical films, and contrast agents in tumor therapy (POSAVEC et al., 2011; RUEDIGER et al., 2012). For example, YALCINKAYA and co-authors used PVB polymer based on its water-insoluble property to produce electrospun nanofibers containing post-synthesized silver nanoparticles. After producing the nanofibers, they synthesized silver nanoparticles by immersing the nanofibers in an aqueous solution of ascorbic acid as a reductant agent (YALCINKAYA et al., 2016).

Besides, PVB nanofibers containing bentonite are produced by electrospinning technique, and they have shown 86% absorbance of 100 mg/L methylene blue after a 7-hour immersion (JALIL and ISMAIL, 2019). In addition, electrospun PVB nanofibers enriched by copper nanoparticles, vanadium oxide, and thymol have shown high antibacterial activity, and they have suppressed the growth of *E. coli*, *S. aureus*, and *K. pneumoniae*. The authors suggested that these nanofibrous membranes could be suitable textile for medical masks and wastewater treatment (YALCINKAYA and KOMAREK, 2019; LU et al., 2021).

## 5. CONCLUSION

Biological and chemical routes synthesized selenium nanoparticles as green synthesis approaches. Organic red selenium nanoparticles with about 250 nm were transformed by probiotic bacteria like *Lactobacillus acidophilus*, which is amorphous in shape. Organic selenium nanoparticles with sizes 50 to 500 nm at 2000 mg/kg with yogurt as powder also have been produced by the one-step method. That means selenium-enriched yogurt powder has been produced by the combination of steps for conversion of selenium nanoparticles and yogurt making at the same time without any exceptional condition. Inorganic red amorphous elemental selenium from 100 nm to 100  $\mu\text{m}$  was converted from 500 mg/L selenium precursor as selenite and 10 g/L reducing agents as ascorbic acids. In addition, organic and inorganic grey hexagonal selenium nanoparticles were converted through the heat treatment, a thermodynamically stable form. High concentrations of sodium selenite and ascorbic acids were suitable ratios without any precipitator to obtain selenium nano-granules. This study produced red and grey selenium nanopowder by simple and novel methods. The synthesized organic and inorganic red or grey selenium nanoparticles in aqueous and powder forms can be applied in animal nutrition as a nutritional or functional additive.

Moreover, in this study, PVC and silicone tubes have successfully coated with red and grey selenium nanoparticles by simple and rapid method. Silicone surfaces are more efficient to coat with selenium nanoparticles than PVC. The selenium nanolayer is coated on the silicon surface with a thickness of 16  $\mu\text{m}$  and evenly distributed, and on the PVC tube has 2  $\mu\text{m}$  aggregates. The adaptability of the coating method presented in this study recognizes coating tubes of various lengths and diameters with selenium nanoparticles. It is also opening the way for several applications of these tubes coated with selenium nanoparticles in various fields. Selenium ions are slowly released from the surface of the tube. Therefore, in the future, studies of the antibacterial activity and selenium enrichment of these selenium-coated tubes in water or irrigation system may be of great interest. They can also be fascinating in medicine and microbiological research like cell culture, ventilators, *etc.*

We found that the biologically synthesized selenium nanoparticles at 800 mg/L have no toxic effect on *Paramecium caudatum*. Moreover, they have shown an antidote effect

on the silver- and selenium-mediated toxicity of *Paramecium*. The supplementation with selenium nanoform reduced the lethal concentrations of toxic substances by 2-fold compared to the un-supplemented group. Namely, the lethal concentrations were decreased in the selenium supplemented groups from 1.25 mg/L to 2.50 mg/L for silver nanoparticles, 2.50 mg/L to 5.0 mg/L for silver nitrate, 10.0 mg/L to 20.0 mg/L for sodium selenite, and from 20.0 mg/L to 40.0 mg/L for sodium selenate. In addition, the survival time of *Paramecium* has significantly extended by supplementation with selenium nanoparticles. These data indicate that supplementary selenium nanoparticles can increase endurance and reduce toxicity.

In this study, nanofibers containing three types of selenium nanoparticles with a size of approximately 500 nm, a specific surface area of  $8 \text{ m}^2 \text{ g}^{-1}$ , and a length of 5093  $\text{km cm}^{-3}$  were produced by the electrospinning technique. In the presence of red and grey selenium nanopowder, they were distributed like beads on the outside and inside the nanofibers. Increasing the concentration of red-SeNPs and grey-SeNPs from 1% to 10% increases bead formation but does not affect fiber size. Electrospinning conditions may control the fiber size. In the presence of in-situ synthesized SeNPs, they were distributed inside the fiber less than 50 nm in size.

Interestingly, the allotropes of selenium were found not to affect the nanofibers' morphology and size or diameter. The use of nanofibers will be more effective by combining the properties of nanofiber with a high specific surface area and porosity and interconnected pore structure with the antioxidant, antibacterial, anti-cancer, and protective properties of selenium nanoparticles. Therefore, selenium-enriched nanofibers can be used as medical pads, sponges, rolls for animal treatment, filter membranes for air and water treatment, and as protective fibers against environmental hazards such as chemical and biological or biochemical hazards.

## 6. NEW SCIENTIFIC RESULTS

1. Red amorphous selenium nanoparticles with sizes ranging from 100 nm to 100  $\mu\text{m}$  in aqueous and powdered form were produced by reacting sodium selenite and ascorbic acid at low (500 mg/L Se with 10 g/L ascorbic acids) and high (10,000 g/L Se with 100 g/L ascorbic acids) concentrations, respectively. Grey hexagonal selenium nanoparticles in aqueous and powdered form were converted by heat treatment at 85  $^{\circ}\text{C}$  for 10 minutes.
2. A homogeneous nanolayer of selenium nanoparticles with a thickness of 16  $\mu\text{m}$  on the inner surface of the silicone tube and an aggregate of 2  $\mu\text{m}$  on the inner surface of the PVC tube was created in a simple and rapid method.
3. The biosynthesized selenium nanoparticles at 800 mg/L have shown no toxic effect on *Paramecium caudatum*. Moreover, they have shown an antidote effect on the silver- and selenium-mediated toxicity of *Paramecium caudatum*. The supplementation with selenium nanoparticles reduced the lethal concentrations of sodium selenite, sodium selenate, silver nanoparticles, and silver nitrate by 2-fold compared to the un-supplemented group. In addition, the survival time of *Paramecia* was significantly extended by supplementation with selenium nanoparticles.
4. Different types of selenium nanoparticles enriched nanofibers in amorphous shape with a main diameter of 500 nm and a specific surface area of 8  $\text{m}^2 \text{g}^{-1}$  were produced by the electrospinning technique. 10% of PVB polymer is an excellent matrix for forming nano selenium-enriched nanofibers and nanofibrous sheets.

## 7. PRACTICAL APPLICABILITY OF RESULTS

1. Comparative studies of aqueous and powdered nano selenium in animal supplements will be needed in the future.
2. Nano selenium coated tubes could fortify the water system in the animal houses and greenhouse. In this case, selenium nanoparticles can show functional effects such as disinfection and enrichment in water. Plants and animals can uptake the selenium nanoparticles without any toxicity from the water. Furthermore, it could be fascinating to use in medicine and microbiological research such as cell culture, ventilators, *etc.*
3. A method with *Paramecium caudatum* could be suitable for chemical education and toxicological research, such as testing the acute toxicity of toxic metals, metalloid compounds, mycotoxins, insecticides, *etc.*
4. Nano selenium-enriched nanofibers can be used as medical pads, sponges, rolls for animal treatment, filter membranes for air and water treatment, and as protective fibers against environmental hazards such as chemical and biological or biochemical hazards.

## 8. SUMMARY

According to the literature data, it is well known that selenium has much more attention in various sectors everywhere. The selenium supplementation of animals is essential in Hungary, especially in the Hortobágy region. Therefore, every feed must be contained a selenium additive. There is an outbreak of white muscle disease in Mongolia for grazing animals, especially young animals in spring, caused by selenium shortage in soil and plant for geographical reasons. However, there are a limited number of products that contain selenium. Therefore, it is imperative to enrich the soil, plants and feed with selenium. The beneficial effect of selenium is caused by its chemical forms. The most common forms of selenium, such as selenate and selenite, can easily be overdosed on in plants and animals. There is a small space between the beneficial and toxic effects of selenium. Surprisingly, selenium nanoparticles have shown higher biological properties with lower toxic risk than other forms. Therefore, the synthesis or production of selenium nanoparticles is attracting attention, and their application is increasing over the days in nutrition, medicine, and others. For example, a regular daily intake of selenium in animal nutrition can be provided multifaceted results, including protecting animal health, reducing the financial risks of farmers, enriching animal-derived products, and supplementing humans. For these reasons, we focus on synthesizing selenium nanoparticles by biological and chemical methods, confirming their properties, and making products containing selenium nanoform.

In our study, selenium nanoparticles were synthesized by the biological method using probiotic bacteria *Lactobacillus acidophilus* (LA-5) according to the patent of Prokisch and Zommara (2011), and by the chemical method using various concentrations of sodium selenite with 25 mg/L to 500 mg/L, and ascorbic acids with 1 g/L, 5 g/L, and 10 g/L.

The formation of selenium nanoparticles and their morphological characterization was carried out by UV/vis spectroscopy, dynamic light scattering (DLS), scanning electron microscope (SEM), energy-dispersive X-ray spectroscopy (EDS), and X-ray diffraction analysis (XRD) with selected area electron diffraction (SAED).

The antidote or protective effect of the biosynthesized selenium nanoparticles at 800 mg/L was determined by a simple method with a light microscope and SEM using a starter

culture of *P. caudatum* obtained from a fish laboratory (Faculty of Agricultural and Food Sciences and Environmental Management, University of Debrecen). Toxic concentrations of silver nanoparticles, silver nitrate, sodium selenite, and sodium selenate were used for this experiment.

Nano selenium-enriched nanofibers were produced from PVB polymer containing different selenium nanoparticles by electrospinning technique. The morphology and diameter of fiber were characterized by a light microscope, SEM, and X-ray analysis.

The results show that organic red selenium nanoparticles around 250 nm were transformed by bacteria like *Lactobacillus acidophilus*, which is amorphous in shape. Organic selenium nanoparticles with sizes from 50 to 500 nm within yogurt as powder also have been produced by the one-step method. That means selenium-enriched yogurt powder has been produced by the combination of steps for conversion of selenium nanoparticles and yogurt making at the same time without any exceptional conditions. In that case, selenium nanoparticles with yogurt have been produced by mixing starter culture (Lyofast Y 250: *S. thermophilus* and *L. delbrueckii* sp. *Bulgaricus*) with selenium source as sodium selenite in skim milk at 37 °C for 24-36 hours. After the yogurt making time, 10 mg/L of ascorbic acids in powder was added, and the mixture was maintained at room temperature for 30 minutes. Finally, 2000 mg/kg of selenium-enriched yogurt powder was obtained by lyophilization and grinding.

Inorganic red amorphous selenium nanoparticles with sizes from 100 nm to 100 μm have been synthesized from the reaction of 500 mg/L sodium selenite and 10 g/L ascorbic acids at room temperature for 30 minutes. This ratio was suitable compared to other concentrations of precursor and reducing agents. Moreover, organic and inorganic grey hexagonal selenium nanoparticles were converted through heat treatment, a thermodynamically stable form. Selenium nano-granules were obtained from the reaction of sodium selenite at 10,000 mg/L and ascorbic acids at 100 g/L at room temperature for 2 hours without any precipitator agents. The selenium nano-granules were precipitated within 30 minutes of the mixing time. Finally, red selenium nanopowder is prepared by washing with ethanol and distilled water, drying, and grinding. At the same time, grey selenium nanopowder, which is hexagonal crystalline form, is converted by heat treatment at 85 °C for 10 minutes from red powder.

During this experiment, the selenium layer on the inner surface of the medical tube was created by a circulating flow of selenium nanoparticle's solution using a peristaltic pump with a flow rate of 95 rpm at room temperature for 30 minutes. After stabilizing the red color, it was washed with distilled water several times. Also, the selenium nanolayer with crystal structure was converted at a higher temperature of 85 °C from the red selenium-coated tubes. In this process, the color change is visible, and it indicates the formation of grey hexagonal selenium on the inner surface of the tube. SEM and EDS analysis performed the morphological and structural characterization of the selenium nanolayer. PVC tubes are coated with selenium nanoparticles with a size of 100–200 nm, and these single and small particles attach to form more significant clusters with a size of 2 µm. These structures were detected in the top-down and cross-sectional areas and are unevenly and sparsely distributed within the tube. The silicone surfaces were also covered with a considerable amount of selenium nanoparticles and are evenly distributed over all surfaces. The thickness of the nanolayer is approximately 16 µm.

We found that the biologically synthesized selenium nanoparticles at 800 mg/L have no toxic effect on *P. caudatum*; they accumulate in the cells within 5 minutes. After feeding, dark spots inside *P. caudatum* are visible under a microscope, resulting from red particles. Therefore, this accumulation of selenium nanoparticles inside the cell was confirmed by light and SEM with X-ray analysis. Moreover, they have shown an antidote effect on the silver- and selenium-mediated toxicity of *P. caudatum*. The supplementation with selenium nanoparticles reduced the lethal concentrations of toxicants by 2-fold compared to the un-supplemented group. Namely, the lethal concentrations were decreased in the selenium supplemented groups from 1.25 mg/L to 2.50 mg/L for silver nanoparticles, 2.50 mg/L to 5.0 mg/L for silver nitrate, 10.0 mg/L to 20.0 mg/L for sodium selenite, and from 20.0 mg/L to 40.0 mg/L for sodium selenate. The liner curve shows the correlation between concentration and survival time in experimental and control groups on the logarithmic scale. It illustrates the survival time of Paramecia for each concentration of toxicants by experimental and control groups and the difference in the lethal concentration of toxicants by such groups.

Surprisingly, the survival time of Paramecium has significantly extended by supplementation with selenium nanoparticles in the experimental group. Also, they did not show any changes in locomotion and morphology, including shape, blebbing, lysis, and swimming. The morphological changes lasted longer in the experimental groups than

in the control groups. Paramecium's swimming stopped entirely in the control groups, not supplemented with nano selenium, but his ciliates continued to move until the cells were lysed. As the concentration decreased, continuous changes in swimming speed, changes (circular motion), immobility, and cytolysis were observed. Swimming speed gradually decreases with increasing exposure time, probably caused by toxic substances on cell metabolism and morphological alterations. Silver-affected Paramecium showed systematic changes in its shape, primarily by causing irregular bleb formation of the cell membrane before cytolysis. Single or multiple blebs (vesicles) have developed on the cell membranes, which is a common occurrence during cell apoptosis. Macronucleus fragmentation and decay were also observed with increasing exposure time.

In the final step of the work, we tested selenium nanoparticles in nanofiber production using the electrospinning technique. As a result, 10% of PVB polymer solution with a density of  $0.81 \text{ g mL}^{-1}$  and a viscosity of  $474 \text{ mm}^2 \text{ s}^{-1}$  was compatible with a flow rate of  $10 \text{ mL h}^{-1}$ , a distance of 25 cm between stainless-steel collector and needle tip, and 40 kV of voltage, a humidity of 34%, and a temperature of  $24 \text{ }^\circ\text{C}$ . PVB polymer solution in 10% was proper for resuspension of selenium nanopowder from 1% to 10% by ultrasonication for 30 minutes. The optical images with multiple structures like linear, spiral, and zigzag lines of nanofiber are created by a conventional light microscope with  $400\times$  magnification. The samples were prepared by covering some fibers on the coverslip during electrospinning. Generally, we have produced nanofiber or nanofibrous sheets containing pre-synthesized red and grey selenium nanopowder and in-situ synthesized selenium nanoparticles.

In the presence of selenium nanopowder, 1% to 10% red and grey selenium nanopowder was mixed with 10% PVB polymer, and the mixture was loaded into the electrospinning process. Concentrations above 5% of the nanopowder were affected by the viscosity, density, and conductivity of the PVB polymer solution, slowing productivity. Finally, we have produced a nanofibrous sheet containing selenium nanoparticles with beads. The nanofibrous sheets are pink and black with smooth and flexible surfaces. Interestingly, there was no significant difference in the dimension, structure, or morphology of the nanofibers produced from the amorphous and crystalline forms of selenium, as well as in the electrospinning process, which was identified by scanning electron microscopic technique within X-ray and EDS analysis. The resulting nanofibers are typically amorphous with a diameter range of 100 nm to  $100 \text{ }\mu\text{m}$  and a

specific surface area of around 4 to 40 m<sup>2</sup> g<sup>-1</sup>. Significantly, the mean diameter was approximately 500 nm with a specific surface area of 8 m<sup>2</sup> g<sup>-1</sup> at all concentrations of selenium nanopowder. In addition, the length of the nanofibers is calculated by the equation for the volume and surface of cylinders, based on their diameter size. As a calculation, the length of the nanofibers is 5093 km cm<sup>-3</sup> with a diameter of 500 nm, which is derived from one mL of 10% polymer solution. We found that the highest concentration of nanopowder produced more beads formation than the lowest concentration.

In the presence of in-situ synthesized selenium nanoparticles, we have synthesized selenium nanoparticles in a polymer solution by dissolving 500 mg/L of sodium selenite with 10 g/L of ascorbic acids in 80% ethanol at ultrasonic for 30 minutes. Subsequently, 10% (w/v) of PVB was mixed and treated with ultrasound for 30 minutes. Then, these solutions were mixed with ultrasound in equal proportions for 30 minutes to obtain a homogenous polymer with selenium nanoparticles. After synthesizing selenium nanoparticles in PVB polymer, they were diluted with a pure PVB polymer solution and loaded into the electrospinning process. Eventually, we have a pink nanofibrous sheet with a smooth and soft surface containing 1250 mg/L of selenium and smaller than 50 nm. They are also amorphous with 500 nm of average diameter size. The in-situ synthesized selenium nanoparticles are well dispersed in a PVB polymer solution and located inside the fiber. These nano-selenium enriched nanofibrous sheets are new material.

## 9. REFERENCES

1. AADIL, K.R. – MUSSATTO, S.I. – JHA, H. (2018). Synthesis and characterization of silver nanoparticles loaded poly(vinyl alcohol)-lignin electrospun nanofibers and their antimicrobial activity. *International Journal of Biological Macromolecules*. 120, 763–767.
2. AHMED, M.K. – MANSOUR, S. F. – AL-WAFI, R. – EL-DEK S.I. – USKOKOVIC, V. (2019). Tuning the mechanical, microstructural, and cell adhesion properties of electrospun epsilon-polycaprolactone microfibers by doping selenium-containing carbonated hydroxyapatite as a reinforcing agent with magnesium ions. *Journal of Material Sciences*. 54, 14524–14544.
3. ALAGESAN, V. – VENUGOPAL, S. (2019): Green synthesis of selenium nanoparticle using leaves extract of *Withania somnifera* and its biological applications and photocatalytic activities. *BioNanoScience*. 9(1), 105–116.
4. ALAM, H. – KHATOON, N. – RAZA, M. – GHOSH, P.C. – SARDAR, M. (2019): Synthesis and characterization of nano selenium using plant biomolecules and their potential applications. *BioNanoScience*. 9(1), 96-104.
5. AMANCHI, NAGESWARA RAO. – MOHD MASOOD HUSSAIN. (2010): Cytotoxicity assessment of monocrotophos in *Paramecium caudatum* and *Oxytricha fallax*. *Journal of Environmental Biology*. 31 (5), 603–7.
6. AN, C. – WANG, S. (2007): Diameter-selected synthesis of single-crystalline trigonal selenium nanowires. *Materials Chemistry and Physics*. 101(2-3), 357-361.
7. ANDREONI, V. – LUISCHI, M.M. – CAVALCA, L. – ERBA, D. – CIAPPELLANO, S. (2000): Selenite tolerance and accumulation in the *Lactobacillus species*. *Annals of Microbiology*. 50, 77–88.
8. ANGAMUTHU, A. – VENKIDUSAMY, K. – MUTHUSWAMI, R.R. (2019): Synthesis and characterization of nano-selenium and its antibacterial response on some important human pathogens. *Current Science*. 116(2), 285.
9. ANNA, H. – ROBIN, D.G. – OLAV, A.C. – GRAHAM, H.L. (2007): How to use the world's scarce selenium resources efficiently to increase the selenium concentration in food. *Microbial Ecology in Health and Disease*. 19(4), 209–228.
10. ANNA, V.T. – ALEXANDER, A.K. (2017): Proteins in microbial synthesis of selenium nanoparticles. *Talanta*. 174, 539–547.

11. ANSAR, S. – ALSHEHRI, SM. – ABUDAWOOD, M. – HAMED, SS. – AHAMAD, T. (2017): Antioxidant and hepatoprotective role of selenium against silver nanoparticles. *International Journal of Nanomedicine*. 12 (October), 7789–97.
12. ARORA, S. – JAIN, J. – RAJWADE, JM. – PAKNIKAR, KM. (2008): Cellular responses induced by silver nanoparticles: in vitro studies. *Toxicology Letters*. 179(2), 93–100.
13. BADADE ZG, M.K. – NARSHETTY J.G. (2011): Oxidative stress adversely affects spermatogenesis in male infertility. *Biomedical Research*. 22(3), 323–328.
14. BAI, K. – HONG, B. – HE, J. – HONG, Z. – TAN, R. (2017): Preparation and antioxidant properties of selenium nanoparticles-loaded chitosan microspheres. *International Journal of Nanomedicine*. 12, 4527-4539.
15. BAPTISTA, P. V. – MCCUSKER, M.P. – CARVALHO, A. – FERREIRA, D.A. – MOHAN, N.M. – MARTINS, M. – FERNANDES, A.R. (2018): Nano-Strategies to Fight Multidrug Resistant Bacteria “A Battle of the Titans.” *Frontiers in Microbiology*. 9, 1441.
16. BASAGLIA, M. – TOFFANIN, A. – BALDAN, E. – BOTTEGAL, M. – SHAPLEIGH, J.P. – CASELLA, S. (2007): Selenite-reducing capacity of the copper-containing nitrite reductase of *Rhizobium sllae*. *FEMS Microbiology Letters*. 269(1), 124–130.
17. BENBOUZID, H. – BERREBBAH, H. – DJEBAR, M.R (2015): Toxicity of the *Chlorfenapyr*: Growth inhibition and induction of oxidative stress on a freshwater protozoan: *Paramecium sp.* *Advances in Environmental Biology*. 9, 281–285.
18. BENKO, I. – NAGY, G. – TANCZOS, B. – UNGVARI, E. – SZTRIK, A. – ESZENYI, P. – PROKISCH, J. – BANFALVI, G. (2012): Subacute toxicity of nano-selenium compared to other selenium species in mice. *Environmental Toxicology and Chemistry*. 31(12), 2812–2820.
19. BHATTARAI, N. – EDMONDSON, D. – VEISEH, O. – MATSEN, F.A. – ZHANG, M.Q. (2005). Electrospun chitosan-based nanofibers and their cellular compatibility. *Biomaterials*. 26, 6176– 6184.
20. BHATTARAI, N. – ZHANG, M.Q. (2007). Controlled synthesis and structural stability of alginate-based nanofibers. *Nanotechnology*. 18(45), 455601.

21. BOAKYE, M.A.D. – RIJAL, N.P. – ADHIKARI U. – BHATTARAI, N. (2015). Fabrication and characterization of electrospun PCLMgO-Keratin-based composite nanofibers for biomedical applications. *Materials*. 8(7), 4080–4090.
22. BOROUMAND, S. – SAFARI, M. – SHAABANI, E. – SHIRZAD, M. – FARIDI-MAJIDI, R. (2019): Selenium nanoparticles: Synthesis, characterization and study of their cytotoxicity, antioxidant and antibacterial activity. *Materials Research Express*. 6(8), 0850d8.
23. BRANCO VASCO. – ANA GODINHO-SANTOS. – JOAO GONCALVES. – JUN LU. – ARNE HOLMGREN. – CRISTINA CARVALHO. (2014): Mitochondrial thioredoxin system as a primary target for mercury compounds. *Toxicology Letters*. 229 (September), S57-S58.
24. BREHM, P. – ECKERT, R. (1978): An electrophysiological study of the regulation of ciliary beating frequency in *Paramecium*. *The Journal of Physiology*. 283(1), 557–568.
25. BRUMMER, F. – PIRELLI, J. – JEAN, A.H. (2014): Selenium Supplementation Strategies for Livestock in Oregon. 9.
26. BURKE, L. – MORTIMER, C.J. – CURTIS, D.J. – LEWIS, A.R. – WILLIAMS, R. – HAWKINS, K. – MAFFEIS, T.G.G. – WRIGHT, C.J. (2017): In-situ synthesis of magnetic iron-oxide nanoparticle-nanofiber composites using electrospinning. *Materials Science and Engineering: C*. 70, 512–519.
27. CAVALU, S. – KAMEL, E. – LASLO, V. – FRITEA, L. – COSTEA, T. – ANTONIAC, I.V. – VASILE, E. – ANTONIAC, A. – SEMENESCU, A. – MOHAN, A. – SACELEANU, V. – VICAS, S. (2018): Eco-friendly, facile and rapid way for synthesis of selenium nanoparticles production, structural and morphological characterization. *Revista de Chimie*. 68(12), 2963–2966.
28. CHAN, J.M. – DARKE, A.K. – PENNEY, K.L. – TANGEN, C.M. – GOODMAN, P.J. – LEE, G.M. – SUN, T. – PEISCH, S. – TINIANOW, A.M. – RAE, J.M. – KLEIN, E.A. – THOMPSON, I.M. – KANTOFF, P.W. – MUCCI, L.A. (2016): Selenium- or vitamin E-related gene variants, interaction with supplementation, and risk of high-grade prostate cancer in SELECT. *Cancer epidemiology, biomarkers & prevention: a publication of the American Association for Cancer Research, cosponsored by the American Society of Preventive Oncology*. 25(7), 1050–1058.

29. CHANGBING, W. – CHEN, H. – CHEN, D. – ZHAO, M. – LIN, Z. – GUO, M. – XU, T. – CHEN, Y. – HUA, L. – LIN, T. – TANG, Y. – ZHU, B. – LI, Y. (2020): The inhibition of H1N1 influenza virus-induced apoptosis by surface decoration of selenium nanoparticles with  $\beta$ -Thujaplicin through reactive oxygen species-mediated AKT and p53 signaling pathways. *ACS Omega*, 5(47), 30633–30642.
30. CHEN, T. – WONG, Y.S. – ZHENG, W. – BAI, Y. – HUANG, L. (2008): Selenium nanoparticles fabricated in *Undaria pinnatifida* polysaccharide solutions induce mitochondria-mediated apoptosis in A375 human melanoma cells. *Colloids and Surfaces. B, Biointerfaces*: 67(1), 26–31.
31. CHEN, H. – YOO, J. B. – LIU, Y. – ZHAO, G. (2011): Green synthesis and characterization of se nanoparticles and nanorods. *Electronic Materials Letters*. 7(4), 333-336.
32. CHEN, H. – SHIN, D.W. – NAM, J.G. – KWON, K.W. – YOO, J.B. (2010): Selenium nanowires and nanotubes synthesized via a facile template-free solution method. *Materials Research Bulletin*. 45(6), 699–704.
33. CHEN, Y. – LI, Q. – XIA, C. – YANG, F. – XU, N. – WU, Q. – HU, Y. – XIA, L. – WANG, C. – ZHOU, M. (2019): Effect of selenium supplements on the antioxidant activity and nitrite degradation of lactic acid bacteria. *World Journal of Microbiology and Biotechnology*. 35(4), 61.
34. CHIERA, N.M. – EICHLER, R. – VÖGELE, A. – TÜRLER, A. (2015). Vapor deposition coating of fused silica tubes with amorphous selenium. *Thin Solid Films*, 592, 8–13.
35. CHUNG, S. – ERCAN, B. – ROY, A.K. – WEBSTER, T.J. (2016). Addition of selenium nanoparticles to electrospun silk scaffold improves the mammalian cell activity while reducing bacterial growth. *Frontiers in Physiology*, 7.
36. CHUNG, S. – ZHOU, R. – WEBSTER, T.J. (2020): Green synthesized BSA-coated selenium nanoparticles inhibit bacterial growth while promoting mammalian cell growth. *International Journal of Nanomedicine*. 15, 115–124.
37. CREMONINI, E. – ZONARO, E. – DONINI, M. – LAMPIS, S. – BOARETTI, M. – DUSI, S. – MELOTTI, P. – LLEO, M.M. – VALLINI, G. (2016): Biogenic selenium nanoparticles: Characterization, antimicrobial activity and effects on human dendritic cells and fibroblasts. *Microbial Biotechnology*. 9(6), 758–771.

38. COLLÉN, J. – PINTO, E. – PEDERSÉN, M. – COLEPICOLO, P. (2003): Induction of oxidative stress in the red macroalga *Gracilaria tenuistipitata* by pollutant metals. *Archives of Environmental Contamination and Toxicology*. 45(3), 337–342.
39. COOPER, A. – OLDINSKI, R. – MA, H. – BRYERS, J.D. – ZHANG, M. (2013). Chitosan-based nanofibrous membranes for antibacterial filter applications. *Carbohydrate Polymers*. 92(1), 254–259.
40. COGUN, H. Y. – FIRAT, Ö. – FIRAT, Ö. – YÜZEREROĞLU, T. A. – GÖK, G. – KARGIN, F. – KÖTEMEN, Y. (2012): Protective effect of selenium against mercury-induced toxicity on hematological and biochemical parameters of *Oreochromis niloticus*. *Journal of Biochemical and Molecular Toxicology*. 26(3), 117-122.
41. COMBS G.F, JR. (2001): Selenium in global food systems. *British Journal of Nutrition*. 85(5), 517–547.
42. CSAPÓ, J. – HOLLÓ, G. – HOLLÓ, I. – SALAMON, R.V. – SALAMON, SZ. – TORÓ, SZ. – KISS, ZS.C. (2015): Production of selenium-enriched milk and dairy products. *Acta Universitatis Sapientiae, Alimentaria*, 8(1), 5–29.
43. DALTON, P.D. – GRAFAHREND, D. – KLINKHAMMER, K. – KLEE, D. – MÖLLER, M. (2007). Electrospinning of polymer melts: Phenomenological observations. *Polymer*. 48(23), 6823–6833.
44. DE MAN, J.C. – ROGOSA, M. – SHAPE, M.R. (1960): A medium for the cultivation of lactobacilli. *Journal of Applied Bacteriology*, 23, 130-135.
45. DE OLIVEIRA, GR – DE ANDRADE, C. – SOTOMAIOR, CS. – COSTA, LB. (2021): Advances in nanotechnology and the benefits of using cellulose nanofibers in animal nutrition, *Veterinary World*. 14(11): 2843-2850.
46. DEEPA, B. – GANESAN, V. (2015): Biogenic synthesis and characterization of selenium nanoparticles using the flower of *Bougainvillea spectabilis* Willd. *International Journal of Science and Research*. 4(1), 690–694
47. DERMAUW, V. – YISEHAK, K. – BELAY, D. – VAN HECKE, T. – DU LAING, G. – DUCHATEAU, L. – JANSSENS, G.P.J. (2013): Mineral deficiency status of ranging zebu (*Bos indicus*) cattle around the Gilgel Gibe catchment, Ethiopia. *Tropical Animal Health and Production*. 45(5), 1139–1147.

48. DKHIL, M.A. – KHALIL, M.F. – DIAB, M.S.M. – BAUOMY, A.A. – SANTOURLIDIS, S. – AL-SHAEBI, E.M. – AL-QURAI SHY, S. (2019): Evaluation of nanoselenium and nanogold activities against murine intestinal schistosomiasis. *Saudi Journal of Biological Sciences*. 26(7), 1468–1472.
49. DHANJAL, S. – CAMEOTRA, S.S. (2010): Aerobic biogenesis of selenium nanospheres by *Bacillus cereus* isolated from coalmine soil. *Microbial Cell Factories*. 9(1), 52.
50. DONG, R.H. – JIA, Y.X. – QIN, C. C. – ZHAN, L. – YAN, X. – CUI, L. – ZHOU, Y. – JIANG, X. – LONG, Y.Z. (2016). In situ deposition of a personalized nanofibrous dressing via a handy electrospinning device for skin wound care. *Nanoscale*. 8, 3482 –3488.
51. DOOSTMOHAMMADI, M. – FOROOTANFAR, H. – SHAKIBAIE, M. – TORKZADEH-MAHANI, M. – RAHIMI, H.R. – JAFARI, E. – AMERI, A. – AMIRHEIDARI, B. (2021). Bioactive anti-oxidative polycaprolactone/gelatin electrospun nanofibers containing selenium nanoparticles/vitamin E for wound dressing applications. *Journal of Biomaterials Applications*. 36(2), 193–209.
52. DUAN, M. – YU, S. – SUN, J. – JIANG, H. – ZHAO, J. – TONG, C. – HU, Y. – PANG, J. – WU, C. (2021): Development and characterization of electrospun nanofibers based on pullulan/chitin nanofibers containing curcumin and anthocyanins for active-intelligent food packaging. *International Journal of Biological Macromolecules*. 187, 332–340.
53. DWIVEDI, C. – SHAH, C.P. – SINGH, K. – KUMAR, M. – BAJAJ, P.N. (2011): An organic acid-induced synthesis and characterization of selenium nanoparticles. *Journal of Nanotechnology*. Article ID 651971, 1–6.
54. EC (2003): Regulation (EC) No 1831/2003 of the European Parliament and of the Council of 22 September 2003 on additives for use in animal nutrition
55. EC (2006a): Regulation (EC) No 1924/2006 of the European Parliament and of the Council of 20 December 2006 on nutrition and health claims made on foods
56. EC (2006b): Regulation (EC) No 1925/2006 of the European Parliament and of the Council of 20 December 2006 on the addition of vitamins and minerals and of certain other substances to foods.
57. ECKERT, R. – NAITOH, Y. (1972): Bioelectric Control of Locomotion in the Ciliates. *The Journal of Protozoology*. 19(2), 237–43.

58. EFSA PANEL on DIETETIC PRODUCTS, NUTRITION and ALLERGIES (NDA). (2010): Scientific opinion on the substantiation of health claims related to selenium and maintenance of normal hair (ID 281), maintenance of normal nails (ID 281), protection against heavy metals (ID 383), maintenance of normal joints (ID 409), maintenance of normal thyroid function (ID 410, 1292), protection of DNA, proteins and lipids from oxidative damage (ID 410, 1292), and maintenance of the normal function of the immune system (ID 1750) according to Article 13(1) of Regulation (EC) No 1924/2006. *EFSA Journal*, 8(10), 1727.
59. EFSA PANEL ON DIETETIC PRODUCTS, NUTRITION AND ALLERGIES. (2014): Scientific opinion on dietary reference values for selenium. *EFSA Journal*, 12(10), 3846.
60. EFSA PANEL ON ADDITIVES AND PRODUCTS OR SUBSTANCES USED IN ANIMAL FEED (FEEDAP). (2012): Scientific Opinion on safety and efficacy of selenium in the form of organic compounds produced by the selenium-enriched yeast *Saccharomyces cerevisiae* NCYC R646 (Selemax 1000/2000) as feed additive for all species. *EFSA Journal*. 10(7), 2778.
61. EFSA PANEL ON ADDITIVES AND PRODUCTS OR SUBSTANCES USED IN ANIMAL FEED (FEEDAP). (2016). Safety and efficacy of selenium compounds (E8) as feed additives for all animal species: Sodium selenite, based on a dossier submitted by Todini and Co SpA. *EFSA Journal*. 14(3), 4442
62. EL-DEEP, M.H. – AMBER, K.A. – ELGENDY, S. – DAWOOD, M.A.O. – ZIDAN, A. (2020): In ovo injection of nano-selenium spheres mitigates the hatchability, histopathology image and immune response of hatched chicks. *Journal of Animal Physiology and Animal Nutrition*, 104(5), 1392–1400.
63. EL-RAMADY, H. – FAIZY, S.E.-D. – ABDALLA, N. – TAHA, H. – DOMOKOS-SZABOLCSY, É. – FARI, M. – ELSAKHAWY, T. – OMARA, A.E.-D. – SHALABY, T. – BAYOUMI, Y. – SHEHATA, S. – GEILFUS, C.-M. – BREVIK, E.C. (2020): Selenium and Nano-Selenium Biofortification for Human Health: Opportunities and Challenges. *Soil Systems*, 4(3), 57.
64. EMA/CVMP (2015): European Medicines Agency, Committee for Medicinal Products for Veterinary Use. European public MRL assessment report (EPMAR). Potassium selenate (All food producing species), sodium selenate (All food

- producing species), sodium selenite (All food producing species). EMA/CVMP/187590/2015.
65. EMA/CVMP (2015). European Medicines Agency, Committee for Medicinal Products for Veterinary Use. European public MRL assessment report (EPMAR) for barium selenate in all food producing species, EMA/CVMP/160082/2014.
  66. ESTEVAM, E.C. – GRIFFIN, S. – NASIM, M. J. – DENEZHKIN, P. – SCHNEIDER, R. – LILISCHKIS, R. – DOMINGUEZ-ALVAREZ, E. – WITEK, K. – LATACZ, G. – KECK, C. – SCHÄFER, K.-H. – KIEĆ-KONONOWICZ, K. – HANDZLIK, J. – JACOB, C. (2017): Natural selenium particles from *Staphylococcus carnosus*: Hazards or particles with particular promise? Journal of Hazardous Materials. 324, 22-30.
  67. ESZENYI, P. – SZTRIK, A. – BABKA, B. – PROKISCH, J. (2011): Elemental, nano-sized (100–500 nm) selenium production by probiotic Lactic acid bacteria. International Journal of Bioscience, Biochemistry and Bioinformatics. 148-152.
  68. EUROPEAN COMMISSION, DIRECTORATE-GENERAL FOR HEALTH AND FOOD SAFETY. (2019): Commission Implementing Regulation (EU) 2019/49 of 4 January 2019 concerning the authorization of sodium selenite, coated granulated sodium selenite and zinc-L-selenomethionine as feed additives for all animal species. C/2018/8845.
  69. FARDSADEGH, B. – VAGHARI, H. – MOHAMMAD-JAFARI, R. – NAJIAN, Y. – JAFARIZADEH-MALMIRI, H. (2019): Biosynthesis, characterization and antimicrobial activities assessment of fabricated selenium nanoparticles using *Pelargonium zonale* leaf extract. Green Processing and Synthesis. 8(1), 191–198.
  70. FAO/WHO. (2001): Human Vitamin and Mineral Requirements. Report of a Joint FAO/WHO Expert Consultation, Bangkok, Thailand.
  71. FARIAS, VB. – PIRZADA, T. – MATHEW, R – SIT, TL. – OPPERMAN, C. – KHAN, SA. (2019): Electrospun polymer nanofibers as seed coatings for crop protection. ACS Sustainable Chemistry & Engineering. 7 (24), 19848–19856.
  72. FERNANDES, A.P. – WALLEMBERG, M. – GANDIN, V. – MISRA, S. – TISATO, F. – MARZANO, C. – RIGOBELLO, M.P. – KUMAR, S. – BJÖRNSTEDT, M. (2012): Methylselenol formed by spontaneous methylation of selenide is a superior selenium substrate to the thioredoxin and glutaredoxin systems. PloS One. 7(11), e50727.

73. FESHARAKI, P.J. – NAZARI, P. – SHAKIBAIE, M. – REZAIIE, S. – BANOEE, M. – ABDOLLAHI, M. – SHAHVERDI, A.R. (2010): Biosynthesis of selenium nanoparticles using *Klebsiella pneumoniae* and their recovery by a simple sterilization process. *Brazilian Journal of Microbiology*. 41, 461–466.
74. FORDYCE, F. (2007): Selenium geochemistry and health. *AMBIO: A Journal of the Human Environment*. 36(1), 94–97.
75. FORGHANI, S. – ALMASI, H. – MORADI, M. (2021): Electrospun nanofibers as food freshness and time-temperature indicators: A new approach in food intelligent packaging. *Innovative Food Science & Emerging Technologies*. 73, 102804.
76. FREITAS, A. – FUNCK, V. – ROTTA, M. – BOHRER, D. – MÖRSCHBÄCHER, V. – PUNTEL, R. – NOGUEIRA, C. – FARINA, M. – ASCHNER, M. – ROCHA, J. B. (2009): Diphenyl diselenide, a simple organoselenium compound, decreases methylmercury-induced cerebral, hepatic and renal oxidative stress and mercury deposition in adult mice. *Brain Research Bulletin*. 79(1), 77–84.
77. GALADARI, S. – RAHMAN, A. – PALLICHANKANDY, S. – THAYYULLATHIL, F. (2017): Reactive oxygen species and cancer paradox: To promote or to suppress? *Free radical biology & medicine*. 104, 144–164.
78. GALBRAITH, M.L. – VORACHEK, W.R. – ESTILL, C.T. – WHANGER, P.D. – BOBE, G. – DAVIS, T.Z. – HALL, J.A. (2016): Rumen microorganisms decrease bioavailability of inorganic selenium supplements. *Biological Trace Element Research*. 171(2), 338–343.
79. GALLEGO-VILLAR, L. – PÉREZ, B. – UGARTE, M. – DESVIAT, L.R. – RICHARD, E. (2014). Antioxidants successfully reduce ROS production in propionic acidemia fibroblasts. *Biochemical and Biophysical Research Communications*. 452(3), 457–461.
80. GANGADOO, S. – STANLEY, D. – HUGHES, R.J. – MOORE, R.J. – CHAPMAN, J. (2017): The synthesis and characterization of highly stable and reproducible selenium nanoparticles. *Inorganic and Nano-Metal Chemistry*. 47(11), 1568–1576.
81. GARCÍA, D. A. – MENDOZA, L. – VIZUETE, K. – DEBUT, A. – ARIAS, M.T. – GAVILANES, A. – TERCENIO, T. – ÁVILA, E. – JEFFRYES, C. – DAHOUMANE, S.A. (2020): Sugar-mediated green synthesis of silver selenide semiconductor nanocrystals under ultrasound irradiation. *Molecules*. 25(21), 5193.

82. GATES, B. – MAYERS, B. – CATTLE, B. – XIA, Y. (2002): Synthesis and characterization of uniform nanowires of trigonal selenium. *Advanced Functional Materials*. 12(3), 219-227.
83. GAO, X. – ZHANG, J – ZHANG, L. (2000). Acute toxicity and bioavailability of nano red elemental selenium. *Wei Sheng Yan Jiu*. 29(1), 57–58.
84. LGOMATHI, K. – GOPINATH, D. – RAFIUDDIN AHMED, M. – JAYAKUMAR, R. (2003). Quercetin incorporated collagen matrices for dermal wound healing processes in rat. *Biomaterials*. 24(16), 2767–2772.
85. GOPINATH, P. – GOGOI, S.K. – SANPUI, P. – PAUL, A. – CHATTOPADHYAY, A. – GHOSH, S.S. (2010): Signaling gene cascade in silver nanoparticle induced apoptosis. *Colloids Surface B: Biointerfaces*. 77(2), 240–245.
86. GULYÁS, G. – CSOSZ, E. – JOE, P. – JÁVOR, A. – MEZES, M. – ERDELYI, M. – BALOGH, K. – JANAKY, T. – SZABO, Z. – SIMON, Á. – CZEGLÉDI, L. (2016): Effect of nano-sized, elemental selenium supplement on the proteome of chicken liver. *Journal of Animal Physiology and Animal Nutrition*. 101, 502–510.
87. GUNTI, L. – DASS, R.S. – KALAGATUR, N.K. (2019): Phytofabrication of selenium nanoparticles from *Emblica officinalis* fruit extract and exploring its biopotential applications: antioxidant, antimicrobial, and biocompatibility. *Frontiers in Microbiology*. 10.
88. GUPTA, M. – SHIKHA GUPTA. (2017): An overview of selenium uptake, metabolism, and toxicity in plants. *Frontiers in Plant Science*. 7, 2074.
89. HALL, J.A. – BOBE, G. – HUNTER, J.K. – VORACHEK, W.R. – STEWART, W.C. – VANEGAS, J.A. – ESTILL, C.T. – MOSHER, W.D. – PIRELLI, G.J. (2013): Effect of Feeding Selenium-Fertilized Alfalfa Hay on Performance of Weaned Beef Calves. *PLoS ONE*. 8(3), e58188.
90. HAGEMAN, S.P.W. – VAN DER WEIJDEN, R.D. – STAMS, A.J.M. – BUISMAN, C.J.N. (2017): Bio-production of selenium nanoparticles with diverse physical properties for recovery from water. *International Journal of Mineral Processing*. 169, 7–15.
91. HAO, P. – ZHU, Y. – WANG, S. – WAN, H. – CHEN, P. – WANG, Y. – CHENG, Z. – LIU, Y. – LIU, J. (2017): Selenium administration alleviates toxicity of chromium(VI) in the chicken brain. *Biological Trace Element Research*. 178(1), 127–135.

92. HASHMI, M. – ULLAH, S. – KIM, I.S. (2019): Copper oxide (CuO) loaded polyacrylonitrile (PAN) nanofiber membranes for antimicrobial breath mask applications. *Current Research in Biotechnology*. 1, 1–10.
93. HASSANIN, KMA. – EL-KAWI, S.A. – KHALID, S.H. (2013): The prospective protective effect of selenium nanoparticles against chromium induced oxidative and cellular damage in rat thyroid. *International Journal of Nanomedicine*. 8, 1713–1720
94. HINTZE, K.J. – LARDY, G.P. – MARCHELLO, M.J. – FINLEY, J.W. (2002): Selenium accumulation in beef: Effect of dietary selenium and geographical area of animal origin. *Journal of Agricultural and Food Chemistry*. 50(14), 3938–3942.
95. HUANG, L. – NAGAPUDI, K. P. – APKARIAN, R. – CHAIKOF, E.L. (2001). Engineered collagen–PEO nanofibers and fabrics. *Journal of Biomaterials Science, Polymer Edition*. 12(9), 979–993.
96. HUANG, Z.M. – ZHANG, Y.Z. – KOTAKI, M. – RAMAKRISHNA, S. (2003). A review on polymer nanofibers by electrospinning and their applications in nanocomposites. *Composites Science and Technology*. 63, 2223–53.
97. HUANG, Z.M. – ZHANG, Y.Z. – RAMAKRISHNA, S. – LIM, C.T. (2004). Electrospinning and mechanical characterization of gelatin nanofibers. *Polymer*. 45, 5361–5368.
98. HUANG, Y. – MIAO, Y.-E. – LIU, T. (2014): Electrospun fibrous membranes for efficient heavy metal removal. *Journal of Applied Polymer Science*, 131(19).
99. HUSSAIN, MOHD. – MASOOD, NAGESWARA RAO AMANCHI. – VENKATA RAMANAIAH SOLANKI. – MOHAN BHAGAVATHI. (2008): Low cost microbioassay test for assessing cytopathological and physiological responses of ciliate model *Paramecium caudatum* to carbofuran pesticide. *Pesticide Biochemistry and Physiology*. 90(1), 66–70.
100. HUIZHEN, K. – EMMA, F. – PLINNIO, G. –JESSE, C. – QUFU, W. – BENJAMIN, C. – ABDULLAH, A. – RADWAN, A. – BENJAMIN, S.H. (2016). Electrospun polystyrene nanofibrous membranes for direct contact membrane distillation. *Journal of Membrane Science*, 515.
101. IKEMOTO, T. – KUNITO, T. – TANAKA, N. – BABA, N. – MIYAZAKI, N. – TANABE, S. (2004): Detoxification mechanism of heavy metals in marine mammals and seabirds: Interaction of selenium with mercury, silver, copper, zinc,

- and cadmium in liver. *Archives of Environmental Contamination and Toxicology*. 47, 402–413.
102. IGNATOVA, M. – MANOLOVA, N. – RASHKOV, I. (2007). Electrospinning of poly(vinyl pyrrolidone-iodine complex and poly(ethylene oxide)/poly(vinyl pyrrolidone)-iodine complex – A prospective route to antimicrobial wound dressing materials. *European Polymer Journal*. 43, 1609–1623.
  103. ILONA, B. – NAGY, G. – TANCZOS, B. – UNGVARI, E. – SZTRIK, A. – ESZENYI, P. – PROKISCH, J. – GASPAR, B. (2012). Subacute toxicity of nano-selenium compared to other selenium species in mice. *Environmental Toxicology and Chemistry*. 31, 2812–2820.
  104. JAIN, R. – JORDAN, N. – WEISS, S. – FOERSTENDORF, H. – HEIM, K. – KACKER, R. – HÜBNER, R. – KRAMER, H. – VAN HULLEBUSCH, E.D. – FARGES, F. – LENS, P.N.L. (2015): Extracellular polymeric substances govern the surface charge of biogenic elemental selenium nanoparticles. *Environmental Science & Technology*. 49(3), 1713–1720.
  105. JALIL, A.I.A. – ISMAIL, S. (2019): Adsorption of methylene blue via electrospun polyvinyl butyral/bentonite. *AIP Conference Proceedings* 2124. 030010.
  106. JEONG, L. – LEE, K.Y. – PARK, W.H. (2007). Effect of solvent on the characteristics of electrospin regenerated silk fibroin nanofibers. *ASBM7: Advanced Biomaterials VII*. 342–343, 813–816.
  107. JIA, X. – LI, N. – CHEN, J. (2005): A subchronic toxicity study of elemental Nano-Se in Sprague-Dawley rats. *Life Sciences*. 76(17), 1989–2003.
  108. JIA, H. – ZHU, G. – VUGRINOVICH, B. – KATAPHINAN, W. – RENEKER, D.H. – WANG, P. (2002). Enzyme-carrying polymeric nanofibers prepared via electrospinning for use as unique biocatalysts. *Biotechnology Progress*. 18(5), 1027–1032.
  109. JIN, W.-J. – LEE, H.K. – JEONG, E.H. – PARK, W.H. – YOUK, J.H. (2005). Preparation of polymer nanofibers containing silver nanoparticles by using Poly(N-vinylpyrrolidone). *Macromolecular Rapid Communications*. 26(24), 1903–1907.
  110. JOO KIM, H. – RAJ PANT, H. – HEE KIM, J. – JUNG CHOI, N. – SANG KIM, C. (2014): Fabrication of multifunctional TiO<sub>2</sub>-fly ash/polyurethane nanocomposite membrane via electrospinning. *Ceramics International*. 40(2), 3023–3029.

111. JOSHI, M. – BHATTACHARYYA, A. – ALI, S.W. (2008): Characterization techniques for nanotechnology applications in textiles. *Indian Journal of Fibre & Textile Research*. 33, 304–317.
112. KAMARUZAMAN, N.A. – YUSOFF, A.R.M. – BUANG, N.A. – SALLEH, N.G.N. (2017). Effects on diameter and morphology of polycaprolactone nanofibers infused with various concentrations of selenium nanoparticles. Langkawi, Malaysia. 020013.
113. KAMARUZAMAN, N.A. – YUSOFF, A.R.M. – MALEK, N.A.N.N. – TALIB, M. (2021). Fabrication, characterization and degradation of electrospun poly( $\epsilon$ -caprolactone) infused with selenium nanoparticles. *Malaysian Journal of Fundamental and Applied Sciences*. 17(3), 295–305.
114. KANG, M. – JUNG, R. – KIM, H.-S. – YOUK, J.H. – JIN, H.-J. (2007). Silver nanoparticles incorporated electrospun silk fibers. *Journal of Nanoscience and Nanotechnology*. 7(11), 3888–3891.
115. KAPUR, M. – SONI, K. – KOHLI, K. (2017): Green synthesis of selenium nanoparticles from *Broccoli*, characterization, application and toxicity. *Advanced Techniques in Biology & Medicine*. 05(01).
116. KARUPPANNAN, C. – SIVARAJ, M. – KUMAR, J.G. – SEERANGAN, R. – BALASUBRAMANIAN, S. – GOPAL, D.R. (2017): Fabrication of progesterone-loaded nanofibers for the drug delivery applications in bovine. *Nanoscale Research Letters*. 12(1), 116.
117. KAUR, R. – KAUDAL, T. – SHARMA, A. (2018): Probiotic mediated synthesis of selenium nanoparticles: characterization and biofilm scavenging analysis. *Research Journal of Life Sciences, Bioinformatics, Pharmaceutical and Chemical Sciences*. 4(3), 291.
118. KAZEMPOUR, Z.B. – YAZDI, M.H. – RAFII, F. – SHAHVERDI, A.R. (2013): Sub-inhibitory concentration of biogenic selenium nanoparticles lacks post antifungal effect for *Aspergillus niger* and *Candida albicans* and stimulates the growth of *Aspergillus niger*. *Iranian Journal of Microbiology*. 5(1), 81–85.
119. KESSI, J. – HANSELMANN, K. W. (2004): Similarities between the abiotic reduction of selenite with glutathione and the dissimilatory reaction mediated by *Rhodospirillum rubrum* and *Escherichia coli*. *Journal of Biological Chemistry*. 279(49), 50662–50669.

120. KIELISZEK, MAREK. – STANISŁAW BŁAŻEJAK. (2016). Current knowledge on the importance of selenium in food for living organisms: A Review. *Molecules*. 21(5), E609.
121. KIM, T.S. – YUN, B.Y. – KIM, I.Y. (2003). Induction of the mitochondrial permeability transition by selenium compounds mediated by oxidation of the protein thiol groups and generation of the superoxide. *Biochemical Pharmacology*. 66(12), 2301–2311.
122. KIM, C.W. – FREY, M.W. – MARQUEZ, M. – JOO, Y.L. (2005). Preparation of submicron-scale, electrospun cellulose fibers via direct dissolution. *Journal of Polymer Science Part B: Polymer Physics*. 43, 1673–1683.
123. KIM, H.S. – YOO, H.S. (2010). MMPs-responsive release of DNA from electrospun nanofibrous matrix for local gene therapy: In vitro and in vivo evaluation. *Journal of Control Release*. 145(3), 264–271.
124. KHIL, M.S. – CHA, D. – KIM, H.Y. – KIM, I.S. – BHATTARAI, N. (2003). Electrospun nanofibrous polyurethane membrane as wound dressing. *Journal of Biomedical Materials Research Part B: Applied Biomaterials*. 67B, 675–679.
125. KOMALA, Z. (1995): Notes on the use of invertebrates, especially ciliates, in studies on pollution and toxicity. *Folia Biologica*, 43(1–2), 25–27.
126. KOJOURI, G.A. – SADEGHIAN, S. – MOHEBBI, A. – DEZFOULI, M.R.M. (2012): The effects of oral consumption of selenium nanoparticles on chemotactic and respiratory burst activities of neutrophils in comparison with sodium selenite in sheep. *Biological Trace Element Research*. 146(2), 160–166.
127. KORA, A.J. – RASTOGI, L. (2016): Biomimetic synthesis of selenium nanoparticles by *Pseudomonas aeruginosa* ATCC 27853: An approach for conversion of selenite. *Journal of Environmental Management*. 181, 231–236.
128. KORA, A.J. – RASTOGI, L. (2017): Bacteriogenic synthesis of selenium nanoparticles by *Escherichia coli* ATCC 35218 and its structural characterization. *IET Nanobiotechnology*. 11(2), 179–184.
129. KVITEK LIBOR. – MARKETA VANICKOVA. – ALES PANACEK. – JANA SOUKUPOVA. – MILAN DITTRICH. – EVA VALENTOVA. – ROBERT PRUCEK. – MARTINA BANCIROVA. – DAVID MILDE. – RADEK ZBORIL. (2009): Initial study on the toxicity of silver nanoparticles (NPs) against *Paramecium caudatum*. *The Journal of Physical Chemistry*. C 113(11), 4296–4300.

130. KWAN, J. – KIM, C.H. – DUNN, L.L. – SCHIESSER, C.H. – DAVIES, M.J. (2016). A novel selenium compound enhances wound closure and improves microvascular perfusion: implications for wound healing. *Free Radical Biology and Medicine*. 100, S72–S73.
131. LAMBERTI, C. – MANGIAPANE, E. – PESSIONE, A. – MAZZOLI, R. – GIUNTA, C. – PESSIONE, E. (2011): Proteomic characterization of a selenium-metabolizing probiotic *Lactobacillus reuteri* Lb2 BM for nutraceutical applications. *PROTEOMICS*. 11(11), 2212–2221.
132. LAMPIS, S. – ZONARO, E. – BERTOLINI, C. – BERNARDI, P. – BUTLER, C.S. – VALLINI, G. (2014). Delayed formation of zero-valent selenium nanoparticles by *Bacillus mycoides* SeITE01 as a consequence of selenite reduction under aerobic conditions. *Microbial Cell Factories*. 13(1), 35.
133. LAMPIS, S. – ZONARO, E. – BERTOLINI, C. – CECCONI, D. – MONTI, F. – MICARONI, M. – TURNER, R.J. – BUTLER, C.S. – VALLINI, G. (2017): Selenite biotransformation and detoxification by *Stenotrophomonas maltophilia* SeITE02: Novel clues on the route to bacterial biogenesis of selenium nanoparticles. *Journal of Hazardous Materials*. 324(Pt A), 3–14.
134. LENZ, M. – VAN AELST, A.C. – SMIT, M. – CORVINI, P.F.X. – LENS, P.N. L. (2009): Biological Production of Selenium Nanoparticles from Waste Waters. *Advanced Materials Research*. 71–73, 721–724.
135. LEON, S.A. – BERGMANN, F. (1968): Properties and biological activity of a new peptide antibiotic (Colisan). *Biotechnology and Bioengineering*. 10(4), 429–444.
136. LEU, J.G. – CHEN, S.A. – CHEN, H.M. – WU, W.M. – HUNG, C.F. – YAO, Y.D. – TU, C.S. – LIANG, Y.J. (2012). The effects of gold nanoparticles in wound healing with antioxidant epigallocatechin gallate and  $\alpha$ -lipoic acid. *Nanomedicine: nanotechnology, biology, and medicine*. 8(5), 767–775.
137. LI, Q. – YAM, V.W.-W. (2006): High-yield synthesis of selenium nanowires in water at room temperature. *Chemical Communications*. 9, 1006–1008.
138. LI, S. – SHEN, Y. – XIE, A. – YU, X. – ZHANG, X. – YANG, L. – LI, C. (2007): Rapid, room-temperature synthesis of amorphous selenium/protein composites using *Capsicum annuum* L extract. *Nanotechnology*. 18, 405101.

139. LI, Q. – CHEN, T. – YANG, F. – LIU, J. – ZHENG, W. (2010): Facile and controllable one-step fabrication of selenium nanoparticles assisted by L-cysteine. *Materials Letters*. 64(5), 614–617.
140. LI, J. – LIANG, D. – QIN, S. – FENG, P. – WU, X. (2015): Effects of selenite and selenate application on growth and shoot selenium accumulation of pak choi (*Brassica chinensis* L.) during successive planting conditions. *Environmental Science and Pollution Research International*. 22(14), 11076–11086.
141. LI, H. – SHI, W. – ZENG, X. – HUANG, S. – ZHANG, H. – QIN, X. (2020): Improved desalination properties of hydrophobic GO-incorporated PVDF electrospun nanofibrous composites for vacuum membrane distillation. *Separation and Purification Technology*. 230, 115889.
142. LI, J. – LAING, G.D. – FERRER, I. – LENS, P.N.L. (2021): Selenium biofortification for human and animal nutrition. Chapter 9. *Environmental Technologies to Treat Selenium Pollution: Principles and Engineering*. IWA Publishing. 270.
143. LIMA, L.W. – SCHIAVON, M. (2021): Selenium hyperaccumulation in plants. Chapter 8. *Environmental Technologies to Treat Selenium Pollution: Principles and Engineering*. IWA Publishing.
144. LIN, Z.H. – CHRIS WANG, C.R. (2005): Evidence on the size-dependent absorption spectral evolution of selenium nanoparticles. *Materials Chemistry and Physics*. 92(2–3), 591–594.
145. LIN, W. – ZHANG, J. – XU, J.-F. – PI, J. (2021): The advancing of selenium nanoparticles against infectious diseases. *Frontiers in Pharmacology*. 12, 1971.
146. LING, K. – HENNO, M. – JÖUDU, I. – PÜSSA, T. – JAAKSON, H. – KASS, M. – ANTON, D. – OTS, M. (2017): Selenium supplementation of diets of dairy cows to produce Se-enriched cheese. *International Dairy Journal*. 71, 76–81.
147. LITTLE, EDWARD E. – SUSAN E. FINGER. (1990): Swimming behavior as an indicator of sublethal toxicity in fish. *Environmental Toxicology and Chemistry*. 9(1), 13–19.
148. LIU, W. – LI, X. – WONG, Y.S. – ZHENG, W. – ZHANG, Y. – CAO, W. – CHEN, T. (2012). Selenium nanoparticles as a carrier of 5-fluorouracil to achieve anticancer synergism. *ACS Nano*. 6(8), 6578–6591.

149. LU, W.-C. – CHEN, C.-Y. – CHO, C.-J. – VENKATESAN, M. – CHIANG, W.-H. – YU, Y.-Y. – LEE, C.-H. – LEE, R.-H. – RWEI, S.-P. – KUO, C.-C. (2021): Antibacterial activity and protection efficiency of polyvinyl butyral nanofibrous membrane containing thymol prepared through vertical electrospinning. *Polymers*. 13(7), 1122.
150. LUESAKUL, U. – KOMENEK, S. – PUTHONG, S. – MUANGSIN, N. (2016): Shape-controlled synthesis of cubic-like selenium nanoparticles via the self-assembly method. *Carbohydrate Polymers*. 153, 435–444.
151. LU JUN. – ARNE HOLMGREN. (2014): The thioredoxin antioxidant system. *Free Radical Biology and Medicine, Antioxidants*. 66 (January), 75–87.
152. LUO, H. – WANG, F. – BAI, Y. – CHEN, T. – ZHENG, W. (2012): Selenium nanoparticles inhibit the growth of HeLa and MDA-MB-231 cells through induction of S phase arrest. *Colloids Surf B Biointerfaces*. 94, 304–308.
153. MACKEVICA, A. – SKJOLDING, L.M. – GERGS, A. – PALMQVIST, A. – BAUN A. (2015): Chronic toxicity of silver nanoparticles to *Daphnia magna* under different feeding conditions. *Aquatic Toxicology*. 161, 10–16.
154. MAEDA, S. – KATO, T. – KOGURE, H. – HOSOYA, N. (2015): Rapid response of thermo-sensitive hydrogels with porous structures. *Applied Physics Letters*. 106(17), 171909.
155. MALHOTRA, S. – JHA, N. – DESAI, K. (2014): A Superficial synthesis of selenium nanospheres using wet chemical approach. *International Journal of Nanotechnology and Application (IJNA)*. 3(4), 7–14.
156. MACKINTOSH, S.B. – SERINO, L.P. – IDDON, P.D. – BROWN, R. – CONLAN, R.S. – WRIGHT, C.J. – MAFFEIS, T.G.G. – RAXWORTHY, M.J. – SHELDON, I.M. (2015). A three-dimensional model of primary bovine endometrium using an electrospun scaffold. *Biofabrication*. 7(2), 025010.
157. MARTIN, R.B. – PHILIP, J. W. – ROSIE, J.B. – MARK, C.M. – HELEN, C.B. – SARAH, E.J. – MALCOLM, J.H. – STEVE, P.M. – FANG-JIE, Z. – NEIL, B. – MILES, H. – MARK, T. (2006): Biofortification of UK food crops with selenium. *Proceedings of the Nutrition Society*. 65(2), 169–181.
158. MATTHEWS, J.A. – WNEK, G.E. – SIMPSON, D.G. – BOWLIN, G.L. (2002). Electrospinning of collagen nanofibers. *Biomacromolecules*. 3(2), 232–238.

159. MEDINA CRUZ, D. – MI, G. – WEBSTER, T.J. (2018): Synthesis and characterization of biogenic selenium nanoparticles with antimicrobial properties made by *Staphylococcus aureus*, methicillin-resistant *Staphylococcus aureus* (MRSA), *Escherichia coli*, and *Pseudomonas aeruginosa*. *Journal of Biomedical Materials Research. Part A*, 106(5), 1400–1412.
160. MEGELSKI, S. – STEPHENS, J.S. – CHASE, D.B. – RABOLT, J.F. (2002). Micro- and nanostructured surface morphology on electrospun polymer fibers. *Macromolecules*. 35(22), 8456–8466.
161. MENG, Z.X. – ZHENG W. – LI, W.L. – ZHENG, Y.F. (2010). Fabrication and characterization of three-dimensional nanofiber membrane of PCL–MWCNTs by Electrospinning. *Materials Science and Engineering C*. 30, 1014–1021.
162. MENON, S. – SHRUDHI DEVI, K.S. – AGARWAL, H. – SHANMUGAM, V.K. (2019): Efficacy of biogenic selenium nanoparticles from an extract of ginger towards evaluation on anti-microbial and anti-oxidant activities. *Colloid and Interface Science Communications*. 29, 1-8.
163. MEHRBOD, P. – MOTAMED, N. – TABATABAIAN, M. – ESTYAR, R.S. – AMINI, E. – SHAHIDI, M. – KHEIRI, M.T. (2015): In Vitro Antiviral Effect of “Nanosilver” on Influenza Virus. *DARU Journal of Pharmaceutical Sciences*. 17(2), 88–93.
164. MILEWSKI, S. – SOBIECH, P. – BŁAŻEJAK-GRABOWSKA, J. – WÓJCIK, R. – ŻARCZYŃSKA, K. – MICIŃSKI, J. – ZĄBEK, K. (2021): The Efficacy of a Long-Acting Injectable Selenium Preparation Administered to Pregnant Ewes and Lambs. *Animals*, 11(4), 1076.
165. MISHRA, R.R. – PRAJAPATI, S. – DAS, J. – DANGAR, T.K. – DAS, N. – THATOI, H. (2011): Reduction of selenite to red elemental selenium by moderately halotolerant *Bacillus megaterium* strains isolated from Bhitarkanika mangrove soil and characterization of reduced product. *Chemosphere*. 84(9), 1231–1237.
166. MITTAL, M. – SIDDIQUI, M.R. – TRAN, K. – REDDY, S.P. – MALIK, A.B. (2014). Reactive oxygen species in inflammation and tissue injury. *Antioxidants & Redox Signaling*. 20(7), 1126–1167.
167. MRÁZOVÁ, J. – GAŽAROVÁ, M. – KOPČEKOVÁ, J. – KOLESÁROVÁ, A. – BUČKO, O. – BOBČEK, B. (2020): The effect of consumption of pork enriched by organic selenium on selenium status and lipid profile in blood serum of

- consumers. *Journal of Environmental Science and Health. Part. B, Pesticides, Food Contaminants, and Agricultural Wastes.* 55(1), 69–74.
168. MOHAMMAD, A.W. – TEOW, Y.H. – ANG, W.L. – CHUNG, Y.T. – OATLEY-RADCLIFFE, D.L. – HILAL, N. (2015): Nanofiltration membranes review: Recent advances and future prospects. *Desalination.* 356, 226–254.
169. MONDAL, K. – ROY, P. – SRIVASTAVA, S.K. (2008): Facile biomolecule-assisted hydrothermal synthesis of trigonal selenium microrods. *Crystal Growth and Design.* 8 (5), 1580-1584.
170. MONTAZER, M. – SHAMEI, A. – ALIMOHAMMADI, F. (2014). Synthesis of nanosilver on polyamide fabric using silver/ammonia complex. *Materials Science and Engineering: C.* 38, 170–176.
171. MORENO-MARTIN, G. – PESCUA, M. – PÉREZ-CORONA, T. – MOZZI, F. – MADRID, Y. (2017): Determination of size and mass-and number-based concentration of biogenic SeNPs synthesized by lactic acid bacteria by using a multimethod approach. *Analytica Chimica Acta.* 992, 34–41.
172. MORTUZA, M.G. – TAKAHASHI, T. – TATSUYA UEKI, – KOSAKA, T. – MICHIBATA, H. – HOSOYA, H. (2005): Toxicity and bioaccumulation of hexavalent chromium in green Paramecium, *Paramecium bursaria*. *Journal of Health Science.* 51(6), 676–682.
173. MULLA, N.A. – OTARI, S.V. – BOHARA, R.A. – YADAV, H.M. – PAWAR, S.H. (2020): Rapid and size-controlled biosynthesis of cytocompatible selenium nanoparticles by *Azadirachta indica* leaves extract for antibacterial activity. *Materials Letters.* 264, 127353.
174. NAITOH, Y. (1966): Reversal Response Elicited in Nonbeating Cilia of Paramecium by Membrane Depolarization. *Science.* 154(3749), 660–662.
175. NICASTRO, H. L. – DUNN, B.K. (2013): Selenium and prostate cancer prevention: Insights from the selenium and vitamin E cancer prevention trial (SELECT). *Nutrients.* 5(4), 1122–1148.
176. NRC. (1985): *Nutrient Requirements of Sheep.* 6<sup>th</sup> edition. The National Academies Press. Washington, DC, USA.
177. NRC. (2001): *Nutrient Requirements of Dairy Cattle.* 7<sup>th</sup> Revised edition. The National Academies Press. Washington, DC, USA.

178. NRC (2005). Mineral Tolerance of Animals: 2<sup>nd</sup> Revised edition. The National Academies Press. Washington, DC. USA.
179. ORTMAN, K. – PEHRSON, B. (1999): Effect of selenate as a feed supplement to dairy cows in comparison to selenite and selenium yeast. *Journal of Animal Science*. 77(12), 3365–3370.
180. OHKAWA, K. – CHA, D.I. – KIM, H. – NISHIDA, A. – YAMAMOTO, H. (2004). Electrospinning of chitosan. *Macromolecular Rapid Communications*. 25, 1600–1605.
181. OSANLOO M, – ARISH J, – SERESHTI H (2020): Developed methods for the preparation of electrospun nanofibers containing plant derived oil or essential oil: A systematic review. *Polymer Bulletin*. 77, 6085–6104.
182. PAGAR, T. – GHOTEKAR, S. – PAGAR, K. – PANSAMBAL, S. – OZA, R. (2019): A review on bio-synthesized Co<sub>3</sub>O<sub>4</sub> nanoparticles using plant extracts and their diverse applications. *Journal of Chemical Reviews*. 1(4), 260–270.
183. PALOMO-SIGUERO, M. – GUTIÉRREZ, A.M. – PÉREZ-CONDE, C. – MADRID, Y. (2016): Effect of selenite and selenium nanoparticles on lactic bacteria: A multi-analytical study. *Microchemical Journal*. 126, 488–495.
184. PAN, S.F. – KE, X.X. – WANG, T.Y. – LIU, Q. – ZHONG, L.B. – ZHENG, Y.M. (2019). Synthesis of silver nanoparticles embedded electrospun PAN nanofiber thin-film composite forward osmosis membrane to enhance performance and antimicrobial activity. *Industrial & Engineering Chemistry Research*. 58(2), 984–993.
185. PAPPAS, A.C. – ACAMOVIC, T. – SPARKS, N.H.C. – SURAI, P.F. – MCDEVITT, R.M. (2005): Effects of supplementing broiler breeder diets with organic selenium and polyunsaturated fatty acids on egg quality during storage. *Poultry Science*, 84(6), 865–874.
186. PAPAFAEIRIOU, A.Z. – LAKIS, C. – STEFANOY, S. – YIAKOULAKI, M. – MPOKOS, P. – PAPANIKOLAOU, K. (2016): Trace elements content of plant material growing on alkaline organic soils and its suitability for small ruminant extensive farming. *Bulgarian Journal of Agricultural Science*. 22, 733–739.
187. PAVLOVIĆ, Z. – MILETIĆ, I. – JOKIĆ, Ž. – PAVLOVSKI, Z. – ŠKRBIĆ, Z. – ŠOBAJIĆ, S. (2010): The Effect of Level and Source of Dietary Selenium

- Supplementation on Eggshell Quality. *Biological Trace Element Research*, 133(2), 197–202.
188. PENG, D. – ZHANG, J. – LIU, Q. – TAYLOR, E.W. (2007): Size effect of elemental selenium nanoparticles (Nano-Se) at supranutritional levels on selenium accumulation and glutathione S-transferase activity. *Journal of Inorganic Biochemistry*. 101(10), 1457–1463.
  189. PESCUA, M. – GOMEZ-GOMEZ, B. – PEREZ-CORONA, T. – FONT, G. – MADRID, Y. – MOZZI, F. (2017): Food prospects of selenium enriched–*Lactobacillus acidophilus* CRL 636 and *Lactobacillus reuteri* CRL 1101. *Journal of Functional Foods*. 35, 466–473.
  190. PRABHU, K.S. – LEI, X.G. (2016): Selenium. *Advances in Nutrition* (Bethesda, Md.). 7(2), 415–417.
  191. PRAKAASH S, – BALASUBRAMANIAM L, – PATEL SA, – NAYAK B, – HOWELL C, – SKONBERG D (2021): Antioxidant and antimicrobial modified cellulose nanofibers for food applications. *Food Bioscience*. 44, Part A, 101421.
  192. PRASANTH, S. – SUDARSANAKUMAR, C. (2017): Elucidating the interaction of L-cysteine-capped selenium nanoparticles and human serum albumin: Spectroscopic and thermodynamic analysis. *New Journal of Chemistry*. 41(17), 9521–9530.
  193. PRASAD, K.S. – SELVARAJ, K. (2014): Biogenic synthesis of selenium nanoparticles and their effect on As(III)-induced toxicity on human lymphocytes. *Biological Trace Element Research*. 157(3), 275–283.
  194. PROKISCH, J. – ZOMMARA, M. (2011): Process for producing elemental selenium nanospheres. 2011.08.23. Patent No. US 8003071 B2.
  195. P.S. ANALYTICAL. (1999): APP092: Using the Millenium Excalibur for selenium speciation. P.S. Analytical Application Notes, Kent, UK
  196. POPHALY, S. – SINGH, R. – POPHALY, S. – KAUSHIK, J. – TOMAR, S. (2012): Current status and emerging role of glutathione in food grade lactic acid bacteria. *Microbial Cell Factories*. 11, article number: 114.
  197. POSAVEC, D. – DORSCH, A. – BOGNER, U. – BERNHARDT, G. – NAGL, S. (2011). Polyvinyl butyral nanobeads: preparation, characterization, biocompatibility and cancer cell uptake. *Microchimica Acta*. 173(3), 391–399.

198. PUSZTAHELYI, T. – KOVÁCS, S. – PÓCSI, I. – PROKISCH, J. (2015): Selenite-stress selected mutant strains of probiotic bacteria for Se source production. *Journal of Trace Elements in Medicine and Biology*. 30, 96–101.
199. QIN, Y. – JI, X. – JING, J. – LIU, H. – WU, H. – YANG, W. (2010): Size control over spherical silver nanoparticles by ascorbic acid reduction. *Colloids and Surfaces A: Physicochemical and Engineering Aspects*. 372(1-3), 172–176.
200. RAJASREE, R.S.R. – GAYATHRI, S. (2015): Extracellular biosynthesis of selenium nanoparticles using some species of *Lactobacillus*. *Indian Journal of Geo-Marine Sciences*. 44(5), 766–775.
201. RAMAMURTHY, CH. – SAMPATH, K.S. – ARUNKUMAR, P. – KUMAR, M.S. – SUJATHA, V. – PREMKUMAR, K. – THIRUNAVUKKARASU, C. (2013): Green synthesis and characterization of selenium nanoparticles and its augmented cytotoxicity with doxorubicin on cancer cells. *Bioprocess and Biosystems Engineering*. 36(8), 1131–1139.
202. RAMOS, J.F. – WEBSTER, T.J. (2012): Cytotoxicity of selenium nanoparticles in rat dermal fibroblasts. *International Journal of Nanomedicine*. 7, 3907–3914.
203. RAMYA, S. – SHANMUGASUNDARAM, T. – BALAGURUNATHAN, R. (2015): Biomedical potential of actinobacterially synthesized selenium nanoparticles with special reference to anti-biofilm, anti-oxidant, wound healing, cytotoxic and anti-viral activities. *Journal of Trace Elements in Medicine and Biology: Organ of the Society for Minerals and Trace Elements (GMS)*. 32, 30–39.
204. RAN, L. – WU, X. – SHEN, X. – ZHANG, K. – REN, F. – HUANG, K. (2010): Effects of selenium form on blood and milk selenium concentrations, milk component and milk fatty acid composition in dairy cows. *Journal of the Science of Food and Agriculture*. 90(13), 2214–2219.
205. RAYMAN, M.P. (2008): Food-chain selenium and human health: emphasis on intake. *British Journal of Nutrition*. 100(2), 254–68.
206. RANZANI-PAIVA, MARIA. – JULIO LOMBARDI. – ADRIANO GONCALVES. (2011): Acute toxicity of sodium selenite and sodium selenate to Tilapia, *Oreochromis niloticus*, Fingerlings. *Boletim Do Instituto de Pesca*. 37 (January), 191–97.
207. RASHNOO, M. – RAHMATI, Z. – AZARFAR, A. – FADAYIFAR, A. (2020): The effects of maternal supplementation of selenium and iodine via slow-release

- blouses in late pregnancy on milk production of goats and performance of their kids. Italian Journal of Animal Science, 19(1), 502–513.
208. RAO, J. VENKATESWARA. – AREPALLI, S.K. – GUNDA, V.G. – BHARAT KUMAR, J. (2008): Assessment of cytoskeletal damage in *Paramecium caudatum*: An early warning system for apoptotic studies. Pesticide Biochemistry and Physiology. 91(2), 75–80.
209. RATHER, H.A. – THAKORE, R. – SINGH, R. – JHALA, D. – SINGH, S. – VASITA, R. (2018). Antioxidative study of cerium oxide nanoparticle functionalized PCL-gelatin electrospun fibers for wound healing application. Bioactive Materials. 3, 201–211.
210. RAYMAN, M.P. (2000): The importance of selenium to human health. The Lancet, 356(9225), 233–241.
211. RAYMAN, M.P. (2012): Selenium and human health. The Lancet, 379(9822), 1256–1268.
212. REN, F. – CHEN, X. – HESKETH, J. – GAN, F. – HUANG, K. (2012): Selenium promotes T-cell response to TCR-stimulation and ConA, but not PHA in primary porcine splenocytes. PLoS ONE. 7(4), e35375.
213. REGAN, F. – CHAPMAN, J. – SULLIVAN, T. (2012): Nanoparticles in anti-microbial materials: Use and Characterization. RSC Pub. Nanoscience. 23, 1<sup>st</sup> edition.
214. RIDLEY, H. – WATTS, C.A. – RICHARDSON, D.J. – BUTLER, C.S. (2006): Resolution of distinct membrane-bound enzymes from *Enterobacter cloacae* SLD1a-1 that are responsible for selective reduction of nitrate and selenate oxyanions. Applied and Environmental Microbiology. 72(8), 5173–5180.
215. RHO, K.S. – JEONG, L. – LEE, G. – SEO, B.M. – PARK, Y.J. – HONG, S.D. – ROH, S. – CHO, J.J. – PARK, W.H. – MIN, B.M. (2006). Electrospinning of collagen nanofibers: Effects on the behavior of normal human keratinocytes and early-stage wound healing. Biomaterials. 27, 1452–1461.
216. RIEGER, K.A. – BIRCH, N.P. – SCHIFFMAN, J.D. (2013). Designing electrospun nanofiber mats to promote wound healing – A review. Journal of Materials Chemistry B. 1, 4531–4541.
217. ROEKENS, E.J. – ROBBERECHT, H.J. – DEELSTRA, H.A. (1986): Dietary selenium intake in Belgium for different population groups at risk for deficiency.

- Diätetische Selen-Aufnahme in Belgien bei verschiedenen Bevölkerungsgruppen mit den Risiken eines Defizits, 182(1), 8–13.
218. RUEDIGER, T. – BERG, A. – GUELLMAR, A. – RODE, C. – SCHNABELRAUCH, M. – URBANEK, A. – WAGNER, K. – WYRWA, R. – KINNE, R.W. – SIGUSCH, B.W. (2012). Cytocompatibility of polymer-based periodontal bone substitutes in gingival fibroblast and MC3T3 osteoblast cell cultures. *Dental Materials*. 28(10), e239-249.
  219. RUJITANAROJ, P. –PIMPHA, N. – SUPAPHOL, P. (2008). Wound-dressing materials with antibacterial activity from electrospun gelatin fiber mats containing silver nanoparticles. *Polymer*. 49(21), 4723–4732.
  220. SADEGHIAN, S. – KOJOURI, G.A. – MOHEBBI, A. (2012): Nanoparticles of selenium as species with stronger physiological effects in sheep in comparison with sodium selenite. *Biological Trace Element Research*. 146(3), 302–308.
  221. SADAT-HOSSEINI, S.M.A., – MOSLEMI, H.R. – NOURBAKHSH, M.S. – GHAFFARI-KHALIGH, S. (2021): evaluating the effect of electrospun polyvinyl alcohol nanofiber containing eucalyptus globules extract on the healing of experimental achilles tendon injury in rat. *Iranian Journal of Veterinary Surgery*. Online First.
  222. SAQUING, C.D. – MANASCO, J.L. – KHAN, S.A. (2009). Electrospun nanoparticle–nanofiber composites via a one-step synthesis. *Small*. 5(8), 944–951.
  223. SARKAR, J. – DEY, P. – SAHA, S. – ACHARYA, K. (2011): Mycosynthesis of selenium nanoparticles. *Micro & Nano Letters*. 6(8), 599–602.
  224. SCHEIDELER, S.E. – WEBER, P. – MONSALVE, D. (2010). Supplemental vitamin E and selenium effects on egg production, egg quality, and egg deposition of  $\alpha$ -tocopherol and selenium. *Journal of Applied Poultry Research*. 19(4), 354–360.
  225. SCHNEIDER, O.D. – MOHN, D. – FUHRER, R. – KLEIN, K. – KÄMPF, K. – NUSS, K.M.R. – SIDLER, M. – ZLINSZKY, K. – VON RECHENBERG, B. – STARK, W.J. (2011): Biocompatibility and bone formation of flexible, cotton wool-like PLGA/calcium phosphate nanocomposites in sheep. *The Open Orthopaedics Journal*. 5, 63–71.

226. SELVARAJ, S. – FATHIMA, N.N. (2017). Fenugreek incorporated silk fibroin nanofibers-a potential antioxidant scaffold for enhanced wound healing. *ACS Applied Materials & Interfaces*. 9, 5916–5926.
227. ŠEVČÍKOVÁ, S. – SKŘIVAN, M. – DLOUHÁ, G. – KOUCKÝ, M. (2016): The effect of selenium source on the performance and meat quality of broiler chickens. *Czech J. Anim. Sci.* 51(10): 449-457.
228. SHAH, C.P. – KUMAR, M. – BAJAJ, P.N. (2007): Acid-induced synthesis of polyvinyl alcohol-stabilized selenium nanoparticles. *Nanotechnology*. 18(38), 385607.
229. SHAHABADI, N. – ZENDEHCHESHM, S. – KHADEMI, F. (2021): Selenium nanoparticles: Synthesis, in-vitro cytotoxicity, antioxidant activity and interaction studies with ct-DNA and HSA, HHb and Cyt c serum proteins. *Biotechnology Reports*. 30, e00615.
230. SHI LI-GUANG. – YANG RU-JIE. – YUE WEN-BIN. – XUN WEN-JUAN. – ZHANG CHUN-XIANG. – REN YOU-SHE. – SHI LEI. – LEI FU-LIN. (2010): Effect of elemental nano-selenium on semen quality, glutathione peroxidase activity, and testis ultrastructure in male Boer goats. *Animal Reproduction Science*. 118(2), 248–254.
231. SHI, L. – XUN, W. – YUE, W. – ZHANG, C. – REN, Y. – SHI, L. – WANG, Q. – YANG, R. – LEI, F. (2011): Effect of sodium selenite, Se-yeast and nano-elemental selenium on growth performance, Se concentration and antioxidant status in growing male goats. *Small Ruminant Research*. 96(1), 49–52.
232. SHOEIBI, S. – MASHREGHI, M. (2017): Biosynthesis of selenium nanoparticles using *Enterococcus faecalis* and evaluation of their antibacterial activities. *Journal of Trace Elements in Medicine and Biology*. 39, 135–139.
233. SKALICKOVA, S. – MILOSAVLJEVIC, V. – CIHALOVA, K. – HORKY, P. – RICHTERA, L. – ADAM, V. (2017): Selenium nanoparticles as a nutritional supplement. *Nutrition*. 33, 83–90.
234. SOLOMIN, E.V. – SIROTKIN, E.A. – SIROTKIN, A.A. (2017). Universal electrospinning scalable plant for filtering nanofiber production. *Procedia Engineering*. 206, 1371–1375.
235. SONG, D. – LI, X. – CHENG, Y. – XIAO, X. – LU, Z. – WANG, Y. – WANG, F. (2017): Aerobic biogenesis of selenium nanoparticles by *Enterobacter cloacae*

- Z0206 as a consequence of fumarate reductase mediated selenite reduction. *Scientific Reports*. 7(1), 3239.
236. SOWNDARYA, P. – RAMKUMAR, G. – SHIVAKUMAR, M.S. (2017): Green synthesis of selenium nanoparticles conjugated *Clausena dentata* plant leaf extract and their insecticidal potential against mosquito vectors. *Artificial Cells, Nanomedicine, and Biotechnology*. 45(8), 1490–1495.
  237. SPALLHOLZ, J.E. – HOFFMAN, D.J. (2002). Selenium toxicity: cause and effects in aquatic birds. *Aquatic toxicology (Amsterdam, Netherlands)*. 57(1-2), 27–37.
  238. SPEARS, J.W. – WEISS, W.P. (2008): Role of antioxidants and trace elements in health and immunity of transition dairy cows. *Journal of Veterinary Science*. 176, 70–76.
  239. SPILLER, H.A. (2018): Rethinking Mercury: The role of selenium in the pathophysiology of mercury toxicity. *Clinical Toxicology (Philadelphia, Pa.)*. 56 (5), 313–326.
  240. SPYRIDOPOULOU, K. – TRYFONOPOULOU, E. – AINDELIS, G. – YPSILANTIS, P. – SARAFIDIS, C. – KALOGIROU, O. – CHLICHLIA, K. (2021): Biogenic selenium nanoparticles produced by *Lactobacillus casei* ATCC 393 inhibit colon cancer cell growth in vitro and in vivo. *Nanoscale Advances*. 3(9), 2516–2528.
  241. SRIVASTAVA, N. – MUKHOPADHYAY, M. (2013): Biosynthesis and structural characterization of selenium nanoparticles mediated by *Zooglea ramigera*. *Powder Technology*. 244, 26–29.
  242. SRIVASTAVA, N. – MUKHOPADHYAY, M. (2015a): Green synthesis and structural characterization of selenium nanoparticles and assessment of their antimicrobial property. *Bioprocess and Biosystems Engineering*. 38(9), 1723–1730.
  243. SRIVASTAVA, N. – MUKHOPADHYAY, M. (2015b): Biosynthesis and structural characterization of selenium nanoparticles using *Gliocladium roseum*. *Journal of Cluster Science*. 26(5), 1473–1482.
  244. STONE, R. (2009): Diseases. A medical mystery in middle China. *Science*. 324(5933), 1378–1381.
  245. STONEHOUSE, G.C. – MCCARRON, B.J. – GUIGNARDI, Z.S. – EL MEHDAWI A.F. – LIMA, L.W. – FAKRA, S.C. – PILON-SMITS, E.A.H. (2020):

- Selenium metabolism in Hemp (*Cannabis sativa* L.)-potential for phytoremediation and biofortification. *Environment Science & Technology*. 54(7), 4221–4230.
246. SUN, K. – QIU, J. – LIU, J. – MIAO, Y. (2009): Preparation and characterization of gold nanoparticles using ascorbic acid as reducing agent in reverse micelles. *Journal of Materials Science*. 44(3), 754-758.
247. SUNDARAN, S.P. – RESHMI, C.R. – SAGITHA, P. – MANAF, O. – SUJITH, A. (2019): Multifunctional graphene oxide loaded nanofibrous membrane for removal of dyes and coliform from water. *Journal of Environmental Management*. 240, 494–503.
248. SUNDARRAJAN, S. – TAN, K.L. – LIM, S.H. – RAMAKRISHNA, S. (2014). Electrospun nanofibers for air filtration applications. *Procedia Engineering*. 75, 159–163.
249. SUPAPHOL, P. – MIT-UPPATHAM, C. – NITHITANAKUL, M. (2005). Ultrafine electrospun polyamide-6 fibers: effects of solvent system and emitting electrode polarity on morphology and average fiber diameter. *Macromolecular Materials and Engineering*. 290, 933–942.
250. SURYADININGRAT, M. – KURNIAWATI, DY. – MUJIBURRAHMAN, A. – PURNAMA, MTE. (2021): Dietary polyvinyl alcohol and alginate nanofibers ameliorate hyperglycemia by reducing insulin and glucose-metabolizing enzyme levels in rats with streptozotocin-induced diabetes, *Veterinary World*. 14(4): 847-853.
251. SUTTLE, N.F. (2010). *Mineral Nutrition of Livestock*. 4<sup>th</sup> edition. MPG Books Group: London, UK. 565.
252. TAYLOR CAMERON. – MARIANNE MATZKE. – ALEXANDRA KROLL. – DANIEL S.R. – CLAUS SVENDSEN. – ALISON CROSSLEY. (2016): Toxic interactions of different silver forms with freshwater green algae and cyanobacteria and their effects on mechanistic endpoints and the production of extracellular polymeric substances. *Environmental Science: Nano*. 3(2), 396–408.
253. TEJO PRAKASH, N. – SHARMA, N. – PRAKASH, R. – RAINA, K.K. – FELLOWES, J. – PEARCE, C.I. – LLOYD, J.R. – PATTRICK, R.A.D. (2009): Aerobic microbial manufacture of nanoscale selenium: Exploiting nature’s bio-nano mineralization potential. *Biotechnology Letters*. 31(12), 1857–1862.

254. TEO, W.E. – RAMAKRISHNA, S. (2006). A review on electrospinning design and nanofiber assemblies. *Nanotechnology*. 17(14), R89–R106.
255. TIJING, L.D. – WOO, Y.C. – JOHIR, M.A.H. – CHOI, J.-S. – SHON, H.K. (2014): A novel dual-layer bicomponent electrospun nanofibrous membrane for desalination by direct contact membrane distillation. *Chemical Engineering Journal*, 256, 155–159.
256. THOMAS, R. – SOUMYA, K.R. – MATHEW, J. – RADHAKRISHNAN, E.K. (2015). Electrospun polycaprolactone membrane incorporated with biosynthesized silver nanoparticles as effective wound dressing material. *Applied Biochemistry and Biotechnology*. 176(8), 2213–2224.
257. TONG, W. – JIANG, B. – WANG, Y. – YIN, A. – HUANG, C. – WANG, S. – MO, X. (2015): Electrospun poly(L-lactide-co-caprolactone)–collagen–chitosan vascular graft in a canine femoral artery model. *Journal of Materials Chemistry B*. 3(28), 5760–5768.
258. TORRES, S.K. – CAMPOS, V.L. – LEÓN, C.G. – RODRÍGUEZ-LLAMAZARES, S.M. – ROJAS, S.M. – GONZÁLEZ, M. – SMITH, C. – MONDACA, M.A. (2012): Biosynthesis of selenium nanoparticles by *Pantoea agglomerans* and their antioxidant activity. *Journal of Nanoparticle Research*. 14(11), 1236.
259. TRABELSI, H. – AZZOUZ, I. – FERCHICHI, TEBOURBI, SAKLY, M. – ABDELMELEK, H. (2013): Nanotoxicological evaluation of oxidative responses in rat nephrocytes induced by cadmium. *International Journal of Nanomedicine*. 8(1), 3447–3453.
260. UNNITHAN, A.R. – ARATHYRAM, R.S. – KIM, C.S. (2015): Electrospinning of Polymers for Tissue Engineering, Chapter 3: S. Thomas, Y. Grohens, N. Ninan (Eds.), *Nanotechnology Applications for Tissue Engineering*. ISBN: 978-0-323-32889-0, William Andrew Publishing. 45-55.
261. UNGVÁRI, EVA. – ISTVÁN MONORI, – ATTILA MEGYERI, – ZOLTAN CSIKI, – JOZSEF PROKISCH, ATTILA SZTRIK, – ANDRÁS JÁVOR, – ILONA BENKŐ. (2013): Protective effects of meat from lambs on selenium nanoparticle supplemented diet in a mouse model of polycyclic aromatic hydrocarbon-induced immunotoxicity. *Food and Chemical Toxicology*. 64, 298–306.

262. VAHDATI, M. – TOHIDI MOGHADAM, T. (2020): Synthesis and characterization of selenium nanoparticles-lysozyme nanohybrid system with synergistic antibacterial properties. *Scientific Reports*. 10(1), 510.
263. VALLET-REGÍ, M. – GONZÁLEZ, B. – IZQUIERDO-BARBA, I. (2019): Nanomaterials as promising alternative in the infection treatment. *International Journal of Molecular Sciences*. 20(15), 3806.
264. VAN HOUTEN, J. (1978): Two mechanisms of chemotaxis in *Paramecium*. *Journal of Comparative Physiology*. 127(2), 167–74.
265. VAZQUEZ-MUÑOZ ROBERTO. – BELEN BORREGO. – KARLA JUÁREZ-MORENO. – MARITZA GARCÍA-GARCÍA. – JOSUÉ D. MOTA MORALES. – NINA BOGDANCHIKOVA. – ALEJANDRO HUERTA-SAQUERO. (2017): Toxicity of silver nanoparticles in biological systems: Does the complexity of biological systems matter? *Toxicology Letters*. 276(July) 11–20.
266. VENKATESWARA RAO, J. – SRIKANTH, K. – AREPALLI, S.K. – GUNDA, V.G. (2006): Toxic effects of acephate on *Paramecium caudatum* with special emphasis on morphology, behaviour, and generation time. *Pesticide Biochemistry and Physiology*. 86(3), 131–37.
267. VENKATESWARA RAO, J. – GUNDA, V.G. – SRIKANTH, K. – AREPALLI, S.K. (2007): Acute toxicity bioassay using *Paramecium caudatum*, a key member to study the effects of monocrotophos on swimming behaviour, morphology and reproduction. *Toxicological & Environmental Chemistry*. 89(2), 307–317.
268. VERA, P. – ECHEGOYEN, Y. – CANELLAS, E. – NERÍN, C. – PALOMO, M. – MADRID, Y. – CÁMARA, C. (2016): Nano selenium as antioxidant agent in a multilayer food packaging material. *Analytical and Bioanalytical Chemistry*. 408(24), 6659–6670.
269. VERA, P. – CANELLAS, E. – NERÍN, C. (2018): New antioxidant multilayer packaging with nanoselenium to enhance the shelf-life of market food products. *Nanomaterials*. 8(10), 837.
270. VERMA, P. – MAHESHWARI, S.K. (2018): Preparation of silver and selenium nanoparticles and its characterization by dynamic light scattering and scanning electron microscopy. *Journal of Microscopy and Ultrastructure*. 6(4), 182–187.
271. VETCHINKINA, E. – LOSHCHININA, E. – KURSKY, V. – NIKITINA, V. (2013): Reduction of organic and inorganic selenium compounds by the edible

- medicinal basidiomycete *Lentinula edodes* and the accumulation of elemental selenium nanoparticles in its mycelium. *Journal of Microbiology* (Seoul, Korea). 51(6), 829–835.
272. VIEIRA, A. – STEIN, E. – ANDREGUETTI, D. – CEBRIÁN-TORREJÓN, G. – DOMÉNECH-CARBÓ, A. – COLEPICOLO, P. – FERREIRA, A.M. (2017): Sweet Chemistry: A Green way for obtaining selenium nanoparticles active against cancer cells. *Journal of the Brazilian Chemical Society*. 28(10), 2021–2027.
273. VICAS, S.I. – LASLO, V. – TIMAR, A.V. – BALTA, C. – HERMAN, H. – CICEU, A. – GHARBIA, S. – ROSU, M. – MLADIN, B. – FRITEA, L. – CAVALU, S. – COTORACI, C. – PROKISCH, J. – PUSCHITA, M. – POP, C. – MIUTESCU, E. – HERMENEAN, A. (2021a): Nano selenium-enriched probiotics as functional food products against cadmium liver toxicity. *Materials*. 14, 2257.
274. VICAS, S.I. – LASLO, V. – TIMAR, A.V. – BALTA, C. – HERMAN, H. – CICEU, A. – GHARBIA, S. – ROSU, M. – MLADIN, B. – FRITEA, L. – CAVALU, S. – COTORACI, C. – PROKISCH, J. – PUSCHITA, M. – POP, C. – MIUTESCU, E. – HERMENEAN, A. (2021b): Functional food product based on nanoselenium- enriched *Lactobacillus casei* against cadmium kidney toxicity. *Applied Sciences*. 11, 4220.
275. VINCETI, M. – WEI, E.T. – MALAGOLI, C. – BERGOMI, M. – VIVOLI, G. (2001): Adverse health effects of selenium in humans. *Reviews on Environmental Health*. 16(4), 233–251.
276. VINCETI, M. – MANDRIOLI, J. – BORELLA, P. – MICHALKE, B. – TSATSAKIS, A. – FINKELSTEIN, Y. (2014): Selenium neurotoxicity in humans: Bridging laboratory and epidemiologic studies. *Toxicology Letters*. 230(2), 295–303.
277. VISHA, P. – NANJAPPAN, K. – JAYACHANDRAN, S. – SELVARAJ, P. – ELANGO, A. – KUMARESAN, G. (2015): Biosynthesis and structural characteristics of selenium nanoparticles using *Lactobacillus acidophilus* bacteria by wet sterilization process. *International Journal of Advanced Veterinary Science and Technology*. 4(1), 178–183.
278. VYAS, J. – RANA, S. (2018): Synthesis of selenium nanoparticles using *Allium sativum* extract and analysis of their antimicrobial property against gram positive bacteria. *The Pharma Innovation Journal*. 7(9), 262–266.

279. WADHWANI, S.A. – GORAIN, M. – BANERJEE, P. – SHEDBALKAR, U.U. – SINGH, R. – KUNDU, G.C. – CHOPADE, B.A. (2017): Green synthesis of selenium nanoparticles using *Acinetobacter sp.*, SW30: Optimization, characterization and its anticancer activity in breast cancer cells. *International Journal of Nanomedicine*. 12, 6841–6855.
280. WALLACE, L.G. – BOBE, G. – VORACHEK, W.R. – DOLAN, B.P. – ESTILL, C.T. – PIRELLI, G.J. – HALL, J.A. (2017): Effects of feeding pregnant beef cows' selenium-enriched alfalfa hay on selenium status and antibody titers in their newborn calves. *Journal of Animal Science*. 95(6), 2408–2420.
281. WANG, H. – ZHANG, J. – YU, H. (2007): Elemental selenium at nano size possesses lower toxicity without compromising the fundamental effect on selenoenzymes: Comparison with selenomethionine in mice. *Free Radical Biology and Medicine*. 42(10), 1524–1533.
282. WANG, T. – YANG, L. – ZHANG, B. – LIU, J. (2010): Extracellular biosynthesis and transformation of selenium nanoparticles and application in H<sub>2</sub>O<sub>2</sub> biosensor. *Colloids and Surfaces B: Biointerfaces*. 80(1), 94–102.
283. WANG, Q. – MEJÍA JARAMILLO, A. – PAVON, J.J. – WEBSTER, T.J. (2015): Red selenium nanoparticles and gray selenium nanorods as antibacterial coatings for PEEK medical devices: Antibacterial Coatings for Peek Medical Devices. *Journal of Biomedical Materials Research*. 104(7), 352–1358,
284. WANG, H. – CHEN, B. – HE, M. – YU, X. – HU, B. (2017): Selenocysteine against methyl mercury cytotoxicity in HepG2 cells. *Scientific Reports*. 7(1), 147.
285. WANG, Y. – SHU, X. – ZHOU, Q. – FAN, T. – WANG, T. – CHEN, X. – LI, M. – MA, Y. – NI, J. – HOU, J. – ZHAO, W. – LI, R. – HUANG, S. – WU, L. (2018): Selenite reduction and the biogenesis of selenium nanoparticles by *Alcaligenes faecalis* Se03 isolated from the gut of *Monochamus alternatus* (Coleoptera: Cerambycidae). *International Journal of Molecular Sciences*. 19(9), E2799.
286. WANG, K. – WANG, Y. – LI, K. – WAN, Y. – WANG, Q. – ZHUANG, Z. – GUO, Y. – LI, H. (2020): Uptake, translocation and biotransformation of selenium nanoparticles in rice seedlings (*Oryza sativa L.*). *Journal of Nanobiotechnology*, 18(1), 103.
287. WENJUAN, X. – LIGUANG, S. – WENBIN, Y. – CHUNXIANG, Z. – YOUSHE, R. – QIANG, L. – Qian, W. – Lei, S. (2010): Effect of elemental nano-selenium on

- feed digestively, rumen fermentation, and purine derivatives in sheep. *Animal Feed Science and Technology*. 163(2–4), 136–42.
288. WENJUAN, X. – LIGUANG, S. – WENBIN, Y. – CHUNXIANG, Z. – YOUSHE, R. – QIANG, L. (2012): Effect of high-dose nano-selenium and selenium–yeast on feed digestibility, rumen fermentation, and purine derivatives in sheep. *Biol Trace Elem Res*. 150(1–3), 130–136.
289. WILDE, D. (2006): Influence of macro and micro minerals in the peri-parturient period on fertility in dairy cattle. *Animal Reproduction Science*. 96, 240–249.
290. WU, X. – YAO, J. – YANG, Z. – YUE, W. – REN, Y. – ZHANG, C. – LIU, X. – WANG, H. – ZHAO, X. – YUAN, S. – WANG, Q. – SHI, L. – SHI, L. (2011): Improved fetal hair follicle development by maternal supplement of selenium at nano size (Nano-Se). *Livestock Science*. 142(1–3), 270–275.
291. XINHUA, Z. – KWANGSOK, K. – DUFEI, F. – SHAOFENG, R. – BENJAMIN, S.H. – BENJAMIN, C. (2002): Structure and process relationship of electrospun bioabsorbable nanofiber membranes. *Polymer*. 43, 4403–4412.
292. XIONG, Y. – XIA, Y. (2007): Shape-Controlled Synthesis of Metal Nanostructures: The case of palladium. *Advanced Materials*. 19(20), 3385–3391.
293. XU, C. – GUO, Y. – QIAO, L. – MA, L. – CHENG, Y. – ROMAN, A. (2018): Biogenic synthesis of novel functionalized selenium nanoparticles by *Lactobacillus casei* ATCC 393 and its protective effects on intestinal barrier dysfunction caused by enterotoxigenic *Escherichia coli* K88. *Frontiers in Microbiology*. 9, 1129.
294. XU, C. – QIAO, L. – MA, L. – YAN, S. – GUO, Y. – DOU, X. – ZHANG, B. – ROMAN, A. (2019): Biosynthesis of polysaccharides-capped selenium nanoparticles using *Lactococcus lactis* NZ9000 and their antioxidant and anti-inflammatory activities. *Frontiers in Microbiology*. 10, 1632.
295. XUN, W. – SHI, L. – YUE, W. – ZHANG, C. – REN, Y. – LIU, Q. (2012): Effect of high-dose nano-selenium and selenium-yeast on feed digestibility, rumen fermentation, and purine derivatives in sheep. *Biological Trace Element Research*. 150(1–3), 130–136.
296. YALCINKAYA, F. – YALCINKAYA, B. – MARYSKA, J. (2016): Preparation and characterization of polyvinyl butyral nanofibers containing silver nanoparticles. *Journal of Materials Science and Chemical Engineering*. 4(1), 8–12.

297. YALCINKAYA, F. – KOMAREK, M. (2019): Polyvinyl butyral (PVB) nanofiber/nanoparticle-covered yarns for antibacterial textile surfaces. *International Journal of Molecular Sciences*. 20(17), 4317.
298. YUANXIA, L. – ZHU, N. – LIANG, X. – ZHENG, L. – ZHANG, C. – LI, Y.-F. – ZHANG, Z. – GAO, Y. – ZHAO, J. (2020). A comparative study on the accumulation, translocation and transformation of selenite, selenate, and SeNPs in a hydroponic-plant system. *Ecotoxicology and Environmental Safety*. 189, 109955
299. YOON, K.Y. – HOON BYEON, J. – PARK, J.H. – HWANG, J. (2007): Susceptibility constants of *Escherichia coli* and *Bacillus subtilis* to silver and copper nanoparticles. *Science of The Total Environment*. 373(2–3), 572–575.
300. YUAN GAO. – CRANSTON, R. (2008). Recent advances in antimicrobial treatments of textiles. *Textile Research Journal*. 78(1), 60–72.
301. ZARE, B. – BABAIE, S. – SETAYESH, N. – SHAHVERDI, A.R. (2013): Isolation and characterization of a fungus for extracellular synthesis of small selenium nanoparticles. *Nanomedicine Journal*. 1(1), 13–19.
302. ZELST, V.M. – HESTA, M. – GRAY, K. – STAUNTON, R. – DU LAING, G. – JANSSENS, G.P.J. (2016): Biomarkers of selenium status in dogs. *BMC Veterinary Research*. 12, 15.
303. ZHANG, J. – XUEYUN, G. – LIDE, Z. – YONGPING, B. (2001): Biological effects of a nano red elemental selenium. *BioFactors*. 15(1), 27–38.
304. ZHANG, J. – HUALI, W. – XIANGXU, E.Y. – LIDE, Z. (2005): Comparison of short-term toxicity between nano-se and selenite in mice. *Life Sciences*. 76(10), 1099–1109.
305. ZHANG, J. – WANG, X. – XU, T. (2008): Elemental selenium at nano size (Nano-Se) as a potential chemo preventive agent with reduced risk of selenium toxicity: Comparison with Se-Methylselenocysteine in mice. *Toxicological Sciences*. 101(1), 22–31.
306. ZHANG, Y. – WANG, J. – ZHANG, L. (2010): Creation of highly stable selenium nanoparticles capped with hyperbranched polysaccharide in water. *Langmuir*. 26(22), 17617–17623.
307. ZHANG, W. – CHEN, Z. – LIU, H. – ZHANG, L. – GAO, P. – LI, D. (2011): Biosynthesis and structural characteristics of selenium nanoparticles by *Pseudomonas alcaliphila*. *Colloids and Surfaces. B: Biointerfaces*. 88(1), 196–201.

308. ZHANG, H. – ZHOU, H. – BAI, J. – LI, Y. – YANG, J. – MA, Q. – QU, Y. (2019): Biosynthesis of selenium nanoparticles mediated by fungus *Mariannaea sp.* HJ and their characterization. *Colloids and Surfaces A: Physicochemical and Engineering Aspects*. 571, 9–16.
309. ZHENG, S. – LI, X. – ZHANG, Y. – XIE, Q. – WONG, Y.S. – ZHENG, W. – CHEN, T. (2012): PEG-nanolized ultrasmall selenium nanoparticles overcome drug resistance in hepatocellular carcinoma HepG2 cells through induction of mitochondria dysfunction. *International Journal of Nanomedicine*. 7, 3939–3949.
310. ZHENLI, L.H. – JIALI, S. – XIAO, E.Y. (2010): Manganese and selenium. In: *Trace Elements in Soils*. Peter, S. Hooda (ed.). John Wiley & Sons, Ltd. 481–495.
311. ZHILIN, W. – GARY, S.B. – ZHI-QING, L. – YING, L. – LINXI, Y. – XUEBIN, Y. – MIAO, LI. (2015): Biofortification and phytoremediation of selenium in China. *Frontiers in Plant Science*. 6, 136.
312. ZHUANG, Y. – LI, L. – FENG, L. – WANG, S. – SU, H. – LIU, H. – LIU, H. – WU, Y. (2020): Mitochondrion-targeted selenium nanoparticles enhance reactive oxygen species-mediated cell death. *Nanoscale*. 12(3), 1389–1396.
313. ZIA, M.W. – KHALIQUE, A. – NAVEED, S. – HUSSAIN, J. (2016). Impact of selenium supplementation on productive performance and egg selenium status in native Aseel chicken. *Italian Journal of Animal Science*. 15(4), 649–657.
314. ZWOLAK, I. – ZAPOROWSKA, H. (2012): Selenium Interactions and Toxicity: A Review: *Cell Biology and Toxicology*. 28(1), 31–46.

## 10. PUBLICATIONS ON THE TOPIC OF THE DISSERTATION



UNIVERSITY of  
DEBRECEN

UNIVERSITY AND NATIONAL LIBRARY  
UNIVERSITY OF DEBRECEN

H-4002 Egyetem tér 1, Debrecen

Phone: +3652/410-443, email: publikaciok@lib.unideb.hu

Registry number: DEENK/217/2022.PL  
Subject: PhD Publication List

Candidate: Khandsuren Badgar  
Doctoral School: Doctoral School of Animal Husbandry  
MTMT ID: 10065278

### List of publications related to the dissertation

#### Foreign language scientific articles in Hungarian journals (3)

- Badgar, K.,** Prokisch, J.: A simple method for preparing elemental selenium nano- coating inside a silicone surface.  
*Acta agrar. Debr.* 2021 (1), 35-43, 2021. ISSN: 1587-1282.  
DOI: <http://dx.doi.org/10.34101/actaagrar/1/8940>
- Badgar, K.,** Prokisch, J.: Preparation of red and grey elemental selenium for food fortification.  
*Acta Aliment.* 50 (2), 289-298, 2021. ISSN: 0139-3006.  
DOI: <http://dx.doi.org/10.1556/066.2020.00332>  
IF: 0.65 (2020)
- Badgar, K.:** The synthesis of selenium nanoparticle (SeNPs) - Review.  
*Acta agrar. Debr.* 1, 5-8, 2019. ISSN: 1587-1282.  
DOI: <https://doi.org/10.34101/actaagrar/1/2359>

#### Foreign language scientific articles in international journals (7)

- Elsakhawy, T., Omara, A. E. D., Abowaly, M., El-Ramady, H., **Badgar, K.,** Llanaj, X., Törös, G., Hajdú, P., Prokisch, J.: Green Synthesis of Nanoparticles by Mushrooms: A Crucial Dimension for Sustainable Soil Management.  
*Sustainability.* 14, 1-27, 2022. ISSN: 2071-1050.  
DOI: <http://dx.doi.org/10.3390/su14074328>  
IF: 3.251 (2020)
- Badgar, K.,** Abdalla, N., El-Ramady, H., Prokisch, J.: Sustainable Applications of Nanofibers in Agriculture and Water Treatment: A Review.  
*Sustainability.* 14 (1), 1-17, 2022. ISSN: 2071-1050.  
DOI: <http://dx.doi.org/10.3390/su14010464>  
IF: 3.251 (2020)
- Badgar, K.,** Prokisch, J.: Elemental Selenium Enriched Nanofiber Production.  
*Molecules.* 26, 1-9, 2021. ISSN: 1420-3049.  
DOI: <http://dx.doi.org/10.3390/molecules26216457>  
IF: 4.411 (2020)



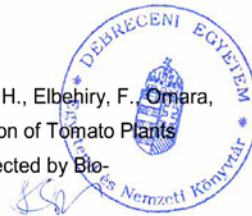


7. **Badgar, K.**, Prokisch, J., El-Ramady, H.: Nanofibers for Sustainable Agriculture: A Short Communication.  
*Egypt. J. Soil Sci.* 61 (3), 373-380, 2021. EISSN: 2357-0369.  
DOI: <http://dx.doi.org/10.21608/ejss.2021.105877.1477>
8. **Badgar, K.**, Prokisch, J.: Testing Toxicity and Antidote Effect of Selenium Nanoparticles with *Paramecium caudatum*.  
*Open J. Anim. Sci.* 11 (04), 532-542, 2021. ISSN: 2161-7597.  
DOI: <http://dx.doi.org/10.4236/ojas.2021.114036>
9. **Badgar, K.**, Prokisch, J.: The production methods of selenium nanoparticles.  
*Acta Univ. Sapientiae, Alim.* 14 (1), 14-43, 2021. ISSN: 1844-7449.  
DOI: <http://dx.doi.org/10.2478/ausal-2021-0002>
10. **Badgar, K.**, Prokisch, J.: The Effects of Selenium Nanoparticles (SeNPs) on Ruminant.  
*Proc. Mong. Acad. Sci.* 60 (4), 1-8, 2020. ISSN: 2310-4716.  
DOI: <http://dx.doi.org/10.5564/pmas.v60i4.1500>

### List of other publications

#### Foreign language scientific articles in international journals (4)

11. El-Ramady, H., Abdalla, N., **Badgar, K.**, Llanaj, X., Törös, G., Hajdú, P., Eid, Y., Prokisch, J.: Edible Mushrooms for Sustainable and Healthy Human Food: Nutritional and Medicinal Attributes.  
*Sustainability.* 14 (9), 1-30, 2022. ISSN: 2071-1050.  
DOI: <http://dx.doi.org/https://doi.org/10.3390/su14094941>  
IF: 3.251 (2020)
12. El-Ramady, H., Abdalla, N., Fawzy, Z., **Badgar, K.**, Llanaj, X., Törös, G., Hajdú, P., Eid, Y., Prokisch, J.: Green Biotechnology of Oyster Mushroom (*Pleurotus ostreatus* L.): A Sustainable Strategy for Myco-Remediation and Bio-Fermentation.  
*Sustainability.* 14 (6), 1-21, 2022. ISSN: 2071-1050.  
DOI: <http://dx.doi.org/10.3390/su14063667>  
IF: 3.251 (2020)
13. Saffan, M. M., Koriem, M. A., Elhenawy, A. S., El-Mahdy, S., El-Ramady, H., Elbehiry, F., Omara, A. E. D., Bayoumi, Y., **Badgar, K.**, Prokisch, J.: Sustainable Production of Tomato Plants (*Solanum lycopersicum* L.) under Low-Quality Irrigation Water as Affected by Bio-Nanofertilizers of Selenium and Copper.  
*Sustainability.* 14 (6), 1-17, 2022. ISSN: 2071-1050.  
DOI: <http://dx.doi.org/10.3390/su14063236>  
IF: 3.251 (2020)





**UNIVERSITY of  
DEBRECEN**

**UNIVERSITY AND NATIONAL LIBRARY  
UNIVERSITY OF DEBRECEN**

H-4002 Egyetem tér 1, Debrecen  
Phone: +3652/410-443, email: publikaciok@lib.unideb.hu

14. Prokisch, J., **Badgar, K.**, El-Ramady, H.: Fortification of Functional Foods for Human Health: A Case Study of Honey and Yogurt for Diabetes.  
*Env. Biodiv. Soil Security*. 5 (1), 331-340, 2021. ISSN: 2536-9415.  
DOI: <http://dx.doi.org/10.21608/jenvbs.2021.110812.1154>

**Total IF of journals (all publications): 21,316**

**Total IF of journals (publications related to the dissertation): 11,563**

The Candidate's publication data submitted to the iDEa Tudóstér have been validated by DEENK on the basis of the Journal Citation Report (Impact Factor) database.

25 April, 2022



## 11. DECLARATION

### DECLARATION

I hereby declare that I have prepared this dissertation in the framework of the Doctoral School of Animal Science, Faculty of Agricultural and Food Sciences and Environmental Management, University of Debrecen, in order to obtain the doctoral (Ph.D.) degree in Animal Husbandry.

Debrecen, 2022/...../.....

-----  
**Khandsuren Badgar**  
*Ph.D. candidate*

### DECLARATION

We hereby declare that **Khandsuren Badgar** Ph.D. candidate has carried out his work under our supervision between 2018 and 2022 within the framework of the Doctoral School of Animal Science, Faculty of Agricultural and Food Sciences and Environmental Management, University of Debrecen. The findings of the dissertation represent the candidate's own ideas and independent work. We recommend accepting the dissertation.

Debrecen, 2022/...../.....

-----  
**Dr. József Prokisch, Ph.D**  
*associate professor*

## ACKNOWLEDGEMENTS

First and foremost, I am extremely grateful to my supervisor **Dr. József Prokisch** (assistant professor at the Institute of Animal Science, Biotechnology and Nature Conservation, University of Debrecen) for his invaluable advice, encouragement, and full support during my research. His great knowledge, innovative ideas, and plentiful experience have guided and shaped me at all times of my academic research. Thank you very much for your special time, and the knowledge and skills instructed me.

I would like to thank **Dr. Lajos Daróczy** (Department of Solid-State Physics, University of Debrecen) for help with the scanning electron microscopic analysis. I would also like to thank **Dr. Attila Bényei** (Department of Physical Chemistry, University of Debrecen) for help with the X-Ray diffraction analysis.

I am also very grateful to **Dr. István Komlósi** (head of Doctoral School of Animal Science, University of Debrecen), **Dr. Levente Czeglédi** (head of Department of Animal Science, University of Debrecen), and **Korcsmáros Marianna Varga** (secretary of Doctoral School of Animal Science, University of Debrecen) and other members of Department of Animal Science, University of Debrecen for the warmest kind supports.

I would like to thank lecturers of the Doctoral School of Animal Science, University of Debrecen for the quality training.

I am grateful to the Stipendium Hungaricum Scholarship Program for the financial support.

I would like to thank my family for giving me time to study and encourage, and for their full support and patience.